DOT/FAA/TC-18/18

Development of Engineered Materials Arresting Systems From 1994 Through 2003

May 2018

Final Report

This document is available to the U.S. public through the National Technical Information Services (NTIS), Springfield, Virginia 22161.

U.S. Department of Transportation
Federal Aviation Administration

NOTICE

1. Report No. DOT/FAA/TC-18/18	2. Government Accession No.	3. Recipient's Catalog No.
4. Title and Subtitle DEVELOPMENT OF ENGINEERED MATERIALS ARRESTING SYSTEMS FROM 1994 THROUGH 2003		5. Report Date May 2018
		6. Performing Organization Code ANG-E261
7. Author(s) White, James and *Subbotin, Nicholas		8. Performing Organization Report No.

9. Performing Organization Name and Address
 	
Applied Research Associates
2628 Fire Road Suite 300
Egg Harbor Township, NJ 08234
 	
*Federal Aviation Administration
  William J. Hughes Technical Center
  Airport Technology Research and Development Branch
  Atlantic City International Airport, NJ 08405
		10. Work Unit No. (TRAIS)

		11. Contract or Grant No.
12. Sponsoring Agency Name and Address U.S. Department of Transportation Federal Aviation Administration Office of Airport Safety and Standards - Airport Engineering Division (AAS-100) 800 Independence Avenue SW Washington, DC 20591		13. Type of Report and Period Covered Final Report
		14. Sponsoring Agency Code AAS-100
15. Supplementary Notes		

16. Abstract

Federal Aviation Administration (FAA) airport design standards require runway safety areas (RSAs) beyond the runway end to minimize the hazards of overruns. However, many runways were built before the adoption of this standard, and construction of a standard RSA may be impracticable. In 1986, the FAA launched a research program to develop an engineered solution for airports with inadequate real estate for standard RSAs. By 1993, the FAA established the feasibility of using a soft-ground arresting system to address this shortcoming. Soft ground is any material that will crush under the wheels of an aircraft and safely and predictably bring an aircraft to a stop.

Between 1994 and 2003, the collaborative research efforts of the FAA, Engineered Systems Company, and the Port Authority of New York and New Jersey, included laboratory testing, mathematical model validation, full-scale aircraft testing, and prototype arrestor system installations at two major airports. The end result enabled the FAA to publish Advisory Circular (AC) 150/5220-22 "Engineered Materials Arresting Systems (EMAS) for Aircraft Overruns." This AC contains standards for planning, design, installation, and maintenance of EMAS in RSAs. The outcome of this research enabled EMAS installations at nine United States airports by 2003.

This report summarizes EMAS research activities between 1994 and 2003.

17. Key Words Engineered materials arresting system, Soft-ground arresting system, Arrestor system, Cellular cement, Phenolic foam, Foamcrete, Arrestor bed, Aircraft rescue and fire fighting, Instrument landing system, Modeling, Overruns, mathematical modeling		18. Distribution Statement This document is available to the U.S. public through the National Technical Information Service (NTIS), Springfield, Virginia 22161. This document is also available from the Federal Aviation Administration William J. Hughes Technical Center at actlibrary.tc.faa.gov.	
19. Security Classif. (of this report) Unclassified	20. Security Classif. (of this page) Unclassified	21. No. of Pages 119	22. Price

Form DOT F 1700.7 (8-72)   Reproduction of completed page authorized

ACKNOWLEDGEMENTS

TABLE OF CONTENTS

APPENDICES

LIST OF FIGURES

LIST OF TABLES

LIST OF SYMBOLS AND ACRONYMS

μ	Mu, coefficient of friction
AC	Advisory Circular
AF	Airway Facilities
ARFF	Aircraft rescue and fire fighting
ATRD	Airport Technology Research and Development Branch
AFFF	Aqueous film forming foam
BOS	Logan International Airport
CG	Center of gravity
CRDA	Cooperative Research and Development Agreement
CRREL	Cold Regions Research and Engineering Laboratory
dB	Decibels
DG	Design Group
EMAS	Engineered Materials Arresting System
ESCO	Engineered Arresting Systems Corporation
F	Fahrenheit
FAA	Federal Aviation Administration
FOD	Foreign object debris
G	G force
GTV	Ground Test Vehicle
GW	Gross weight
ILS	Instrument landing system
JBR	Jet blast resistant
JFK	John F. Kennedy International Airport
kt	Knots
LDA	Laser Doppler anemometer
LGA	LaGuardia International Airport
MAC	Mean aerodynamic chord
MD	McDonnell Douglas
NTSB	National Transportation Safety Board
PANY&NJ	Port Authority of New York and New Jersey
psi	Pounds per square inch
RSA	Runway safety areas
SGAS	Soft-ground arresting system
UDRI	University of Dayton Research Institute
U.S.	United States
WJHTC	William J. Hughes Technical Center

EXECUTIVE SUMMARY

Federal Aviation Administration (FAA) airport design standards require runway safety areas (RSAs) beyond the runway end to minimize the hazards of overruns. Most airports that serve commercial aircraft require an RSA of 1000 feet beyond the end of a runway. However, many runways were built before this standard was implemented and do not have adequate space due to existing structures, bodies of water, large drop-offs, railroads, highways, or other obstructions. If an aircraft overruns the end of these runways, extensive damage to the aircraft, passenger injuries, or loss of lives can be expected.

Aviation accidents in 1982 and 1984 involved aircraft runway overruns that resulted in loss of life and extensive damage to both aircraft. In each case, the aircraft came to rest in a body of water near the end of the runway. The National Transportation Safety Board (NTSB) responded to the risk posed by inadequate RSAs by issuing Safety Recommendation A-84-037 to the FAA to "Initiate research and development activities to establish the feasibility of soft-ground aircraft arresting systems and promulgate a design standard, if the systems are found to be practical."

In 1986, the FAA launched a research program to develop an engineered solution for airports with inadequate real estate for standard safety areas at the end of a runway. From 1986 through 1993, the FAA conducted extensive research and testing on soft-ground arresting systems (SGAS). Soft ground is any material that will crush under the wheels of an aircraft, and safely and predictably bring an aircraft to a stop. FAA report, Soft Ground Arresting System for Airports (DOT/FAA/CT-93/80) details the research conducted during this time. By 1993, the FAA established the feasibility of SGAS, and started working on the second part of the NTSB Safety Recommendation to: "…promulgate a design standard, if the systems are found to be practical."

This report documents the collaborative research efforts of the Port Authority of New York and New Jersey, Engineered Arresting Systems Corporation, and the FAA from 1994 to 2003. This decade of research included laboratory testing, mathematical model validation, full-scale aircraft testing, and prototype arrestor system installations at two major airports. The end result enabled the FAA to publish Advisory Circular (AC) 150/5220-22, "Engineered Materials Arresting Systems (EMAS) for Aircraft Overruns." This AC contains standards for planning, design, installation, and maintenance of EMAS in RSAs, effectively satisfying the NTSB recommendation.

The outcome of this research enabled EMAS installations at nine United States airports by 2003.

1. INTRODUCTION'0'"'

This report summarizes a decade of research and development activities from 1994 through 2003 related to minimizing the risks associated with aircraft that overrun the end of a runway. It provides a chronological review of the collaborative efforts between the Federal Aviation Administration (FAA), Port Authority of New York and New Jersey (PANY&NJ), and Engineered Arresting Systems Corporation (ESCO)[1] to develop a practical soft-ground aircraft arresting system, create an FAA standard, and deploy prototype systems at two major airports; John F. Kennedy International Airport (JFK) and LaGuardia International Airport (LGA).

2. BACKGROUND.

On January 23, 1982, a McDonnell Douglas (MD) DC-10-30 (DC-10-30) aircraft was unable to stop on Runway 15R at Logan International Airport (BOS) and slid into the waters of Boston Harbor at a speed of about 49 knots (kt). The nose section of the fuselage broke off. Two of the 212 passengers could not be found and were presumed dead. [1] A similar overrun accident at JFK occurred on February 28, 1984, when another DC-10-30 aircraft overran Runway 4R after landing and plunged into Thurston Basin, an arm of Jamaica Bay. There were no fatalities, but the aircraft sustained serious damage on impact, as shown in figure 1. The National Transportation Safety Board (NTSB) accident report NTSB/AAR-84/15 [2] indicated that the DC-10 exited the runway at approximately 75 kt (86 miles per hour (mph)) and entered Thurston Basin, 600 feet (ft) beyond the end of the runway, while still moving at approximately 38 kt (44 mph).

On April 16, 1984, the NTSB issued Safety Recommendation A-84-37 [3] to the FAA to "Initiate research and development activities to establish the feasibility of soft-ground aircraft arresting systems and promulgate a design standard, if the systems are found to be practical." This Safety Recommendation makes a specific reference to the accident at BOS.

Figure 1. The DC-10 Overrun on JFK Runway 4R

---

[1] ESCO is now known as Zodiac Arresting Systems America (ZASA).

In 1986, the FAA launched a research program to develop an engineered solution for airports with inadequate real estate for standard runway safety areas (RSAs). A typical RSA is shown in figure 2. Many airports that were built before the RSA became a standard do not have adequate space due to adjacent bodies of water, large drop-offs, railroads, highways, or other obstructions. For example, the RSAs for both the BOS and JFK accidents were limited by adjacent bodies of water. Remediation or relocation of these impediments are often cost prohibitive or environmentally unacceptable.
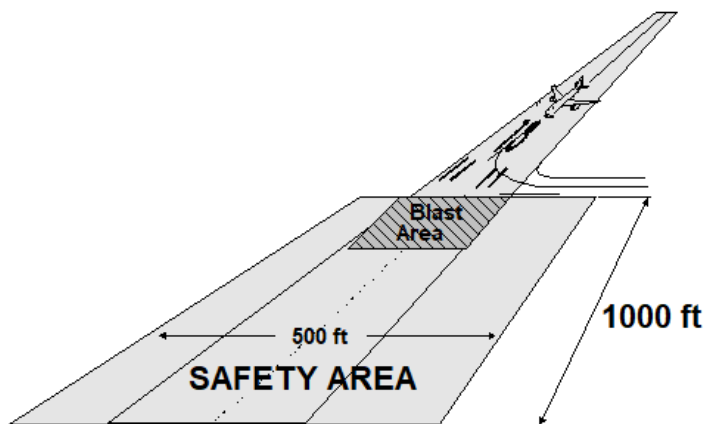
Figure 2. Typical RSA [4]

The initial goal of the research program was to establish the feasibility of placing soft, crushable materials in the RSA to safely stop aircraft that are not able to stop on the runway. One of these materials was phenolic foam, which is a rigid foam board insulation product typically used in roof systems. Soft-ground arresting systems (SGASs) relied on the principle that the aircraft tires will deform or crush the soft material, and the resultant drag forces will safely and predictably decelerate the aircraft. From 1986 through 1993, the FAA conducted extensive research and testing on SGASs. FAA report DOT/FAA/CT-93/80 [4] details the research conducted during this time and concluded the following:

- A mathematical model representing the tire/phenolic foam interface can accurately predict landing gear loads, deceleration, and speed decay of aircraft during simulated overruns.

- A Boeing 727 (B-727) aircraft traveling up to 60 kt can be safely stopped within a bed of phenolic foam in less than 1000 ft.

- Aircraft rescue and fire fighting (ARFF) equipment and personnel were able to maneuver without difficulty on the phenolic foam bed following an aircraft arrestment.

- An aircraft can be extracted from the phenolic foam bed without further damage to the aircraft.

- The phenolic foam bed can be repaired following an aircraft arrestment. [4]

By 1993, the FAA had established the feasibility of SGASs. However, there remained a challenge with the second part of NTSB Safety Recommendation A-84-37 that states, "…promulgate a design standard, if the systems are found to be practical" [3]. The phenolic foam proved adequate for testing purposes but was deemed impractical for operational use. The foam displayed significant elastic behavior, evidenced by rebound forces on the aft side of the tires, and did not have adequate stopping capability for operational use. There were also concerns regarding durability and material behavior in a post-crash fire scenario. Arrestor system materials with higher energy-absorbing characteristics and more durable physical properties were needed.

3. COLLABORATIVE PARTNERSHIPS.

In 1994, the FAA resumed their SGAS research program with the goals of (1) developing a more effective system, (2) demonstrating a prototype, and (3) creating a standard that would provide industry with guidelines for the design, installation, and maintenance of an SGAS.

These three goals aligned with the respective capabilities and needs of ESCO, the PANY&NJ, and the FAA. In 1994, ESCO was a world leader in military aircraft arresting systems, and the company was exploring an expansion into the civil aircraft arresting market. The PANY&NJ had been studying the use of SGAS since 1988 to protect aircraft in the event of another overrun at JFK. The FAA had an objective to develop a standard for SGAS, and they had full-scale aircraft testing capabilities at the William J. Hughes Technical Center (WJHTC) in Atlantic City, New Jersey.

3.1 PARTNERSHIP WITH INDUSTRY.

By 1993, the validated SGAS mathematical model could predict aircraft gear loads and stopping distances for a number of overrun scenarios. However, the FAA had neither the resources to advance the technology nor the mission to commercialize soft ground; industry had both.

FAA Airport Technology Research and Development Branch (ATRD) representatives at the WJHTC established a Cooperative Research and Development Agreement (CRDA) with ESCO to develop a practical aircraft arrestor system. CRDA 94-CRDA-0065 was signed on September 7, 1994. The terms of the CRDA established the obligations and expected benefits for each party. In summary, the FAA agreed to provide a testing venue at the WJHTC, an instrumented B-727 test aircraft, and all necessary engineering and technical support to conduct a series of validation tests and full-scale arrestments. ESCO agreed to provide all resources necessary to develop arresting materials and to design and install full SGASs.

Specific objectives included the following:

- Validate the mathematical model using cement-based arresting materials.
- Develop practical installation details for the placement of a cement-based arrestor system.
- Monitor the durability of a cement-based system in an airport environment.
- Test new materials as soft ground arrestors.
- Develop new and/or improved methods for weather-resistant soft-ground materials.

3.2 PARTNERSHIP WITH PANY&NJ.

The FAA and PANY&NJ partnered to provide an engineered solution to the nonstandard safety overrun area for JFK Runway 4R and use the prototype system as a way of developing practical installation and maintenance details. This information would enable the FAA to develop a national standard for the design and installation of SGASs, later called Engineered Materials Arresting Systems (EMASs).

4. RESEARCH ACTIVITY TIMELINE.

FAA SGAS research activities resumed in 1994 with the signing of the CRDA with ESCO. Table 1 identifies the timeframe for significant research activities and associated milestones. It also identifies the related location of the corresponding narrative in the report.

Table 1. Research Activity and Milestone Timeline

Date	Research Activity	Results and Milestone	Report Section
September 1994	None	FAA established CRDA with ESCO.	3.1
September through November 1994	ESCO and FAA constructed and tested foamcrete arrestor bed.	A full-scale test with B-727 demonstrated improved stopping ability of foamcrete compared to phenolic foam.	5.1
November 17, 1994	B-727 taxied through foamcrete test bed.	Foamcrete displayed improved stopping ability, but it lacked uniformity. Compressive strength and density were unacceptable.	5.1.1
March 1995	FAA developed mathematical model software, ARRESTOR	Simplified the mathematical model for use on desktop application (Microsoft® Windows™ 3.1).	5.2
June 1995	Cellular cement nose gear test	Cellular cement blocks were produced with uniform strength and density appropriate for the intended application at JFK.	5.3
September 1995	None	Preliminary design of prototype arrestor system for JFK.	5.4
May 1996	Full-scale arrest of B-727 in cellular cement test bed	Validated mathematical model, exceeded performance expectations, and demonstrated the need for refined construction methods and weatherproofing.	5.5.2
July 1996	ARFF vehicle maneuverability tests	P-19 vehicle could enter the cellular cement bed and maneuver without difficulty.	5.6.1

Table 1. Research Activity and Milestone Timeline (Continued)

Date	Research Activity	Results and Milestone	Report Section
April 1997	Fire tests at Tyndall Air Force Base	A dual-agent technique using both aqueous film forming foam and a dry chemical was necessary to extinguish the fire in a post-crash scenario.	5.6.2
Fall 1996	None	PANY&NJ and ESCO prepared final design for EMAS prototype for JFK Runway 4R.	6.1
November 1996	None	PANY&NJ and ESCO completed EMAS prototype at JFK.	6.2
August through November 1996	Instrument landing system (ILS) interference testing for proposed EMAS at JFK	No significant effect on the localizer signal during or after placement of a cellular cement bed.	6.2.1.2.1
September 1997	Cold-weather testing at WJHTC	EMAS block acted as a superior thermal insulator.	7.1
November 1997	Cold-weather testing at United States (U.S.) Army Corps of Engineers Cold Regions Research and Engineering Laboratory	The interior portions of the blocks responded slowly to ambient temperature changes. No significant or measurable dislocations were observed at either individual blocks or with the joints between blocks.	7.2
Spring 1998	None	PANY&NJ prepared a design for an EMAS installations to serve LGA Runways 13 and 22.	8
July 1998	ILS Interference testing for proposed EMAS at LGA	No significant effect on signals from both localizers serving LGA Runway 22 from EMAS installation.	8.1
August 21, 1998	None	FAA publishes Advisory Circular (AC) 150/5220-22, "Engineered Materials Arresting System (EMAS) for Aircraft Overruns*"	12
August - September 1998	None	PANY&NJ installed EMAS for LGA Runway 22. Jet blast damage was immediate.	8.2
May 1999	None	Saab® 340B overrun at JFK (no fatalities)	11.1
August 1999	None	LGA Runway 22 EMAS is removed due to jet blast damage.	8.2

5

Table 1. Research Activity and Milestone Timeline (Continued)

Date	Research Activity	Results and Milestone	Report Section
May 2000	FAA and ESCO funded University of Dayton Research Institute (UDRI) jet blast mapping study at LGA	UDRI developed a computer program that enabled jet blast simulation studies at the WJHTC Airflow Induction Test Facility wind tunnel.	9.1
September 2000	UDRI acquired jet blast condition behind the WJHTC Airflow Induction Test Facility.	Data enabled FAA to replicate accelerated jet blast exposure at LGA.	9.2.2
November 2000	FAA tested ESCO designed and installed jet blast resistant (JBR) EMAS at WJHTC wind tunnel.	FAA exposed the test bed to equivalent to 1 year of LGA jet blast at 75 ft from the runway. JBR system resisted blast forces without displacement or damage.	9.2.4
December 2000	None	ESCO installed JBR demo bed at LGA.	9.3
February 2001	FAA inspected LGA demo bed.	No evidence of displacement or damage after 2 months of exposure.	9.3
May 2001 through April 2002	FAA resumed testing JBR EMAS behind WJHTC wind tunnel.	Equivalent jet blast testing at 35-ft setback yields no apparent damage to EMAS.	9.4
May 2001	FAA and ESCO conducted small-wheel penetration tests at WJHTC.	JBR coating would likely affect computer prediction accuracy for aircraft less than 25,000 lb and to a lesser degree with heavier aircraft.	9.6
June 2002	None	PANY&NJ removed LGA demo bed after 18-month exposure to jet blast.	9.5
Fall/Winter 2002	None	PANY&NY and ESCO installed second demo bed for observation. Remained in place until 2004.	9.5
July through September 2002	None	PANY&NJ replaced prototype EMAS at JFK with 200-ft-wide JBR EMAS.	10
May 2003	None	MD-11F overrun at JFK (no fatalities)	11.2

* "Engineered Materials Arresting Systems (EMAS) for Aircraft Overruns," FAA AC 150/5220-22 [5]

5. DEVELOPMENT OF CELLULAR CEMENT AIRCRAFT ARRESTOR SYSTEM.

The SGAS validation tests in 1991 and full-scale arrest demonstrations in 1993 used phenolic foam as the arresting material. This material had several physical characteristics that were ideally suited to validation testing. The foam, which resembles rigid roof insulation, had stable density and compressive strength, and was readily available at commercial establishments. However, due to the elasticity of phenolic foam, it did not have adequate stopping ability for operational use. Consensus at the time favored the use of low-density, low-strength foamed concrete as an arresting material. This material (comprised of Portland cement, water, and foam) is commonly used as construction fill material or as lightweight structural flooring. The cured material will not rebound when crushed, and it is nonflammable.

5.1 FOAMED CONCRETE TEST BED AT THE WJHTC.

In the fall of 1994, ESCO designed and hired a cement producer to construct a foamed concrete bed at the WJHTC. The cast-in-place test bed measured 192 ft long by 40 ft wide and tapered to a maximum height of 12 inches (in.). The lead-in ramp was 80 ft long, the 12-in.-high plateau was 40 ft long, and the exit ramp was 72 ft long. The test plan called for the FAA's instrumented B-727 (formerly N-46 and then called Ground Test Vehicle 1 or GTV-1) [2] to taxi through the bed with an entry speed of 35 kt (40 mph) with engines set to idle thrust and flaps at 15 degrees. The thrust and flap settings offset each other to simulate a coasting scenario. Figure 3 shows the B-727 in the foamed concrete test bed at the WJHTC.

Figure 3. The FAA B-727 Aircraft Entering Foamed Concrete Test Bed at the WJHTC

After placement and curing, compressive strength tests results indicated that the test bed had nonuniform strength and density. Mathematical modeling predictions, which rely on consistent physical characteristics, were uncertain. Original test objectives changed from mathematical model validation to material mode of failure observation and rut depth analysis. Secondary

---

[2] The FAA B-727 aircraft was used for ground tests only and not fit for flight.

7

objectives included test methodology and quality control measures to ensure uniform strength of foamed cement materials in future applications.

5.1.1 Test Results.

On November 17, 1994, the FAA's instrumented B-727 aircraft taxied into the test bed without braking or use of reverse thrust. Onboard data acquisition systems recorded triaxial decelerations at the aircraft center of gravity and cockpit, nose gear loads (vertical, drag, and side), speed decay, and time-coded video of nose gear tire interaction with the test bed material.

Measured values included:

- Aircraft weight = 98,000 lb; 33% mean aerodynamic chord (MAC); 4,300 lb at nose gear

- Maximum nose gear vertical load approximately 20,000 lb (working load limit = 44,000 lb)

- Maximum nose gear drag shear load approximately 3,800 lb (working load limit = 25,000 lb)

- Maximum nose gear side load approximately 4,000 lb (working load limit = 15,000 lb)

- Maximum longitudinal deceleration approximately 0.6 g's.

- B-727 entered bed at 42 mph and exited bed at 17 mph.

Rut depths measurements indicated a full compressive failure of the foamed concreate under the load of the main gear.

5.1.2 Test Findings.

General consensus between the FAA, ESCO, and PANY&NJ personnel was that the foamed concrete displayed improved stopping ability compared to phenolic foam. However, lack of uniformity with regards to cured compressive strength and density was unacceptable. Figure 4 shows the nonuniform mode of failure, which indicates a nonhomogeneous material.

Figure 4. Foamed Concrete Test Bed Mode of Failure

5.2 MATHEMATICAL MODEL DESIGN PROGRAM.

In March 1995, the FAA developed a software application, ARRESTOR[3], to simplify the mathematical model to an interactive desktop environment. ARRESTOR was designed to determine the landing gear loads and airframe dynamic response to both the soft ground and the runway surface roughness. The application computed the aircraft wheel rut depths during landing and takeoff so that surface rehabilitation maintenance can be estimated, and included a model for soil deformation that gave fairly accurate levels of soil or asphalt rutting under aircraft wheel loads. ARRESTOR is outlined in figure 5, where μ is the coefficient of friction and CG is the center of gravity of the aircraft. ARRESTOR was specifically designed for DC-9, DC-10, B-707, B-727-100, B-727-200, and B-747 aircraft due to aircraft data availability from the aircraft manufacturers. After the FAA developed the initial ARRESTOR computer model code, further changes to the code were made as part of the collaborative effort to complete the test and evaluation. ESCO's computer model has been further developed and refined since the initial testing was completed.

---

[3] ARRESTOR was compatible only with a Windows 3.1 operation system.
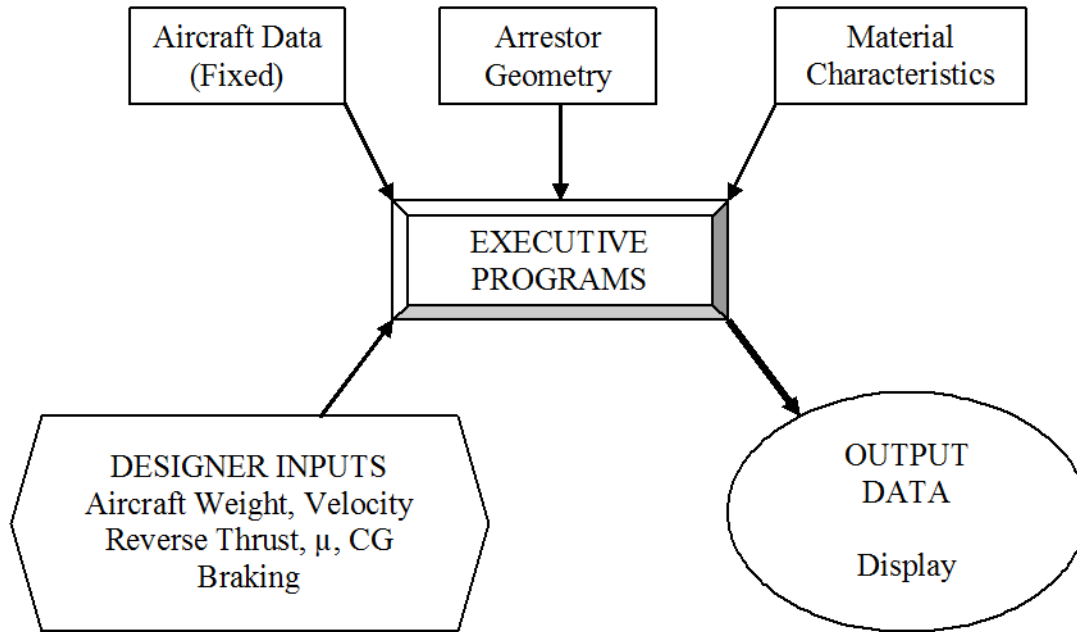
Figure 5. Schematic of ARRESTOR Design Application

5.3 CELLULAR CEMENT NOSE GEAR TEST.

ESCO embarked on a worldwide search for commercially available products that could meet the stringent physical parameters suitable for model validation. These efforts were not successful, and ESCO began an in-house development of a proprietary cellular cement material.

When ESCO realized that commercially available cellular cement products could not provide a product with uniform material strength and density, the company established a laboratory and production facility at a plant near Philadelphia, Pennsylvania, where homogeneous cement-based arrestor system material could be produced. ESCO laboratory tests indicated that uniform compressive strengths between 60 and 80 pounds per square inch (± 5 psi) and low density (20 pounds per cubic foot) could be achieved with careful selection of raw materials and proper mixing. These strengths and density were consistent with the mathematical model input parameters used in the design for the prototype arrestor system for JFK. ESCO elected to identify this new material as cellular cement.

In June 1995, ESCO installed a cellular cement bed on the WJHTC's aircraft apron; the test was intended to be for a nose gear only. The cellular cement blocks were mixed, cast, cured at the ESCO plant, and shipped to the WJHTC. Test objectives included the following:

- Calibration of the mathematical model for cellular cement material
- Evaluation of material uniformity
- Evaluation of anchorage system

5.3.1 Test Plan Specifics.

The specifics for the cellular cement nose gear test plan included the following:

- Test Date: June 26, 1995
- Location: FAA WJHTC aircraft apron
- Bed Size: 10 ft wide by 80 ft long by 15 in. deep with phenolic foam entry and exit ramps (96 ft and 64 ft long, respectively). Bed geometry and strength was simulated in the mathematical model to minimize risk to personnel and equipment.

5.3.1.1 Bed Material.

Details for the bed material used for the cellular cement nose gear test included the following:

- 72 blocks of low-density cellular concrete (approximately 20 per cubic ft)
- Block dimensions were 40 in. by 40 in. by 15 in. deep.
- Blocks were adhered to the concrete ramp with cement grout.

5.3.1.2 Test Aircraft.

Descriptions of the test aircraft used in the cellular cement nose gear test included the following:

- B-727
- 135,000 lb gross weight
- 20% MAC
- Nose gear load = 12,300 lb
- Only the nose gear entered the bed; the main gear straddled the bed.
- Number 2 engine only was set at idle for taxi through test bed.
- Flaps were set at 15 degrees with no brakes applied.

5.3.1.3 Instrumentation.

The instruments were used in the cellular cement nose gear test included the following:

- Triaxial accelerometer at cockpit and CG
- Distance and speed sensors at nose gear
- Strain gauges on all gear to measure vertical, side, and drag loads

5.3.2 Test Results.

The results of the cellular cement nose gear test included the following:

- The aircraft taxied into bed at 40 mph with only the nose gear in cellular cement.

- Aircraft exited bed at 36 mph and taxied an additional 300 ft before stopping as planned.

- Pilots reported a smooth ride through the cellular cement.

- Measured rut depths were consistent with rut depths predicted by the mathematical model.

- Blocks adjacent to passage of nose gear remained intact.

- Measured vertical and drag loads were consistent with those predicted by the mathematical model.

5.3.3 Test Findings.

The findings of the cellular cement nose gear test included the following:

- Cellular cement blocks can be produced with uniform strength and density.

- The strength of the cellular cement used in the nose gear test was appropriate for the intended application at a proposed arrestor system at JFK.

- Anchoring cellular cement blocks to a solid substrate is practical.

Figure 6 shows the path of the B-727's nose gear through the cellular cement blocks, including the phenolic foam lead-in ramp.

Figure 6. The B-727 Nose Gear Ruts

12

5.4 DESIGN OF PROTOTYPE ARRESTOR SYSTEM FOR JFK.

In September 1995, coincident with the development of the ARRESTOR program, the FAA and
PANY&NJ personnel completed a preliminary design for an arrestor system for JFK Runway
4R. The arrestor system was designed to safely stop aircraft with gross weights of 100,000 to
820,000 lb with runway exit speeds ranging from 80 kt for Design Group (DG) III aircraft and
60 kt for DG V aircraft. These weights and speed ranges were established after a review of
accidents reported by the NTSB and the International Civil Aircraft Organization (ICAO). Other
design goals for the arrestor system included:

- Long service life with low maintenance
- Uninhibited access by ARFF
- Simple repair after an aircraft overrun
- No interference with normal airport or aircraft operations
- All-weather capability
- Unattractiveness to wildlife
- Not combustible

The preliminary design was prepared by Robert F. Cook.[4] The design, shown in figure 7, depicts
an arrestor system 400 ft long by 150 ft wide and tapered up to a plateau 30 in. high. Figure 7
shows the initial prototype arrestor system layout. The design resulted from multiple overrun
simulations for a PANY&NJ-specified fleet mix: DC-9, B-707, B-727-100, B-727-200, DC-10,
and B-747. The simulations indicated the arrestor system as an effective means of safely
stopping overrunning aircraft, especially in wet and icy runway surface conditions. The design
used information from three previous reports, one published by the FAA [4] and two authored by
Robert F. Cook [6 and 7].

---

[4] Mr. Robert F. Cook was instrumental in early development of SGASs from the 1980s with the University of
Dayton and the PANY&NJ.
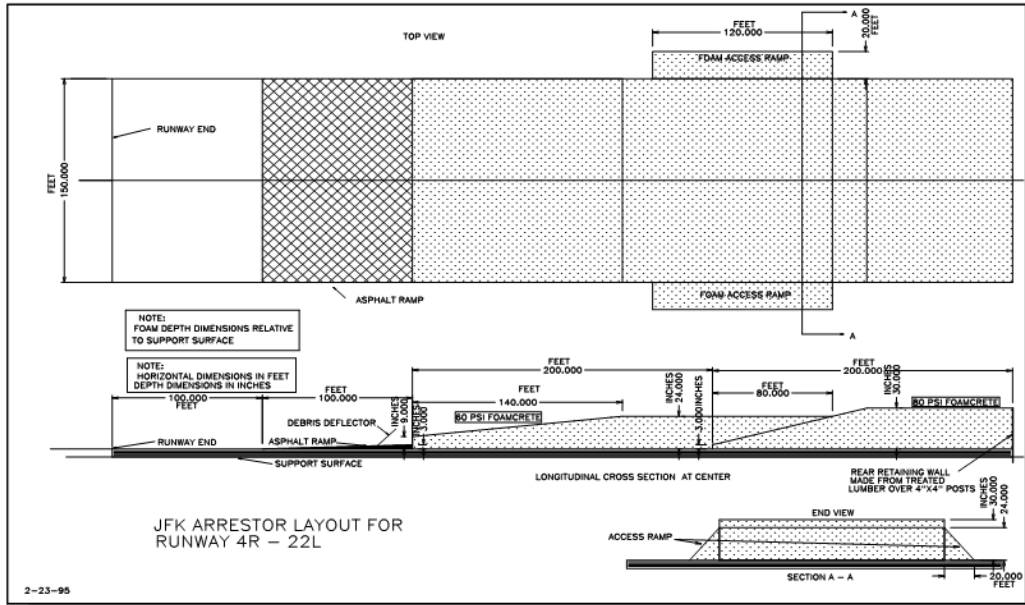
Figure 7. Preliminary Design for Prototype Arrestor System for JFK Runway 4R

The designers assumed that the system would be comprised of a soft cement-based material called foamcrete, a mixture of Portland cement, an air-entraining foaming agent, and water. In the report, further refinements and validation of both material and mathematical modeling were also assumed.

5.5 FULL-SCALE ARREST IN CELLULAR CEMENT.

The success of nose gear test in June 1995 convinced ESCO and the FAA that cellular cement blocks could be produced to a uniform design strength and density. A full-scale arrest of a B-727 in a bed of cellular cement was considered the next logical step prior to prototype deployment at JFK. Consequently, ESCO and the FAA launched a joint effort under the terms of the active CRDA to conduct this demonstration at the WJHTC.

By October 1995, ESCO and the FAA acquired necessary permits and approvals to assemble and operate a cellular cement production facility at the WJHTC, as shown in figure 8. ESCO provided all the material, equipment, and manpower necessary to cast, cure, and install the cellular cement blocks required to conduct a full-scale arrest of the B-727.

14

Figure 8. The ESCO Cellular Cement Block Manufacturing Plant at WJHTC

5.5.1 Test Objectives.

The objectives of the full-scale arrest test were as follows:

- Validate the mathematical model to predict aircraft gear loads, deceleration, and stopping distance in a cellular cement environment.

- Demonstrate the constructability of cellular cement arrestor systems in an airport environment.

5.5.2 Test Plan Specifics.

The final design of the test bed required adequate space to accelerate the B-727 to 55 kt, stabilize velocity, decelerate the aircraft to a safe stop within the arrestor bed, and provide sufficient space for the crew to brake the aircraft to safe stop if the arrestor bed failed to function.

The resultant test bed design, shown in figure 9, measured 376 ft long, 40 ft wide, and with tapered entry and exit ramps to a maximum depth of 25 in.

- Test date: May 21, 1996

- Location: FAA WJHTC Aircraft Apron

- Bed Size: 300 ft long by 40 ft wide by 25 in. deep, with phenolic foam entry and exit ramps (60 ft and 16 ft long, respectively).
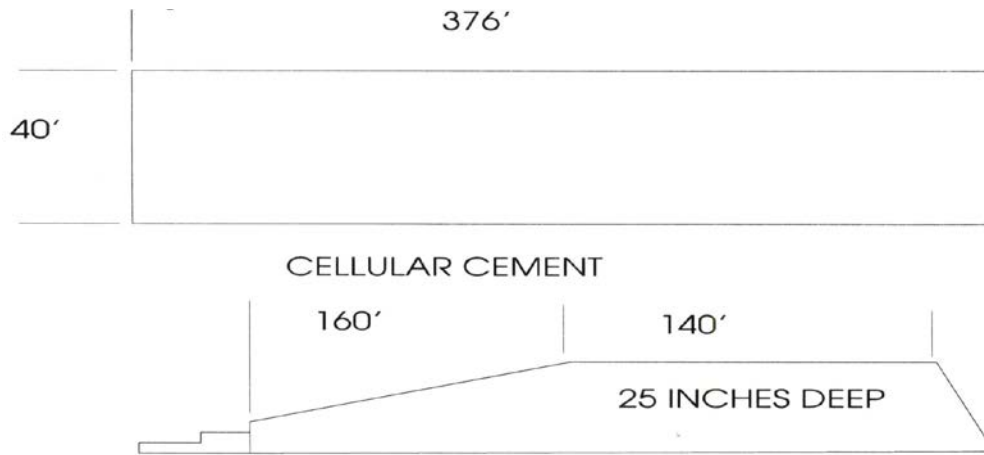
Figure 9. Cellular Cement Test Bed on FAA WJHTC Aircraft Apron

5.5.2.1 Test Bed Material.

Test bed material for the full-scale arrest test included the following:

- Cellular cement blocks 4 ft wide by 8 ft long varying in height up to 24 in.

- A 1-in.-thick cement slurry coat (approximately 120 psi) was applied to the entire top of the test bed.

- Three coats of an elastomeric paint were applied to seal the arrestor from moisture.

- Blocks adhered to concrete ramp with cement grout.

5.5.2.2 Test Aircraft.

Details of the test aircraft for the full-scale arrest test are as follows:

- B-727
- 131,600 lb gross weight
- 23.8% MAC
- Flaps at 15 degrees
- Engines at idle after entering test bed
- No brakes or reverse thrust

5.5.2.3 Instrumentation and Video Documentation.

Aircraft instrumentation included the following:

- Triaxial accelerometer at cockpit and aircraft center of gravity
- Distance and speed sensors at nose gear
- Strain gauges on all gear to measure vertical, side, and drag loads

Video documentation equipment included:

- Nose gear coupled to data acquisition

- High-speed film camera on left main gear

- Video camera on cabin passengers

- Video camera on cockpit

- Eleven additional cameras (video, high-speed film, and stills) with exterior perspectives on test, including two from a helicopter

5.5.3 Test Results.

Figure 10 shows the B-727 entering the test bed at 55 kt.

Figure 10. The B-727 Entering Cellular Cement Test Bed at 55 kt

As the aircraft entered the test bed, the nose gear lifted briefly and only skimmed the top of the bed. The highlighted area in figure 11 shows where this event occurred. As the nose gear reentered the bed, the nose gear structure rotated aft, and the nose wheel and strut separated from the aircraft. Despite the loss of the nose gear, the aircraft maintained a straight trajectory.

Figure 11. Area Highlighted Shows Where Nose Gear Lifted From Test Bed

The aircraft came to a stop 278 ft into the test bed. Figure 12 shows the aircraft after it was arrested. The detached nose gear is circled in yellow.

Figure 12. The B-727 Stopped 278 ft Into the Cellular Cement Test Bed

Post-test analysis indicated that the aircraft's main gear loads did not exceed the landing gear's design limits. Peak deceleration did not exceed 1.0 g, and the aircraft stopped approximately

30 ft short of the predicted location. The unexpected nose gear failure was attributed to corrosion cracks in one of the landing gear support fittings; which was not evident prior to the test.

5.5.4 Comparison With Mathematical Model Predictions.

Comparison of mathematical model simulations and measured results for the main gear only are shown in figures 13 and 14. These graphs compare mathematical model predictions against loads and accelerations measured during the test. Comparisons between the main gear drag loads and main gear vertical loads are shown in figures 13 and 14, respectively.
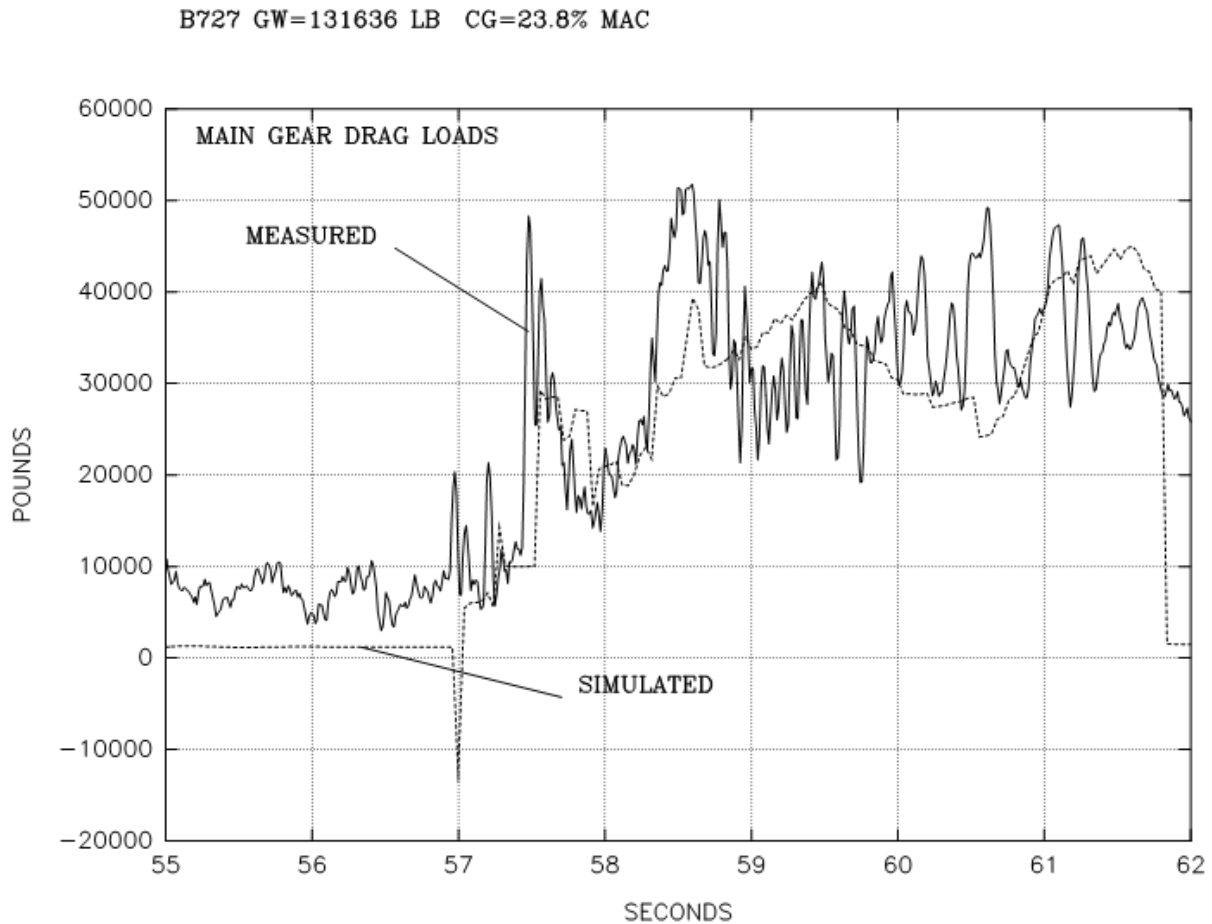
Figure 13. Comparison of Measured and Simulated Main Gear Drag Loads

B727 GW=131636 LB CG=23.8% MAC
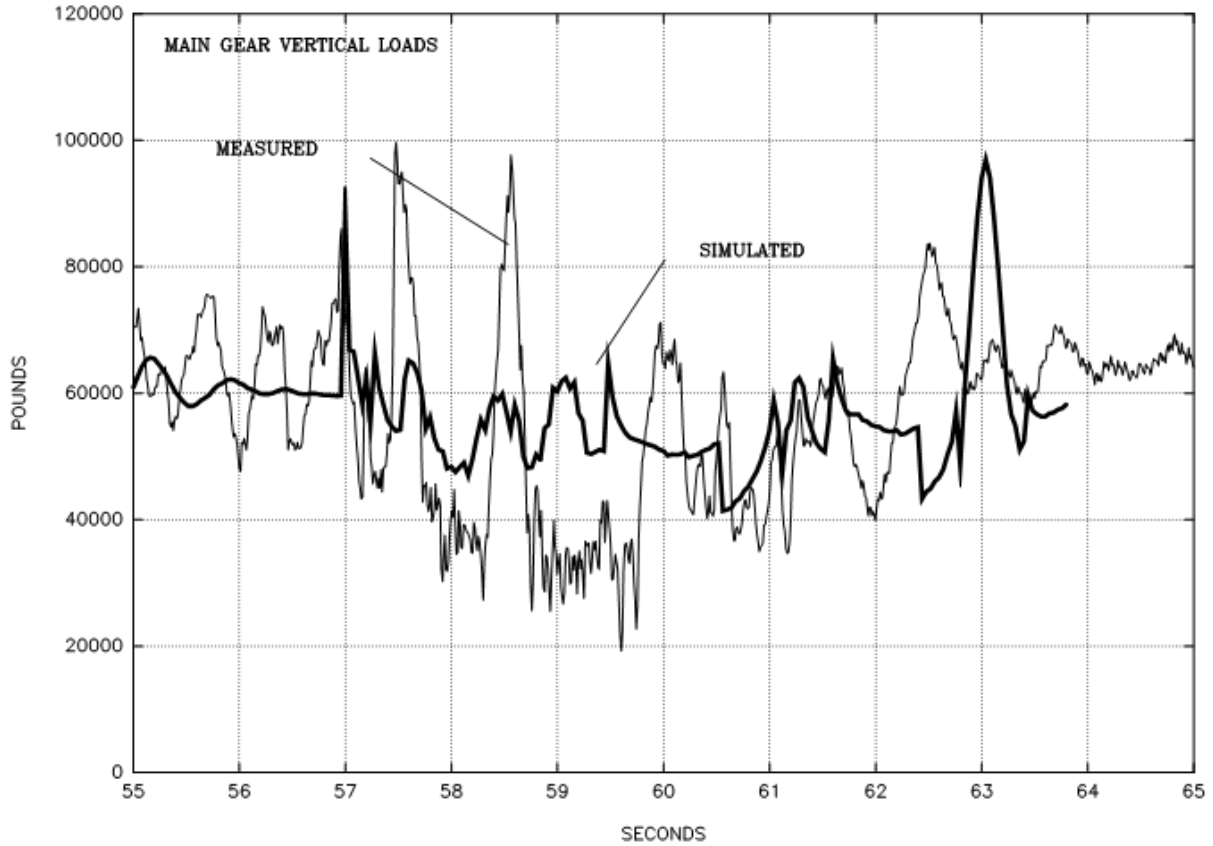
Figure 14. Comparison of Measured and Simulated Main Gear Vertical Loads

The measured and simulated CG longitudinal acceleration data in figure 15 compared very well until the nose gear failure. The measured acceleration shows a very high acceleration at 58.2 seconds, indicating a very large forward force. The source of the force was not determined but coincided with the time that the nose gear failed.

20

B727 GW=131636 LB CG=23.8% MAC

CG LONGITUDINAL ACCELERATION

MEASURED
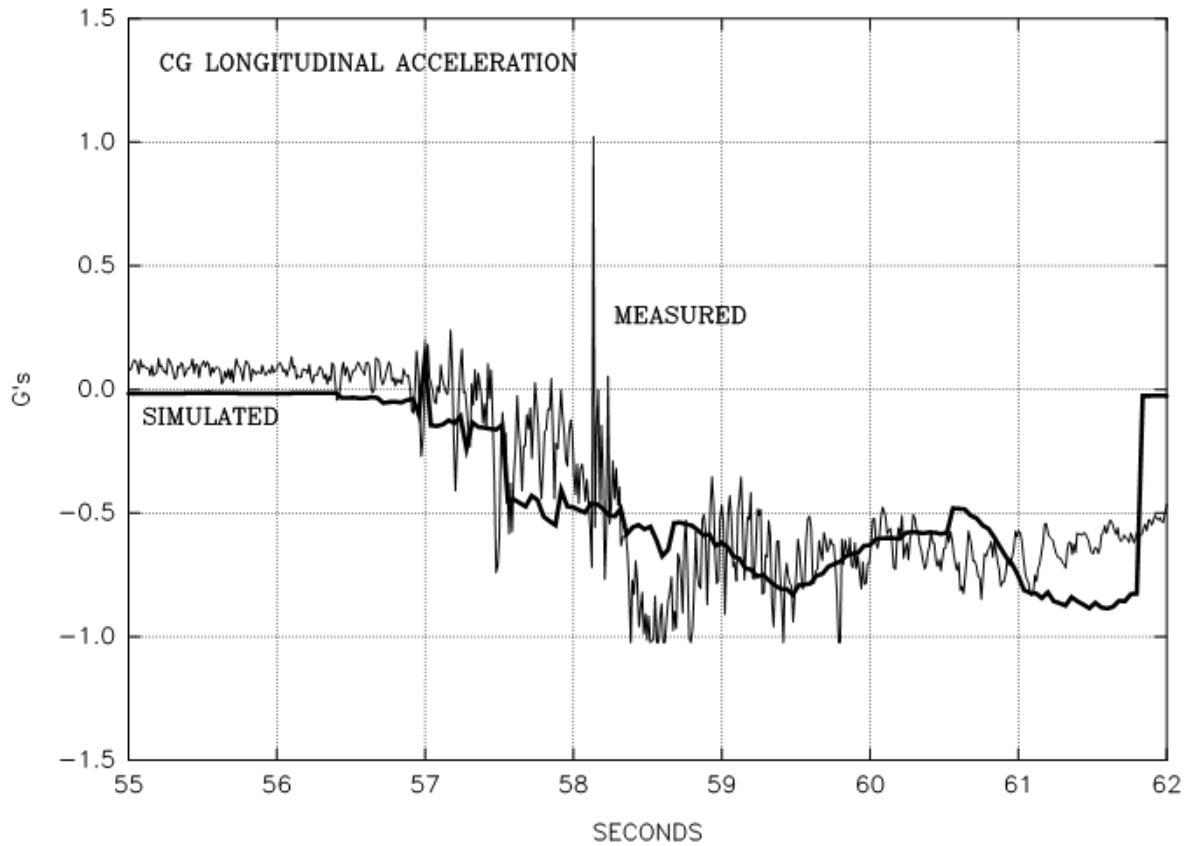
SIMULATED

Figure 15. Comparison of Measured and Simulated Longitudinal Accelerations

The curves in figure 16 were obtained by dividing the measured main gear drag loads by the vertical main gear loads, the definition of the coefficient of friction or braking ability. The statistical average of the drag ratios was 0.6, as measured and predicted by the simulation.

21
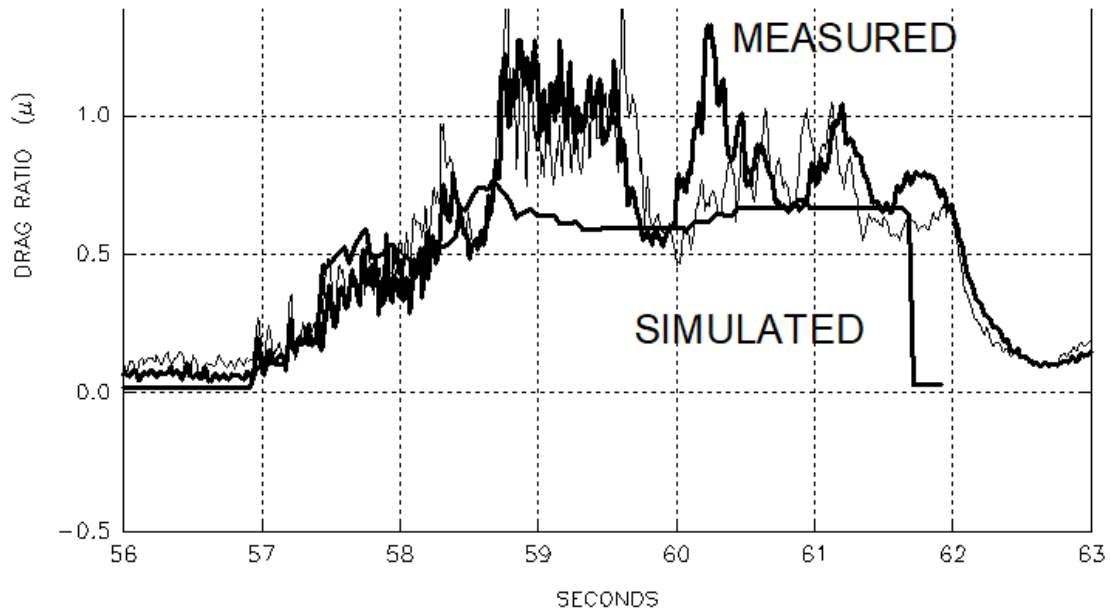
Figure 16. Equivalent Braking Ability in Terms of Mu as a Function of Time

5.5.5 Rut Depths.

Figures 17 and 18 show an FAA research engineer examining the condition of the right main gear after the ruts were cleared of debris. These figures indicate a full depth compression of the cellular cement material.

Figure 17. Right Main Gear Inside the Cellular Cement Test Bed

22

Figure 18. Right Main Gear Material Mode of Failure are Examined

5.5.6 Test Findings.

The findings of the full-scale arrest test were as follows:

- The stopping distance of 278 ft was close to the predicted value of 308 ft.

- The drag ratio, or equivalent braking ability, for the main gear equaled 0.6.

- Rut depth inspection indicated full comprehensive failure of the cellular cement material under the main gear.

- The cellular concrete material exceeded expectations in terms of performance as an arrestor.

- Construction methods related to uniform strength and weatherproofing required additional refinement.

- The PANY&NJ decided to move ahead with the prototype arrestor system installation at JFK as soon as practical.

5.6 POST-CRASH CONSIDERATIONS.

ESCO, the PANY&NJ, and the FAA shared a general interest and some concern regarding the mobility of rescue vehicles in the cellular cement material in the event of an overrun, especially

in a rutted and damaged condition. There was equal concern regarding the risks associated with a post-crash fire. ESCO and the FAA devised a series of demonstrations and tests to address these concerns.

5.6.1 The ARFF Vehicle Maneuverability.

By July 9, 1996, ESCO shortened the original test bed to a 40-ft-wide by 200-ft-long bed by removing the lead-in and exit ramps. The FAA arranged for the use of an Oshkosh Corporation® P-19 ARFF vehicle (gross weight 33,600 lb) provided by the South Jersey Transportation Authority. An extraction vehicle was on stand-by to assist if the test vehicle became immobilized during the test. The plan included numerous maneuverability scenarios. The objective of this test was to demonstrate the ability of an ARFF vehicle to attend to an aircraft in the event of a post-crash fire after an overrun into a damaged cellular cement arrestor bed.

ARFF personnel executed the following maneuvers:

1.   Test vehicle drove the full length of the bed while straddling the nose gear ruts. This allowed the vehicle to traverse undisturbed material.

2.   Test vehicle rode with one set of tires on bed and the other set on the ramp.

3.   Test vehicle rode with one set of tires in a main gear rut and one on undisturbed material.

4.   Test vehicle traversed the bed at a location 25 ft into bed at a height of 14 in., and again at a location of 60 ft into the bed at a height of 18 in.

5.   Test vehicle traversed the bed on a diagonal.

6.   Test vehicle backed through the bed and out again.

Videotape analysis and interviews with the test vehicle operator indicated that the P-19 ARFF vehicle could enter the arrestor bed and maneuver across the bed without difficulty. Figure 19 shows the P-19 ARFF vehicle traversing the arrestor bed on a diagonal.

Figure 19. The P-19 ARFF Vehicle Maneuvering in Arrestor Bed

5.6.2 Fire Tests at Tyndall Air Force Base.

In addition to the P-19 ARFF vehicle mobility tests, a series of medium-scale fire tests were conducted on the cellular cement blocks and debris with consideration that ARFF personnel may encounter a post-crash fire within a cellular cement arrestor system following an aircraft arrestment. The tests were designed to provide rescue personnel with information regarding firefighting techniques within an arrestor system.

The Air Force Material Command at the Wright Laboratory Flight Dynamics Directorate, the ATRD, and the PANY&NJ jointly developed a test plan to be executed at the live fire test facility at Tyndall Air Force Base, Florida. The test protocol followed the experimental and analytical program used by the U.S. Air Force and the FAA in 1996 to investigate the adequacy of the Theoretical and Practical Fire Area (TCA/PCA) methodology equation for determining minimum agent quantities and flow rates published in the National Fire Protection Association (NFPA) 403 [8].

In April 1997, four medium-scale fire tests were performed by Air Force Research Laboratory's Fire Research Group at the fire test facility located at Tyndall Air Force Base, Florida. The tests conducted within a 30-ft-diameter containment steel ring with 6-in. sides. Two cellular cement blocks, each measuring 8 ft long by 4 ft wide by 2 ft high, were placed in the center steel ring and manually crushed to simulate broken cellular cement from an aircraft arrestment. Each test consisted of dousing the cellular cement in 100 gallons of fuel and igniting a fire. The test objectives were to measure the time and amounts of firefighting agent necessary to extinguish a fire in cellular cement. Figure 20 shows firefighters discharging agent during a fire test. After each test, the containment ring was cleared and another test was conducted using new cellular cement material.

25

Figure 20. Firefighters Discharging Extinguishing Agent

Video cameras recorded the fire tests from two perspectives, northerly and westerly views. The footage was timecoded and analyzed to provide extinguishment times and determine amounts of agents used. The westerly view faced the backs of the firefighters, and the northerly view faced right angles to the firefighters. The northerly view provided better visual information regarding flame extinguishment.

5.6.2.1 Fire Test 1.

Test 1 used 87 octane gasoline. Once the ring was fully involved with fire, firefighters used a 95 gallons-per-minute hand line nozzle discharging aqueous film forming foam (AFFF) (3% concentrate) to attempt to extinguish the fire. Approximately 700 gallons of AFFF was discharged for 7 minutes and 14 seconds. The AFFF extinguished approximately 95% of the fire within 6 minutes; however, small flames persisted in the large debris pieces. It was then decided on the next test to discharge dry chemical powder (Purple K) simultaneous with AFFF. This technique is more commonly used when attempting to extinguish running fuel fires.

5.6.2.2 Fire Test 2.

Test 2 used 87 octane gasoline. Firefighters again used AFFF along with a simultaneous dry chemical discharge of 5 to 7 pounds per second from the same hand line nozzle. Approximately 380 gallons of AFFF and 450 lb of dry chemical were discharged in 4 minutes to extinguish the fire.

<u>5.6.2.3 Fire Test 3</u>.

Test 3 used JP-8 jet fuel. JP-8 is a more realistic scenario airport firefighters would encounter for commercial aircraft. Firefighters used the same technique as in Test 2 with an AFFF and dry chemical simultaneous discharge. Approximately 60 gallons of AFFF and 90 lb of dry chemical were discharged in 31 seconds to extinguish the fire.

<u>5.6.2.4 Fire Test 4</u>.

Test 4 used JP-8 jet fuel. Firefighters used the same technique as previous tests. Approximately 52 gallons of AFFF and 96 lb of dry chemical were discharged in 31 seconds to extinguish the fire.

<u>5.6.2.5 Fire Test Results</u>.

Fire test results indicate that in the event of a post-crash fire, ARFF personnel would encounter a debris field that requires a dual-agent technique using both AFFF and a dry chemical to extinguish the fire. Gasoline fires are more difficult to extinguish due to the cellular cement absorbing the fuel similar to what is experienced in a loose sand environment. The fire was reduced and immediately knocked down, but AFFF and dry chemical could not effectively seal or react to the fuel vapors causing a delay in total extinguishment. Cellular cement arrestor systems are primarily designed to safely stop commercial aircraft, and it is unlikely that a post-crash fire will involve gasoline. The fire tests fueled by JP-8 provided a more realistic firefighting environment. In each case, the use of AFFF and dry chemical completely extinguished the JP-8 fire in approximately 30 seconds.

<u>6. FINAL DESIGN AND INSTALLATION OF PROTOYPE ARRESTOR SYSTEM AT JFK</u>.

In the Fall of 1996, the FAA provided the preliminary design of the arrestor system (figure 7) to the PANY&NJ. The PANY&NJ then contracted ESCO to finalize the design after review and analysis of test results from the cellular cement tests conducted by the FAA in June 1995 and May 1996 (sections 5.4 and 5.5, respectively).

<u>6.1 THE ARRESTOR SYSTEM FINAL DESIGN</u>.

The final design called for an arrestor system 150 ft wide by 400 ft long and tapered to 30 in. deep. Once aircraft wheels enter into arresting materials, the modeled arrestor performance did not rely on any braking from the aircraft. Friction was not used in the model after the wheels entered into the arrestor system. The leading edge of the system was set back 100 ft from the end of the runway, as opposed to the preliminary design's 200-ft setback. This setback allowed airport maintenance and emergency personnel to drive behind the system and remain on a roadway. However, by moving the system closer to the runway, there was a subsequent loss of performance in the overrun simulations. This is because the mathematical modeling allowed for some aircraft braking on paved surfaces during overrun simulations. The design change reduced the predicted arrestor system performance by 5 to 7 kt on wet surfaces (effective braking coefficient = 0.35 g). For example, the original plan (200-ft setback) was designed to stop a DC-10 weighing 385,000 lb exiting the runway at 75 kt under wet runway conditions. In the

revised plan, the runway exit speed was reduced to 70 kt. Under icy conditions or with complete loss of brakes, there is no difference in predicted stopping distances or system performance.

The revised system included tapered access ramps for the full 400-ft length along both edges and eliminated the rigid structure at the rear.

The arrestor system used 4-ft by 8-ft cellular cement blocks of varying heights and with compressive strengths of either 60 or 80 psi. The 60 psi blocks comprised the forward section of the system with the 80 psi blocks at the back section. This blend of block strengths afforded maximum stopping power in the deeper bed sections while minimizing nose gear loads for smaller aircraft in the shallower forward section. A topcoat of 1/2-in.-thick, higher-strength, cast-in-place cement slurry covered the top of the blocks. This topcoat provided a substrate for application of an elastomeric coating to weatherproof the system. Although the topcoat could not be factored into the mathematical simulations, its thin profile and low strength (150 psi max) were regarded as insignificant during the passage of an aircraft tire.

ESCO elected to refer to their completed design as an EMAS. The intent was to differentiate their system from the generic SGAS term used by the FAA.

6.2 THE PROTOTYPE EMAS INSTALLATION.

The PANY&NJ funded the final design and installation of the EMAS prototype for JFK Runway 4R. They selected ESCO as the designer and supplier for all materials. The PANY&NJ selected a separate firm to provide construction management and a general contractor for installation. Figure 21 shows the construction at JFK with Thurston Basin and the localizer in the foreground. EMAS construction was completed in November 1996. The onset of cold weather precluded the application of an elastomeric coating to the top of the system until the spring of 1997. As a result, the cellular cement material was exposed to the elements and absorbed significant amounts of water. Planned moisture-monitoring efforts were judged to be of limited value and cancelled. The PANY&NJ and ESCO expended substantial effort to maintain the top surface of the arrestor system. It proved very difficult to adhere protective sealants to the surface.

Figure 21. The EMAS Prototype Serving JFK Runway 4R

6.2.1 Impact to Navigational Aids.

The PANY&NJ and the FAA considered impact to existing air navigation aids due to the placement of the EMAS in the safety overrun area at the departure end of JFK Runway 4R.

6.2.1.1 Impact to Approach Lights Serving JFK Runway 22L.

Several sets of approach lights serving JFK Runway 22L were situated within the footprint of the arrestor system. FAA Airway Facilities (AF) personnel adjusted the height of the lights at first light bar station (100 ft into the system) to clear the top of the arrestor system. The second set of approach lights (300 ft into the system) was high enough to clear the top of the system. The EMAS blocks were cut out around the five conduits supporting the lights. AF personnel also made a determination regarding the re-aiming of the lights, the need for a waiver on this height revision, and the need for a flight check at the end of construction.

6.2.1.2 Impact to Instrument Landing Systems.

The FAA Eastern Region AF engineers raised concerns during the planning stages of the JFK prototype EMAS regarding the effect of the cellular cement blocks on nearby instrument landing systems (ILSs). The critical areas for the Runway 4R Category III localizer and the JFK Runway 22L glide slope encompass the area designated for the prototype EMAS. Personnel from WJHTC and PANY&NJ arranged a series of actions to address these concerns:

29

- Perform ILS mathematical modeling on signal interference EMAS for JFK Runway 4R.
- Conduct flight tests during installation of the arrestor system.
- Perform ILS ground checks during installation of the arrestor system.
- Conduct FAA flight check at the completion of the arrestor system.
- Monitor pilot reports related to changes in the ILS performance.

6.2.1.2.1 The ILS Mathematical Modeling.

The events mentioned in the following sections occurred between August through November 1996. JFK Runway 4R was served by a Category IIIA localizer. The array is located approximately 486 ft from the outboard edge of the prototype EMAS. Members of the Navigation Branch at the WJHTC used two mathematical models to determine the effects on localizer performance: the Ohio State University Geometric Theory of Diffraction (OUGTD) model and the Ohio State University Near-Zone Basic Scattering Code (NZBSC33) model. Simulations were conducted for four different stages of construction with the provision that the outboard face of the arrestor system at each stage was symmetrical with respect to the localizer signal. The cellular cement was modeled in both dry and wet conditions. No significant signal errors were evident in the simulated approaches, and the modeled clearance structure was well within tolerance.

Appendix A includes a memorandum that details the results of the mathematical modeling.

6.2.1.2.2 Flight Tests.

WJHTC test pilots flew a specially instrumented Convair 580 along the localizer signal for JFK Runway 4R and measured signal strength and course width. A typical flight test included three straight-in approaches with the autopilot flying the localizer and glide path signals. Four arcs at prescribed elevation intercept followed the approaches. Onboard differential global positioning system (DGPS) and ILS recording equipment measured aircraft position and signal strength. Flight testing was conducted prior to construction to establish a baseline condition. Flight testing during construction and at completion of the prototype EMAS indicated no significant effect on the localizer signal.

6.2.1.2.3 The ILS Ground Checks.

FAA AF personnel at JFK conducted regular ground checks on the localizer signal throughout the installation of the prototype EMAS. No significant problems were reported.

6.2.1.2.4 Flight Checks.

Scheduled FAA flight checks did not identify any effect on ILS signals due to the presence of the prototype EMAS.

6.2.2 Findings.

Approach light fixtures that lie within the prototype EMAS footprint were elevated to provide visual clearance to the approach path. Mathematical model simulations, interim flight tests, ILS

ground checks, and FAA-certified flight checks indicated no significant effect on the localizer signal during or after placement of the EMAS. In addition, there were no reported adverse effects from pilots using the ILS systems serving JFK Runway 4R/22L from 1996 through 2003.

7. COLD-WEATHER TESTING.

The installation of the EMAS prototype at JFK in 1996 provided the FAA with an opportunity to monitor the impact of environmental stressors on the durability of the system in an operational setting. This monitoring effort consisted primarily of routine visual inspections by PANY&NJ operations personnel and site visits by ESCO and FAA personnel.

The FAA also conducted a series of accelerated temperature experiments on similar EMAS blocks under controlled conditions at the WJHTC and the Cold Regions Research and Engineering Laboratory (CRREL) in Hanover, New Hampshire. The work at the WJHTC examined temperature gradients inside arrestor blocks that occur as ambient conditions fall below the freezing point. Research at the CRREL Environmental Laboratory examined the effect of fluctuating temperatures (freeze and thaw) on a system of blocks. The primary focus of the CRREL tests was on the construction joints between the individual blocks.

7.1 ENVIRONMENTAL CHAMBER AT WJHTC.

On September 8, 1997, a 4-ft-high by 4-ft-wide by 27-in.-deep EMAS block was placed inside an environmental chamber constructed at the WJHTC. The block was instrumented with thermocouples set at 1, 2, 4, 8, and 13.5 in. below the surface. The temperature was set to 0 degrees Fahrenheit (0°F) from an ambient temperature of approximately 70°F. The following were the test results from the environmental chamber:

- The chamber reached 0°F within 3 hours.
- Material at 1 in. reached 32°F in 3 hours.
- Material at 2 in. reached 32°F in excess of 6 hours.
- Material at 4 in. reached 32°F in approximately 24 hours.
- Material at 8 in. reached a low of 46°F in 30 hours.
- Material at 13.5 in. (center of block) reached a low of 55°F at 46 hours.

7.2 ENVIRONMENTAL LABORATORY AT CRREL.

In November 1997, ESCO installed two EMAS test beds in the CRREL Environmental Laboratory. The test beds measured 24 ft long by 16 ft wide by 2 ft thick, and 8 ft square by 2 ft thick. The objective of the tests was to identify surface anomalies due to thermal loading on a cellular cement arrestor system. Figure 22 shows the sizes and placements of the test beds in the CRREL Environmental Laboratory. The number inside each block indicates either a 60- or 80-psi-strength material.

31

CRREL EMAS TEST BED

WOODEN SUPPORT TYPICAL

80	80	80	60	60	60
80	80	80	60	60	60
80	80	60/80	60	60	60
80	80	60/80	60	60	60

BARE BLOCKS

TOP COAT ONLY

ELASTOMERIC & TOP COAT

12'-0" 16'-0"

8'-0"

MINI TEST BED

1" NOMINAL TOP COAT & ELASTOMERIC

EMAS MATERIAL
SUPPORT BASE

EMAS SECTION TYPICAL

4'-0" TYPICAL

24'-0"

MAIN BED

CHAMBER WALL TYPICAL

FOAM INSULATION BOARD TYPICAL

MSC 3 DEC 97
NO SCALE
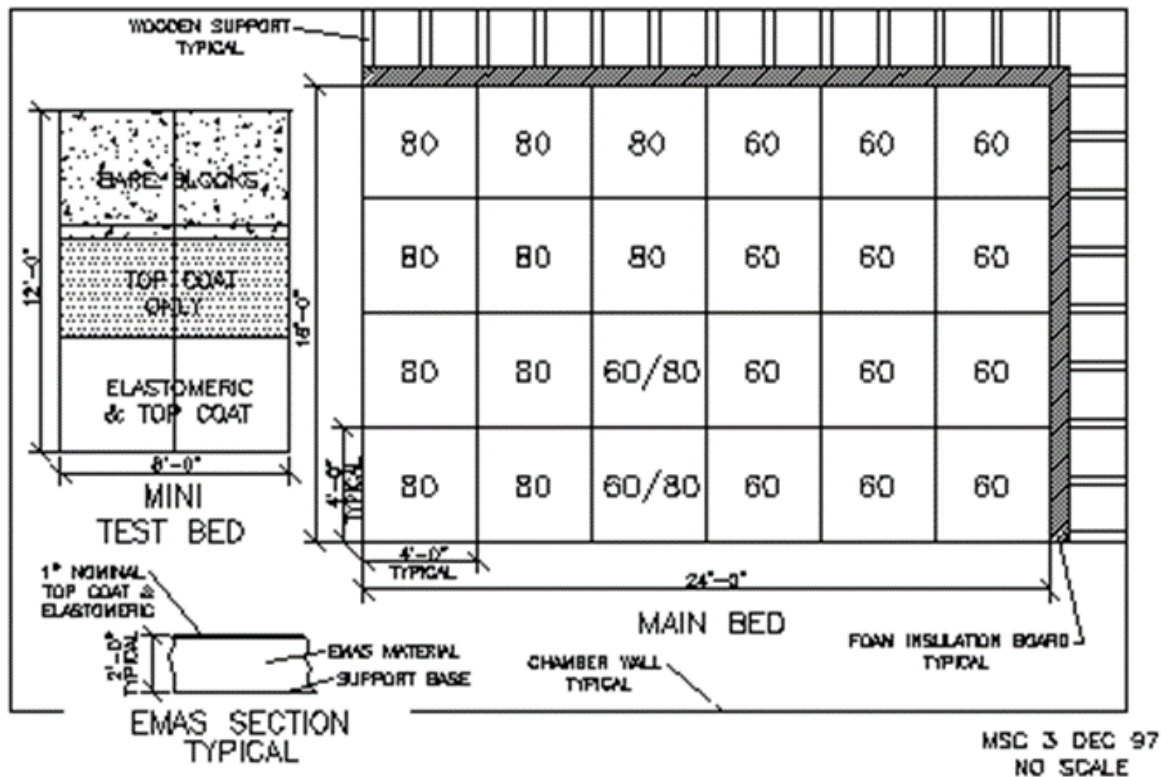
Figure 22. The EMAS Test Beds in the CRREL Environmental Laboratory

The general plan for thermal cycling was to subject the test beds to the temperature oscillations experienced by the prototype arrestor system at JFK. The National Oceanic and Atmospheric Administration (NOAA) database contains the following information for JFK:

- Normal daily mean temperature for January = 31.2°F

- Normal daily maximum temperature for January = 37.5°F

- Normal daily minimum temperature for January = 24.9°F

- Lowest temperature of record at JFK = -2°F (in January)

- Mean number of days in January with minimum temperature 32°F or less = 23

- Greatest variation in a two-day period is approximately 46 degrees (on January 27-28, 1994).

Thermocouples placed inside the bed recorded temperatures during the cycling events at different depths. CRREL personnel conducted visual inspections during temperature cycling

with an emphasis on the joints between blocks. The condition of the bed was noted on a daily basis. Any noticeable bed displacement or surface anomalies were photographed.

7.3 COLD-WEATHER TEST FINDINGS.

As expected, the highly air-entrained material (roughly 80% air) in the EMAS blocks acted as an insulator. Portions of the bed more than a foot below the surface reacted very slowly to external temperature changes. The findings of the CRREL tests parallel the WJHTC tests in that the cellular cement acts as a superior thermal insulator. The interior portions of the blocks responded slowly to ambient temperature changes. No significant or measurable dislocations were observed at either individual blocks or with the joints between blocks.

8. INSTALLATION AT LGA RUNWAY 22.

In Spring of 1998, the PANY&NJ prepared a design for an EMAS installation to serve LGA Runways 13 and 22. The overrun area for Runway 13 measured 382 ft from the end of the runway to the localizer. The overrun area for Runway 22 measured 359 ft from the end of the runway to the localizer. The limited real estate influenced the PANY&NJ decision to locate the leading edge of the Runway 22 EMAS only 35 ft from the end of Runway 22. The outboard edge of the EMAS was located only 53 ft from the Runway 22 localizer. In addition, the EMAS was positioned in the critical area for the Runway 22 offset localizer directional type aid.

8.1 THE LGA ILS TESTING.

Due to the close proximity of the EMAS installation at both locations, the FAA conducted mathematical simulations, flight tests, and ground checks at LGA that were similar to those conducted at JFK. The mathematical modeling indicated that the EMAS would have negligible effect in the localizer approach region ±10 degrees from centerline, but could have some impact in the localizer clearance region that would result in restrictions on the use of the localizer beyond ±10 degrees from centerline. Appendix B includes specific information regarding the ILS mathematical modeling for LGA Runways 13 and 22.

In July 1998, prior to construction, the FAA conducted a series of flight tests to establish a baseline condition for the localizer and laser Doppler anemometer (known as LDA) signals for Runway 22. Measurements from subsequent flight tests were compared to the baseline. Subsequent flight tests during construction indicated that signal errors were well within tolerance, and the measured course widths were only a few hundredths of a degree different from published figures.

Similar to the process during the installation of the EMAS at JFK, FAA AF personnel performed ILS ground checks each morning before the beginning of daily flight operations. No significant ILS disturbances were recorded during construction of the LGA Runway 22 EMAS. Subsequent FAA flight checks and a lack of pilot complaints indicated that the EMAS had no significant impact on the performance of either localizer.

8.2 JET BLAST DAMAGE AT LGA.

The PANY&NJ and ESCO began the EMAS installation for LGA Runway 22 in August 1998, and completed installation in September 1998. The leading edge of the EMAS was installed 35 ft outboard from the end of Runway 22, which was only 35 ft from the departure end of Runway 4. Soon after installation, jet blast forces from Runway 4 departures eroded the hard topcoat of the EMAS and exposed the softer cellular cement material to subsequent jet blast. ESCO and the PANY&NJ implemented several remedial actions to halt further deterioration of the system, including hardened topcoats, redesigned debris deflector, and relocation of the leading edge of the system to 75 ft outboard from the end of the runway. Despite these measures, deterioration of the EMAS continued until the PANY&NJ elected to remove the entire system in August 1999.

9. DEVELOPMENT OF JET BLAST RESISANT EMAS.

The removal of the LGA EMAS in 1999 triggered a joint effort between the PANY&NJ, ESCO, and the FAA to evaluate a jet blast resistant (JBR) EMAS. The plan included:

- Investigating and characterizing jet blast forces in an overrun area.

- Testing various systems under equivalent jet blast conditions at the FAA Airflow Induction Test Facility's wind tunnel.

- Constructing a demonstration EMAS at the exact location of the original LGA EMAS.

- Conducting small wheel penetration tests and evaluating the mode of failure of the JBR EMAS in relationship to small aircraft overruns and foreign object debris (FOD).

 The goal was to rebuild a JBR EMAS to serve LGA Runway 22 as soon as practical.

9.1 MAPPING JET BLAST FORCES AT LGA.

In May 2000, the FAA and ESCO jointly funded a study by University of Dayton Research Institute (UDRI) to measure key jet blast parameters at LGA. The objectives of the study included:

- Measure ground vibration levels on the EMAS base along with acoustic pressure, wind speed, and temperature of the air above the EMAS base under LGA operating conditions

- Correlate these data with the types of aircraft with the LGA fleet mix.

- Record typical operations of aircraft (hold at end of runway, roll and go, etc.) and typical times that aircraft depart LGA Runway 4.

- Use the measured data to project expected loading for the EMAS service life.

9.1.1 Instrumentation at LGA Safety Overrun Area.

UDRI installed instrumentation packages in six locations end of LGA Runway 22. Figure 23 shows the general layout of the instrumentation, figure 24 shows a schematic of each measurement station, and figure 25 is a photograph of a typical measurement station.
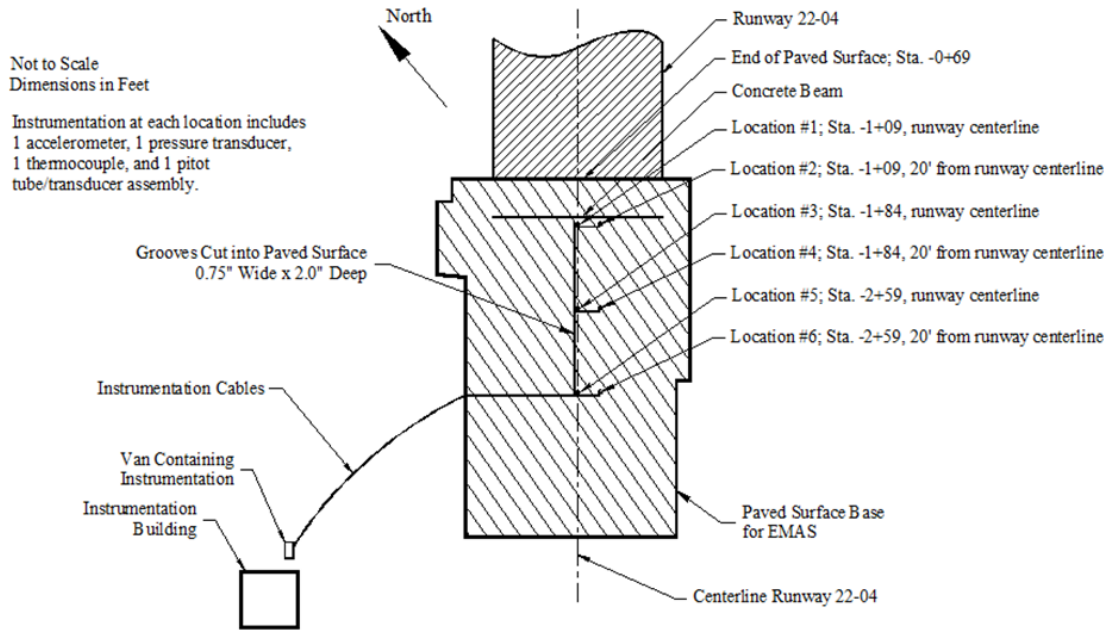

Figure 23. Jet Blast Instrumentation Layout at LGA
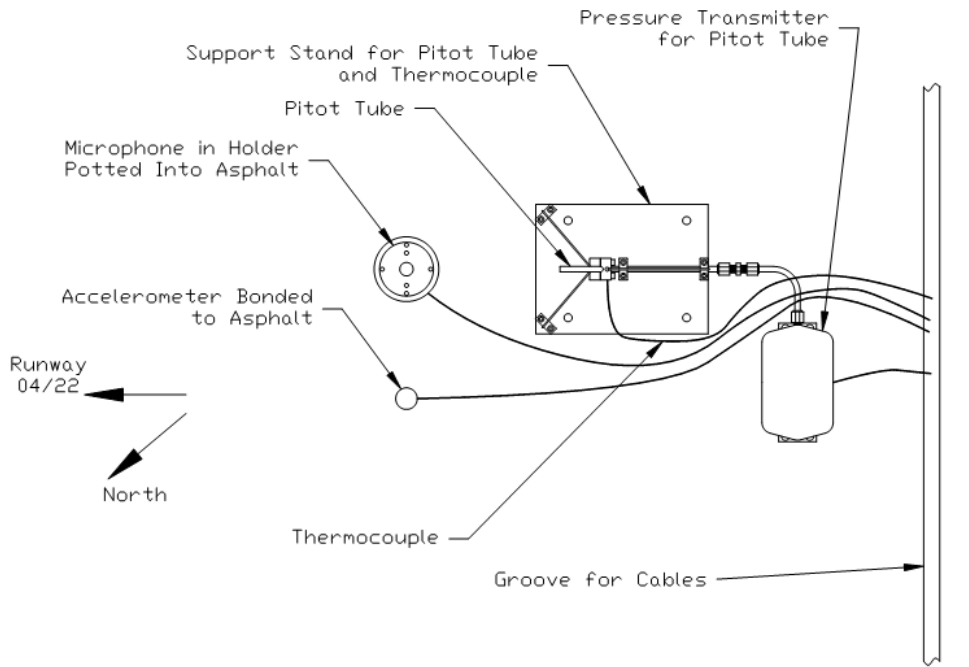
Figure 24. Typical Instrumentation at Each Station on the LGA Runway 22 Overrun Area

Figure 25. Typical Instrumentation Package

9.1.2 Data Collection and Summary.

UDRI personnel recorded takeoff and landing data on May 30 and 31, 2000; June 6 and 7, 2000; and June 19 and 20, 2000. Video recording and simultaneous voice recordings were used to synchronize instrumentation data sets with type of aircraft and manner of operation (takeoff, landing, and rollout). Instrumentation was removed from the overrun area on June 22, 2000.

The UDRI study results are summarized below:

- Ground vibrations were very low with maximum levels not exceeding 0.1 g

- The highest acoustic levels during takeoff occasionally occurred as high as 151 decibels (dB) for B-727, B-737, and DC-9 aircraft. Acoustic levels were also high for landing aircraft when thrust reversers were used, resulting in levels as high as 145 dB.

- Temperature rises were short in duration, but maximum measured rise during takeoff (relative to the ambient temperature) was 42°F. However, typical rise in temperature was only 10°F to 20°F.

- Airspeeds reached a maximum 175 mph, but were generally below 125 mph.

UDRI prepared a computer program to scan the data and determine jet blast loads as a function of aircraft type and number of departures. This program predicted jet blast loads on future EMAS installations. The program also allowed the FAA to proceed with plans to simulate jet blast conditions at the WJHTC Airflow Induction Test Facility.

9.2 WIND TUNNEL TESTING AT THE WJHTC AIRFLOW INDUCTION TEST FACILITY.

The main component of the WJHTC Airflow Induction Test Facility is a wind tunnel powered by two Pratt & Whitney® J-57 turbine engines exhausting into the diffuser cone of the facility. The high-speed exhaust provides the primary flow that induces a secondary flow through the test sections that can approach 0.9 Mach. At the exhaust end of the tunnel, winds speeds are much lower, but they include sound pressure waves, particulate matter, and heat not found on the induction side of the facility. As a result, the exhaust end of the tunnel replicates jet blast conditions near the departure end of a runway. Figure 26 shows the exhaust end of the WJHTC Airflow Induction Test Facility wind tunnel.

Figure 26. The Wind Tunnel at the WJHTC Airflow Induction Test Facility

The FAA tasked UDRI to acquire jet blast data from behind the tunnel. The objective was to determine if the wind tunnel could replicate jet blast conditions measured on the LGA Runway 22 overrun area.

9.2.1 Initial Wind Tunnel Instrumentation and Data Acquisition.

On August 24, 2000, UDRI personnel recorded temperature, vibration, and sound pressure levels at two elevations at each of the eight locations behind the wind tunnel. Figure 27 shows the layout of the instrumentation packages at the wind tunnel.

Figure 27. Instrumentation Locations Behind the Wind Tunnel

The instrumentation mounting system resulted in wind speed measurements 16 in. above ground, temperature measurements 12 in. above ground, and sound pressure measurements 4 in. above ground.   Vibration measurements were also made with an accelerometer mounted directly to plywood.   These accelerations are indicative of the plywood motion rather than the ground vibration.   Higher elevation measurements were taken with the plywood base mounted to a 36-in.-high metal stand (figure 28), thus increasing the elevation of all measurements by 36 in.

Figure 28. Instrumentation Package Mounted on a 36-in.-High Metal Stand Behind the
Wind Tunnel

The data showed that wind speed and sound pressures behind the wind tunnel, particularly at
locations 1 and 3 on the elevated stand, were reasonably comparable for testing purposes with
conditions measured at LGA. Figure 29 shows the data set collected at location 3 on the elevated
stand.

Figure 29. Data Showing Run-up From Idle to Full Power and 45-Second Hold at Full Power

9.2.2 Elevated Platform Testing at Wind Tunnel.

Test results from the initial wind tunnel test led ESCO personnel to construct an elevated concrete platform behind the wind tunnel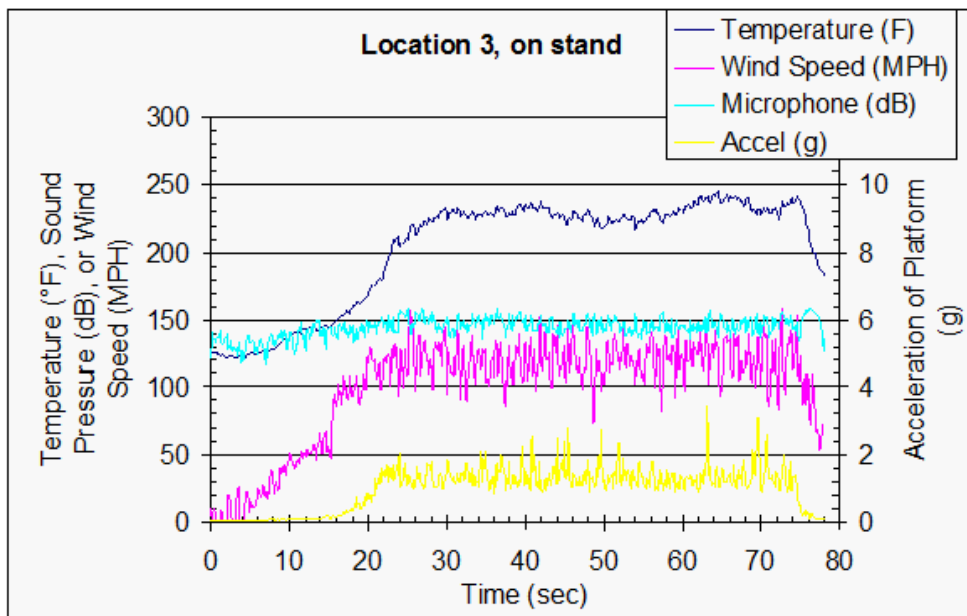 at a location and elevation where jet blast conditions most closely resembled those measured at LGA. UDRI personnel installed data acquisition packages similar to previous testing at three locations on the elevated platform. Figure 30 shows the uplift pressure sensor.
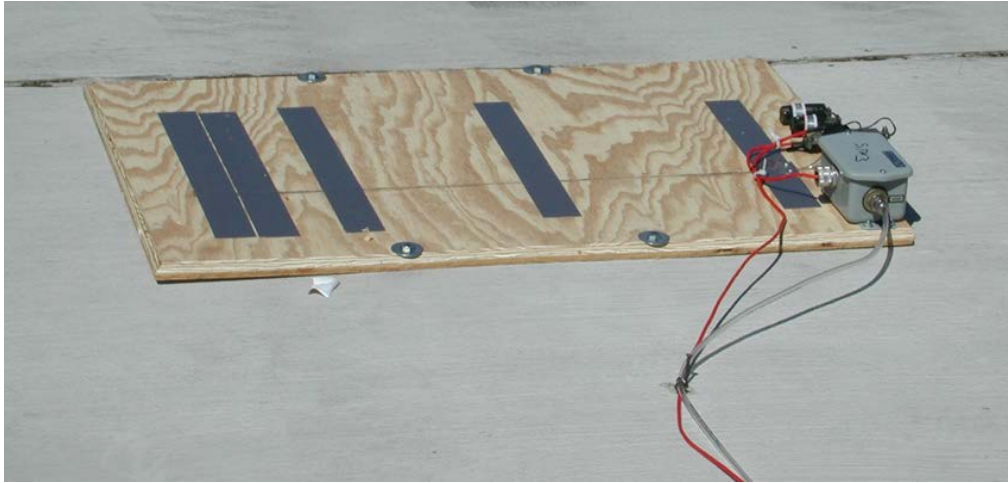
Figure 30. Uplift Pressure Sensor on Elevated Platform

On September 20, 2000, UDRI personnel collected data to map wind speed, temperature, ground vibration, sound pressure levels, and uplift pressure at different wind tunnel power settings. This information enabled UDRI personnel to calculate the power setting and times necessary to replicate 1 month of jet blast exposure at LGA. Table 2 shows the time in seconds at different power settings that are equivalent to 1 month of operations at LGA at three different setback locations. Complete data sets and analyses are included in appendices C and D.

Table 2. Estimated Exposure Times Behind Wind Tunnel Equal to 1-Month Operation at LGA

Power Setting (% Rated Speed)	Exposure Time in Seconds		
	40-ft Setback	115-ft Setback	190-ft Setback
85	5500	2200	720
92	1500	340	60
100	185	25	0

9.2.3 Findings From Initial Wind Tunnel Testing.

Analysis of the jet blast data measured behind the wind tunnel influenced ESCO's design for the next generation JBR EMAS. The cellular cement core material would remain unchanged.   This part of the system was fragile by design with a compressive strength of 60 psi. Any protective-coating system must be able to withstand severe acoustic shock, high temperature swings, and high wind speeds. The exterior coating must also provide protection from rain, snow, and

moisture intrusion. In addition, the wind tunnel testing indicated significant uplift forces associated with high wind speeds. Any weakness in the bond between the coating and base block would eventually lead to the loss of the topcoat, exposing the cellular cement material that would erode with subsequent jet blasts. With these factors in mind, ESCO personnel developed a JBR system that incorporated the use of thin, rigid boards at the top and bottom of the cellular cement blocks. A thin layer of closed cell foam was placed between the top board and the base block to absorb some of the acoustic energy. The entire 4 ft by 4 ft block was then then wrapped with scrim netting to prevent delamination. The top board received factory-applied, moisture-resistant coatings. The bottom board was adhered to a typical overrun base with hot asphalt.

9.2.4 The JBR System Testing Simulating a 75-ft Setback at Wind Tunnel.

In November 2000, ESCO personnel installed a 12 ft by 12 ft JBR system behind the wind tunnel. Figure 31 shows the location of the first two of three rows of blocks on the elevated platform.

Figure 31. View From Top of Platform Facing Into Exhaust End of the Wind Tunnel

Figure 32 shows a view from inside the wind tunnel facing the raised platform and the JBR EMAS test bed.

Figure 32. View From Inside the Wind Tunnel Facing the Platform With JBR Test Bed

FAA and ESCO personnel selected a wind tunnel power-setting plan to simulate LGA jet blast conditions with a 75-ft setback. Figure 33 shows the wind tunnel power setting as a function of time.
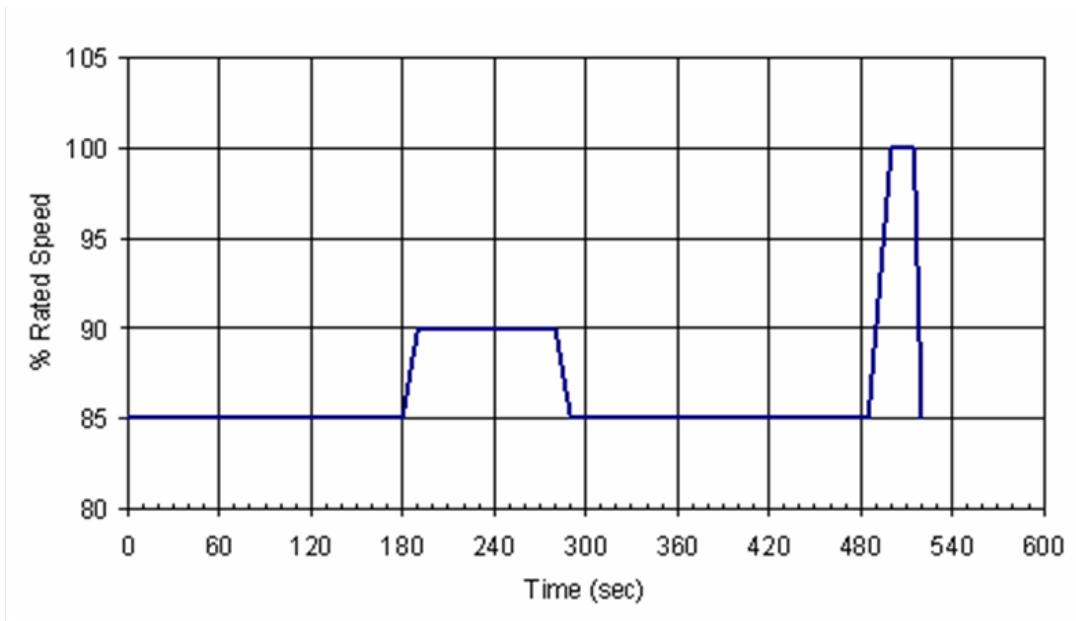

Figure 33. Wind Tunnel Testing Profile for a 75-ft Setback

Between November 16 and November 30, 2000, FAA personnel exposed the test bed to a series of 14 cycles, which was equivalent to 1 year of LGA jet blast. Figure 34 shows one cycle of jet blast testing at the wind tunnel at 100% rated speed. Inspection of the test bed during and after the series of tests indicated the JBR system resisted blast forces without displacement or damage.

Figure 34. Wind Tunnel Jet Blast at 100% Rated Speed

The FAA personnel commenced a second series of jet blast exposure tests behind the wind tunnel in December 2000. The test bed was covered with snow and had been experiencing freeze and thaw cycles. Testing continued through the winter, including numerous freeze and thaw cycles. After 19 months of simulated exposure, there was no apparent damage or significant wear to the test bed surface.

9.3 INSTALLATION OF JBR DEMONSTRATION BED AT LGA.

The success of the JBR wind tunnel testing encouraged ESCO and PANY&NJ personnel to move forward with the installation of the demonstration JBR blocks at LGA. The objective of this effort was to demonstrate the ability of the JBR blocks to withstand jet blast forces produced during LGA Runway 4 departures over a full year.

On December 9, 2000, ESCO personnel installed four rows of JBR blocks across the overrun area for LGA Runway 22. Each row was 148 ft across with a nominal 8 in. height. The first row started 75 ft from the departure end of Runway 4. The leading edge was protected by a metal debris deflector. The tops of the blocks in the first two rows were sealed with polyurethane, and the third and fourth rows were sealed with an asphalt-based coating. All blocks were adhered to the base with hot asphalt. All joints were filled with backer rod and caulk. Figures 35 through 38 show the installation sequence.

Figure 35. Aluminum Debris Deflector at Leading Edge of JBR Blocks at LGA

Figure 36. Typical 8-in.-Deep JBR Block Showing Rigid Boards at Top and Bottom and Mesh Scrim

Figure 37. Leading Edge of JBR Blocks Were 75-ft From Departure End of LGA Runway 4

Figure 38. Polyurethane Coating at Front and Asphalt Coating at Rear

FAA AF personnel performed ground checks on the Runway 22 localizer and LDA signals. PANY&NJ Airport Operations personnel conducted a visual inspection each morning prior to

opening the runway for traffic each day. The inspectors looked for loose or delaminated sections and noted any remarkable conditions.

On February 15, 2001, ATRD personnel conducted a site visit to the demonstration bed. Visual and tactile inspection indicated the blocks were in sound condition. There was no evidence of displacement, delamination, or loose blocks. The coating system appeared intact. The paint on the debris deflector shield was worn away in several locations. Figure 39 shows the condition of the blocks after more than 2 months of exposure to Runway 4 traffic. Figure 40 shows a view from behind the Runway 22 localizer as an aircraft departs Runway 4.

Figure 39. Visual Inspection of JBR Demonstration Blocks

Figure 40. Dark Horizontal Strip is the Rear Face of the JBR Demonstration Bed
(Runway 22 localizer is in the foreground.)

46

9.4 WIND TUNNEL TESTING AT A 35-FT SETBACK.

By May 2001, the JBR demonstration blocks at LGA were still intact and showing only minor abrasion wear on the aluminum debris deflector and some loss of sealant on the top surface of the blocks. This and the results of the jet blast tests behind the FAA wind tunnel prompted the PANY&NJ personnel to consider replacement of the Runway 22 EMAS at the 35-ft setback in lieu of the more conservative 75-ft setback. The additional 40 ft of EMAS provided better arrestor performance. Consequently, ESCO and PANY&NJ personnel requested a series of wind tunnel jet blast tests that simulated this more severe jet blast condition. The UDRI report in appendix C includes two wind tunnel power setting profiles at a simulated 40-ft setback. The more conservative of the two profiles was selected to account for the difference between the simulated setback distance of 40 ft and the planned installation setback at LGA of 35 ft. This recommended profile is shown in figure 41.

Recommended Profile for Simulating Exposure 40' from Runway at LGA
Using the FAA Wind Tunnel - Conservative Data Profile
(Repeat this Profile 16 Times for Each Months Equivalent Exposure)
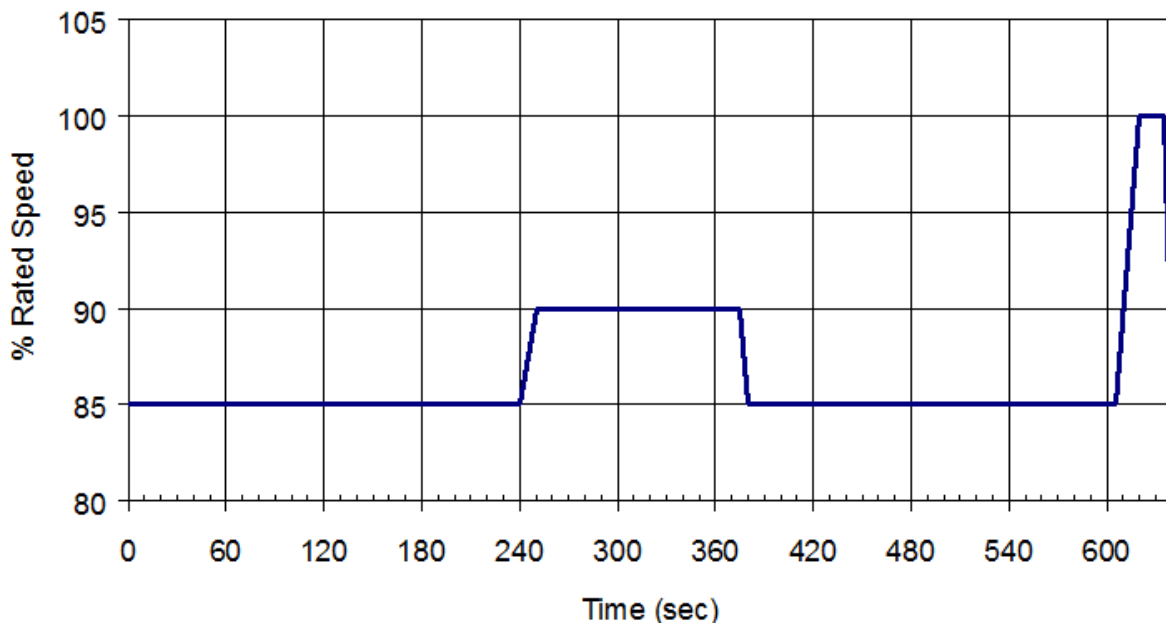
Figure 41. Wind Tunnel Power Setting for 35-ft Setback at LGA

In May 2001, FAA and ESCO personnel intentionally damaged JBR blocks and exposed these sections to maximum jet blast for 5 minutes. The objective was to categorize the modes of failure of the damaged test bed under severe conditions. Figure 42 shows the damaged sections that included surface punctures and saw cuts at different angles through the JBR surface material. Figure 43 shows removal of a full-depth section of the test bed.

Figure 42. Intentional Damage to JBR System

Figure 43. Full-Depth Section Removal From JBR System

After 5 minutes of jet blast testing, video documentation confirmed that the JBR blocks were not susceptible to a domino effect mode of failure. The surface punctures did not increase in size, but the loose material was merely blown out. The saw cuts did not lead to surface separations at the cuts. The section that was removed did experience some removal of additional loose material, but the adjacent blocks remained intact. The test concluded that if the JBR system does sustain damage in an operation setting that there is limited risk that portions of the bed will break loose and pose collateral damage as FOD.

After removing the original JBR test bed from behind the FAA wind tunnel, ESCO personnel installed a new test bed with the same configuration as the original test bed. The only substantive difference was a change in the mesh scrim material from fiberglass to polyester.

From May 2001 through April 2002, the FAA personnel exposed the second test bed the equivalent of 1 year of LGA jet blast at the 75-ft setback and 1 year of LGA jet blast at the 40-ft setback. There was no apparent damage to the surface or integrity of the test.

9.5 FINDINGS OF JBR TESTING AT WIND TUNNEL AND LGA.

On June 29, 2002, over 18 months after installation of the demonstration bed, PANY&NJ and ESCO personnel inspected the LGA demonstration bed prior to removal. The following comments were extracted from the inspection report:

- All four rows of blocks were intact.

- The first two rows of blocks exhibited spiderweb-type cracks in the polyurethane sealant. This may have allowed moisture intrusion.

- The asphaltic sealant on the third and fourth rows was worn off in most places.

- The caulk joints between the blocks were compromised in several locations.

- At least 9 of the 140 blocks were saturated with water.

- Several blocks were damp at the bottom 3 in. and dry at the top.

- The tops of the bottom rigid boards were damp, while the bottoms of the top rigid boards were dry.

- ESCO and PANY&NJ personnel extracted samples from the demonstration bed for further testing.

The general consensus between the PANY&NJ, ESCO, and FAA personnel was that the source and control of moisture in the demonstration bed must be understood prior to installation of the 35-ft setback EMAS at LGA. A second demonstration bed was later installed in 2002 for additional observation, and it remained in place until 2004.

49

9.6 SMALL-WHEEL PENETRATION TESTS.

The introduction of a rigid board and mesh scrim to the cellular cement arrestor system provided protection from jet blast forces, but they also introduced unknowns related to the mode failure under wheel load and mathematical model predictions. The mathematical model used by ESCO personnel to predict aircraft braking performance while traversing through a cellular cement arrestor system assumes that the material is homogeneous throughout its full depth. The JBR coating contradicted this assumption. Consequently, ESCO personnel developed a small wheel test program to determine if modifications to the mathematical model were necessary for predicting aircraft performance in a JBR EMAS.

In May 2001, ESCO and FAA personnel conducted a series of small-wheel load tests to address these issues. ESCO personnel modified an FAA-owned truck with an outrigger that trailed an instrumented 19.5 by 6.75-8 King Air® aircraft tire. The objectives of these tests were to demonstrate the ability of a small wheel to penetrate the JBR protective cap, validate the accuracy of the mathematical model predictions, and document the mode of failure of the JBR system as it relates to FOD risk.

The EMAS computer program assumed that only small aircraft wheel loads would likely be affected by the JBR coating. Since a Beechcraft® 1900C was the smallest commuter in operation at the time of testing, the mass above the test wheel was adjusted to 3800 lb in a static mode with a tire pressure of 100 psi, similar to a Beechcraft 1900C maximum single main wheel load. Tests were conducted at three speeds: 1 kt, 15 kt, and 30 kt, through both JBR coated and uncoated blocks. ESCO personnel conducted the 1-kt and 15-kt tests at their own facility.

At the WJHTC, ESCO personnel installed a test bed comprised of 25 JBR cellular cement blocks, 2 ft by 2 ft, varying from 8 to 12 in. deep. In April 2001, the FAA-owned truck pulled the instrumented test wheel at 30 kt through the JBR block test bed.

During the first test, at 15 kt, the wheel entered the leading edge of the bed and crushed the top layer of the JBR coating without difficultly. The wheel bounced three times within the bed before exiting it. Figure 44 shows the wheel ruts from the small-wheel test through the JBR blocks. The back half of the bed had been removed, and the photograph does not show the other two sections where the wheel bounced out of the bed.

Figure 44. Wheel Ruts From the Small-Wheel Test Through the JBR Blocks

The second test, at 30 kt, tested the same setup and configuration as the first test, but this time used non-JBR-coated cellular cement blocks. The wheel bounced slightly as it entered the bed, but not enough to raise the wheel out of the bed. Figure 45 shows that the wheel stayed in the bed for the full 100 ft.

Figure 45. Wheel Ruts From the Small-Wheel Test Through the Non-JBR Blocks

The third test, at 30 kt, used the same test setup and configuration as the second test, and also used the same JBR-coated blocks. The wheel experienced the similar bouncing sequence as the first test with JBR-coated blocks.

The small-wheel tests, representing a small commuter aircraft, demonstrated that the tires will penetrate the JBR coating of the EMAS. Data analysis indicates that the JBR coating does affect mathematical model prediction accuracy for small-aircraft performance and gear loads. For aircraft weighing more than 25,000 lb, the model remains a suitable means of predicting EMAS performance. Model accuracy increases for aircraft above 50,000 lb. The JBR coating appears to restrain the broken pieces of the blocks. The cement board that comprises the top layer of the JBR coating failed to a degree that no large pieces were ejected. The FOD risk does not appear any worse than a non-JBR EMAS.

The limited data set did not allow analysis of small-aircraft performance in a JBR EMAS at higher entry speeds. Additional tests at these higher speeds are necessary to determine this high speed effect. Additional information regarding the impact of the JBR topcoat is included in appendix E.

10. REPLACEMENT OF PROTOTYPE EMAS AT JFK.

PANY&NJ and ESCO personnel experienced significant difficulty maintaining the integrity of the top surface of the prototype EMAS installed on JFK Runway 4R in November 1996. The original construction sequence postponed applying the sealant on top of the EMAS from November 1996 until spring 1997. By then, significant moisture had entered the EMAS, and bonding sealants on top of the system became problematic.

By 2002, the EMAS maintenance had become very expensive and time consuming. In addition, loose pieces of arrestor system material posed an increasing FOD risk. The PANY&NJ personnel decided to replace the EMAS to coincide with the decision to widen JFK Runway 4R/22L from 150 ft wide to 200 ft wide. The new EMAS would be expanded to cover the full 200-ft-width and use the newly developed and tested JBR blocks with factory-applied moisture protection. The new EMAS construction started in July 2002 and was completed in September 2002. Figure 46 shows the completed JBR EMAS replacement at JFK.

Figure 46. The JBR EMAS Replacement at JFK

11. AIRCRAFT OVERRUNS INTO EMAS AT JFK.

Two aircraft overruns occurred during the development of the EMAS. In each case, the EMAS at the end the runway successfully stopped the aircraft and possibly prevented a catastrophic event.

11.1 THE SAAB 340B OVERRUN AT JFK IN 1999.

On May 8, 1999, a Saab 340B landed long on JFK Runway 4R. The aircraft touched down at a speed of 157 kt with only 1400 ft of remaining runway. The pilot applied reverse thrust and maximum braking but traveled off the end of the runway and entered the EMAS at 75 kt. The aircraft traveled approximately 248 ft into the 400 ft-long EMAS. Figure 47(a) shows the crushed debris deflector, crushed cellular cement, and three sets of wheel ruts that trace the path of the aircraft. Figure 47(b) also shows the nose gear fully penetrating the 30-in.-deep EMAS. The aircraft sustained minimal damage to the nose gear, fuselage, and propellers. Twenty seven passengers and three crew members were unharmed, and one passenger was injured exiting the aircraft. The NTSB concluded that without the EMAS, the aircraft would have traveled 500 to 1000 ft beyond the end of Runway 4R and likely entered Thurston Basin, the site of the 1984 DC-10 overrun accident [9]. The PANY&NJ personnel extracted the aircraft and repaired the EMAS.

(a)	(b)

Figure 47. Saab 340B Aircraft in JFK Runway 4R EMAS

Figure 48 is an overhead view of the Saab 340B overrun at JFK Runway 4R, showing the overrun path and the proximity of Thurston Basin. This photograph was taken after the crushed EMAS was removed.
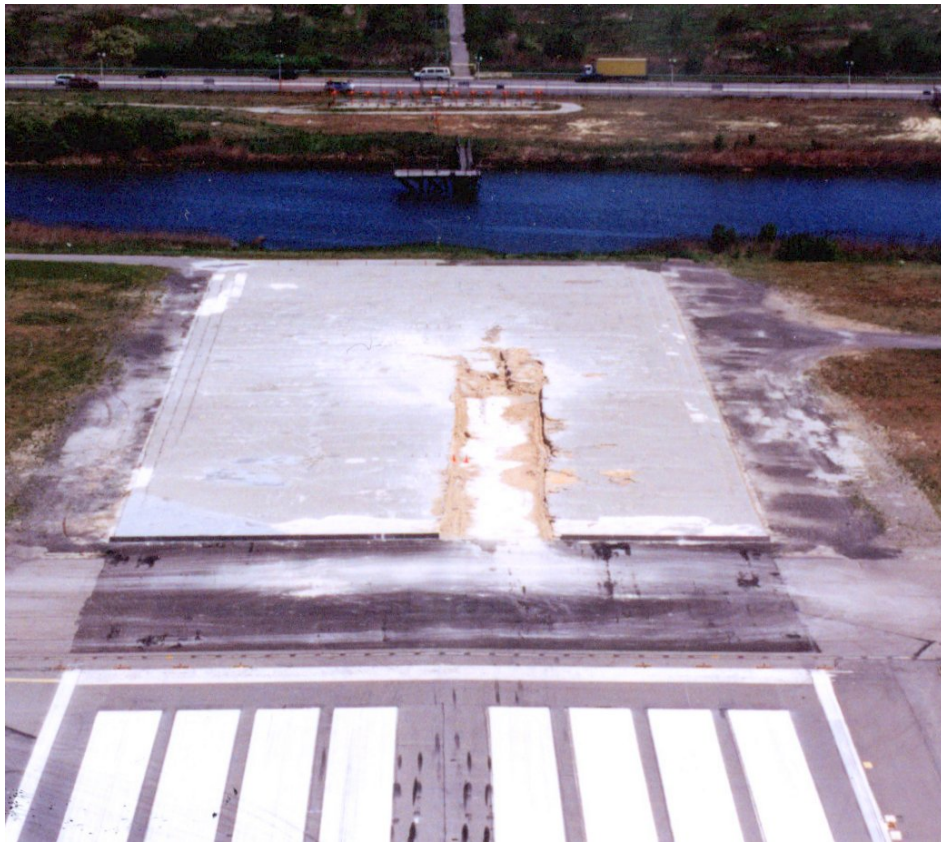

Figure 48. Overhead View of Saab 340B Overrun at JFK Runway 4R

11.2 THE MD-11F OVERRUN AT JFK IN 2003.

On May 30, 2003, an MD-11F overran JFK Runway 4R after landing. Figures 49(a) and (b) shows the final location of the aircraft relative to the end of the runway. These photographs show the mode of failure of the JBR EMAS. The nose gear of the aircraft traveled 115 ft into the EMAS, and the main gear traveled 35 ft into the system. The nose gear entered the EMAS in a yaw position, while the gear rolled through the system under a braking action condition. There were no reported injuries to the two crew members. Five main gear tires and the right nose gear tire were damaged as well as several threshold light fixtures. The PANY&NJ personnel repaired the EMAS following the accident.

(a)   (b)

Figure 49. The MD-11F Overrun at JFK Runway 4R

12. CONCLUSIONS.

By 1993, the Federal Aviation Administration (FAA) had established the feasibility of safely stopping an aircraft in a soft-ground arresting system. From 1994 to 2003, personnel from the FAA, Port Authority of New York and New Jersey, and Engineered Arresting Systems Corporation planned and executed a research program to develop a practical version of this system called Engineered Materials Arresting Systems (EMAS). This decade-long collaborative research included laboratory testing, mathematical model validation, full-scale aircraft testing, jet blast testing, and prototype arrestor system installations at two major airports. The end result enabled the FAA to publish, Advisory Circular (AC) 150/5220-22, "Engineered Materials Arresting Systems (EMAS) for Aircraft Overruns" in 1998. This AC contains standards for planning, designing, installing, and maintaining EMAS in runway safety areas, effectively satisfying the National Transportation Safety Board Safety Recommendation. The outcome of this research enabled EMAS installations at nine United States airports by 2003.

13. REFERENCES.

1.   National Transportation Safety Board (NTSB), "Safety Recommendations A-82-152 through -169," issued December 23, 1982, available at http://www.ntsb.gov/safety/safety-recs/RecLetters/A82_152_169.pdf (date last visited April 11, 2017).

2.   NTSB, "Scandinavian Airlines System, Flight 901, McDonnell Douglas DC-10-30, John F. Kennedy International Airport, Jamaica, New York, February 28, 1984," Aircraft Accident Report NTSB/AAR-84/15, available at https://www.ntsb.gov/investigations/AccidentReports/Reports/AAR8415.pdf (date last visited April 11, 2017).

3.   NTSB, "Safety Recommendation(s) A-84-21 through -41," issued April 16, 1984, available at http://www.ntsb.gov/safety/safety-recs/recletters/A84_21_41.pdf (date last visited April 11, 2017).

4.   White, J.C. and Agrawal, S.A., "Soft Ground Arresting System for Airports," Federal Aviation Administration (FAA) report DOT/FAA/CT-93/80, December 1993.

5.   Federal Aviation Administration, "Engineered Materials Arresting Systems (EMAS) for Aircraft Overruns," FAA Advisory Circular 150/5220-22, August 21, 1998.

6.   Cook, R.F., "Soft-Ground Aircraft Arresting Systems," FAA report DOT/FAA/PM-87/27, August 1987.

7.   Cook, R.F., "Evaluation of a Foam Arrestor Bed for Aircraft Safety Overrun Areas," UDR-TR-88-07, University of Dayton Research Institute, Dayton, Ohio, 1988.

8.   National Fire Protection Association (NFPA), "NFPA 403: Standard for Aircraft Rescue and Fire-Fighting Services at Airports," 2014 edition.

9.   NTSB, "NTSB Identification: NYC99FA110," available at http://www.ntsb.gov/_layouts/ntsb.aviation/brief2.aspx?ev_id=20001212X18850&ntsbno=NYC99FA110&akey=1 (date last visited April 11, 2017).

APPENDIX A—INSTRUMENT LANDING SYSTEM MATHEMATICAL MODELING AT JOHN F. KENNEDY INTERNATIONAL AIRPORT

U.S. Department of Transportation
Federal Aviation Administration

Memorandum

Subject: INFORMATION: ILS Mathematical Modeling, Additional Modeling of the JFK Runway 4R Soft Concrete Arrestor Pad

Date: August 15, 1996

From: Manager, Navigation Branch, ACT-360

Reply to Attn. of:

To: Manager, Airport Technology Research and Development Branch, AAR-410

BACKGROUND: Mr. Jim White of AAR-410 requested additional math modeling using new data he supplied to determine the effects on localizer performance of a concrete arrestor pad to be installed at the stop end of Runway 04R at John F. Kennedy International Airport (JFK). Mr. White also asked for math modeling of various stages of construction for the arrestor pad. This site was previously studied using the Ohio University Geometric Theory of Diffraction (OUGTD) model. A newer model, the Ohio State University Near-Zone Basic Scattering Code (NZBSC33), was used for this study. This model was not available previously, and has proven invaluable at sites that don't fit assumptions made by other math models. Runway 04R is served by an ILS providing Category IIIA operation. The localizer array is set back 9427 feet from threshold. ILS Point E is located at 6400 feet from threshold, based on the runway length of 8400 feet. With a glide path angle of 3.00° and glide slope mast setback of 1007 feet, the runway 04R threshold crossing height (TCH) is calculated to be 52.8 feet. The operating frequency of the localizer is 109.5 MHz with a course width of 4.50 degrees. A vertical profile of the concrete arrestor pad and runway centerline profile are shown in Figure 1. Figure 2 shows the layout of the arrestor pad with respect to the localizer. The numbers indicate the order of construction of various segments of the arrestor pad examined in this report.

MATH MODELING PERFORMED: The NZBSC33 model uses the Uniform Theory of Diffraction (UTD) to calculate fields in the presence of scattering surfaces in three dimensions. Standard array geometry and excitation were assumed for a 14-element self-clearing localizer. Each log-periodic dipole (LPD) antenna was modeled as seven dipoles having geometry consistent with a typical FA-9913 LPD localizer antenna. The currents on each dipole have been previously determined using a Moment of Methods program called NEC-2. The dipole excitations were multiplied by the array distributions and the geometry offset by the array dimensions in order to synthesize the localizer. This technique has been used many times with great success. A partial orbit was modeled to determine the scaling factor for a 4.5° course

width and to verify that adequate clearances will exist. The topography of the ground plane was first determined. The arrestor was then superimposed on the ground plane. Approaches were modeled as straight inbound flights from 4 nmi descending along extended runway centerline at the glide path angle (passing through the TCH) to 12 feet above ground. The approach continued level to ILS Point E. A post-processor computed course deviation indication (CDI) from the electric field output of NZBSC33. The approach data was modified by applying a low-pass filter representative of CDI needle damping. The arrestor pad was modeled for the various stages of construction. The concrete was modeled as dry for the various stages of construction (modeled as a dielectric slab over ground having dielectric constant of 2.5 and loss tangent of 11, values consistent with cement). The completed pad was also modeled as wet. Because the array and arrestor are symmetric with the flight profile, an approach was modeled along the localizer half-width angle to verify that mathematical cancellation was not causing an underprediction in the modeling. This approach was from 4 nmi to threshold along an azimuth 1.125° from centerline.

RESULTS: Figures 3 through 6 illustrate the modeled path structure in the presence of the concrete arrestor pad at different phases of construction. No significant errors are evident on the simulated approaches. Figure 7 is a plot of the modeled clearance structure, which is also well within tolerance. Table 1 summarizes the math modeling approach results.

Table 1 - Comparison of Localizer Performance - Approach

Stage	Dry % Tolerance / nmi	Wet % Tolerance / nmi
1	0.6 / 0.05	
2	0.7 / 0.00	
3	3.3 / 0.00	
4	0.2 / 0.00	0.3 / 0.00

Table 2 summarizes the math modeling half angle approach results. The half-width approach when only Phase 1 is complete is shown in Figure 8. While CDI errors can become large during construction while off course, they are less than ±1.4 uA when construction of the arrestor pad is complete. It is possible that the model may be overpredicting the construction errors.

Table 2 - Comparison of Localizer Performance - Half Angle

Stage	Nominal	+ / -
1	69.8	8.3 / 8.7 uA
2	48.4	22.9 / 8.9 uA
3	82.1	7.7 / 21.6 uA
4	76.0	1.3 / 0.6 uA

CONCLUSIONS: The concrete arrestor pad is predicted to have an insignificant effect on the localizer. This is due to the symmetrical placement of the pad with respect to the localizer. Some small amount of roughness may be observed when flying off centerline in ILS Zone 3. It should be noted that there are no roughness criteria in the United States Flight Inspection Manual for approaches not on centerline.

If you have any questions about this modeling or for any other modeling requirements we can assist you with, please contact Jesse Jones at (609) 485-4573 or cc:Mail.

John Townsend
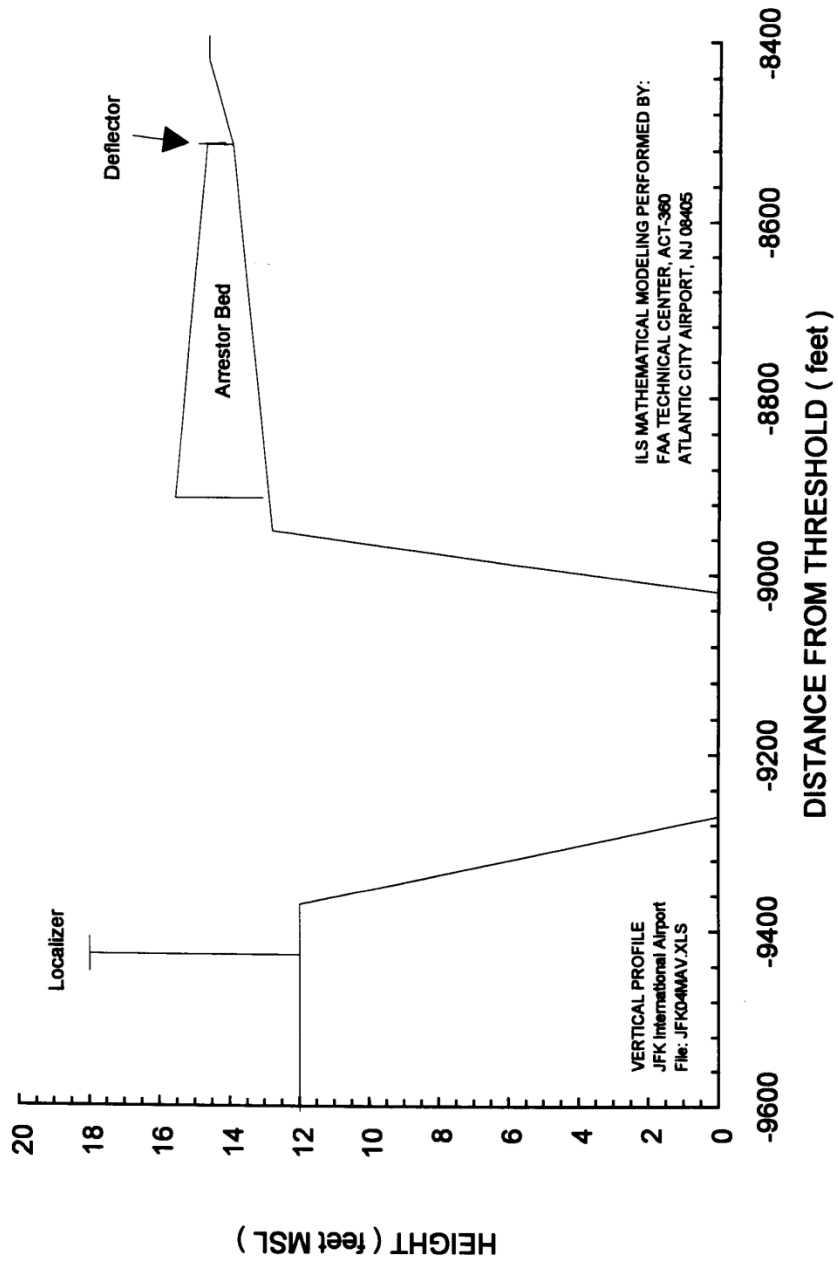
cc: Gary Skillicorn, AND-520

Figure 1. Centerline Vertical Profile of JFK International Airport Runway 04 as Modeled.
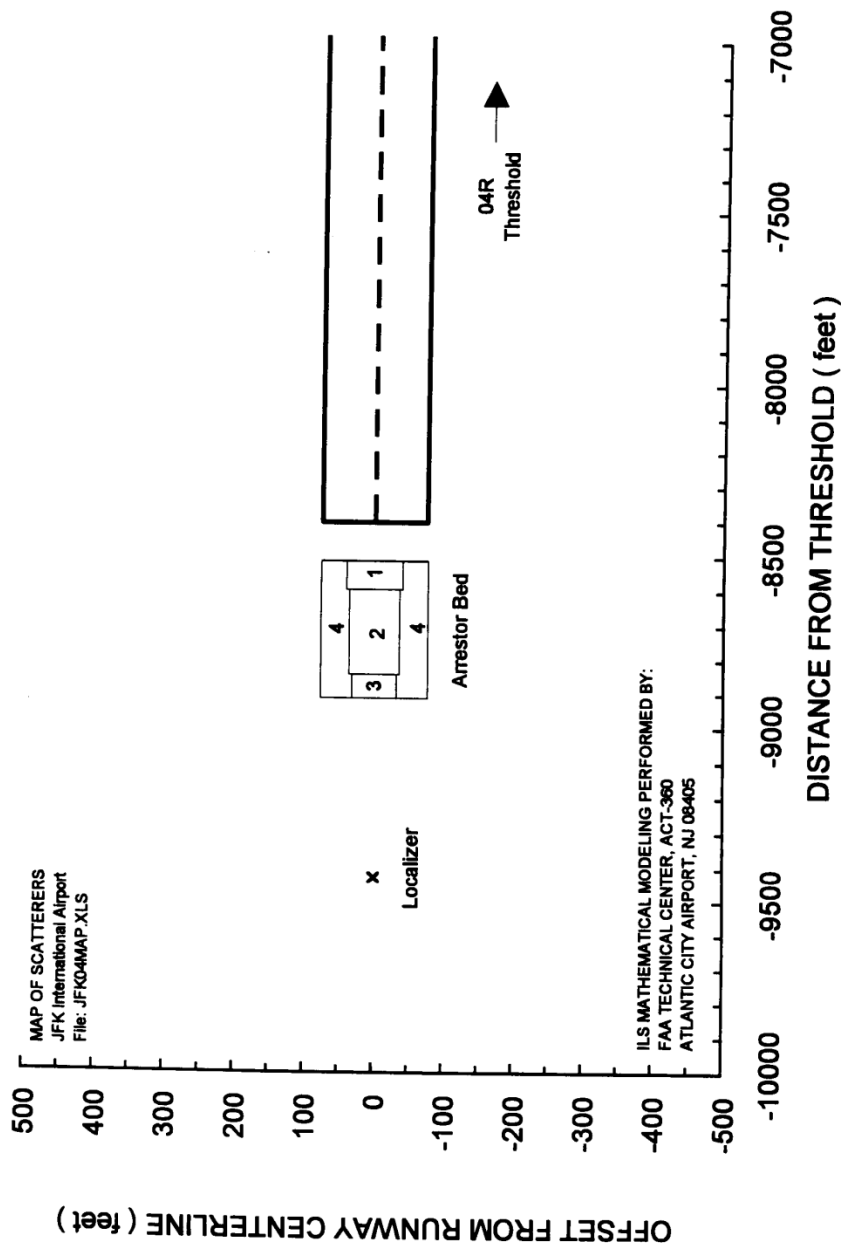
MAP OF SCATTERERS
JFK International Airport
File: JFK04MAP.XLS

ILS MATHEMATICAL MODELING PERFORMED BY:
FAA TECHNICAL CENTER, ACT-360
ATLANTIC CITY AIRPORT, NJ 08405

OFFSET FROM RUNWAY CENTERLINE (feet)

500   400   300   200   100   0   -100   -200   -300   -400   -500

x

Localizer

4   3
2
4   1

Arrestor Bed

04R
Threshold

DISTANCE FROM THRESHOLD (feet)

-10000   -9500   -9000   -8500   -8000   -7500   -7000

Figure 2. Layout of Concrete Arrestor Pad at JFK International Airport as Modeled.
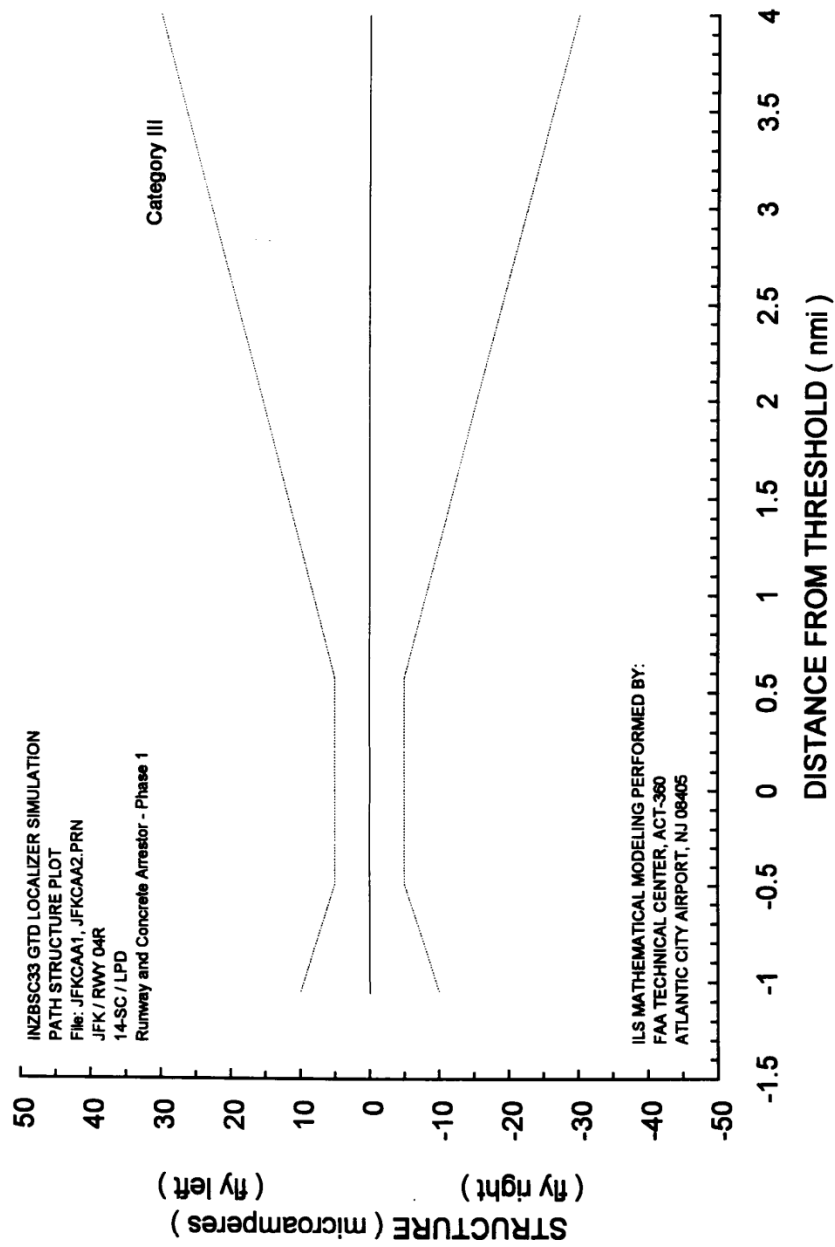
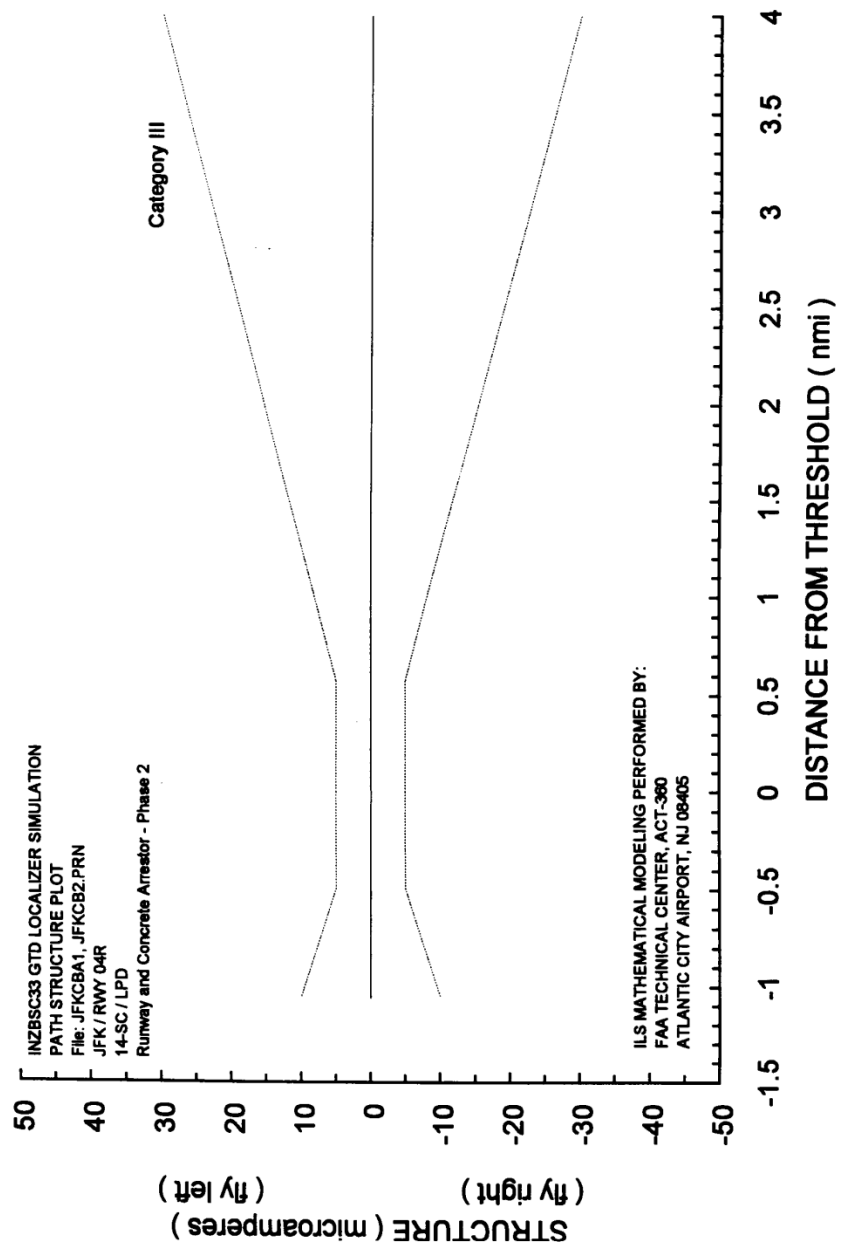Figure 3. Modeled Path Structure from Concrete Arrestor - Phase 1.

STRUCTURE (microamperes)

50
40
30
20
10
0
-10
-20
-30
-40
-50

(fly left)

(fly right)

INZBSC33 GTD LOCALIZER SIMULATION
PATH STRUCTURE PLOT
File: JFKCBA1, JFKCB2.PRN
JFK / RWY 04R
14-SC / LPD
Runway and Concrete Arrestor - Phase 2

Category III

ILS MATHEMATICAL MODELING PERFORMED BY:
FAA TECHNICAL CENTER, ACT-360
ATLANTIC CITY AIRPORT, NJ 08405

-1.5   -1   -0.5   0   0.5   1   1.5   2   2.5   3   3.5   4

DISTANCE FROM THRESHOLD (nmi)

Figure 4. Modeled Path Structure from Concrete Arrestor - Phase 2.
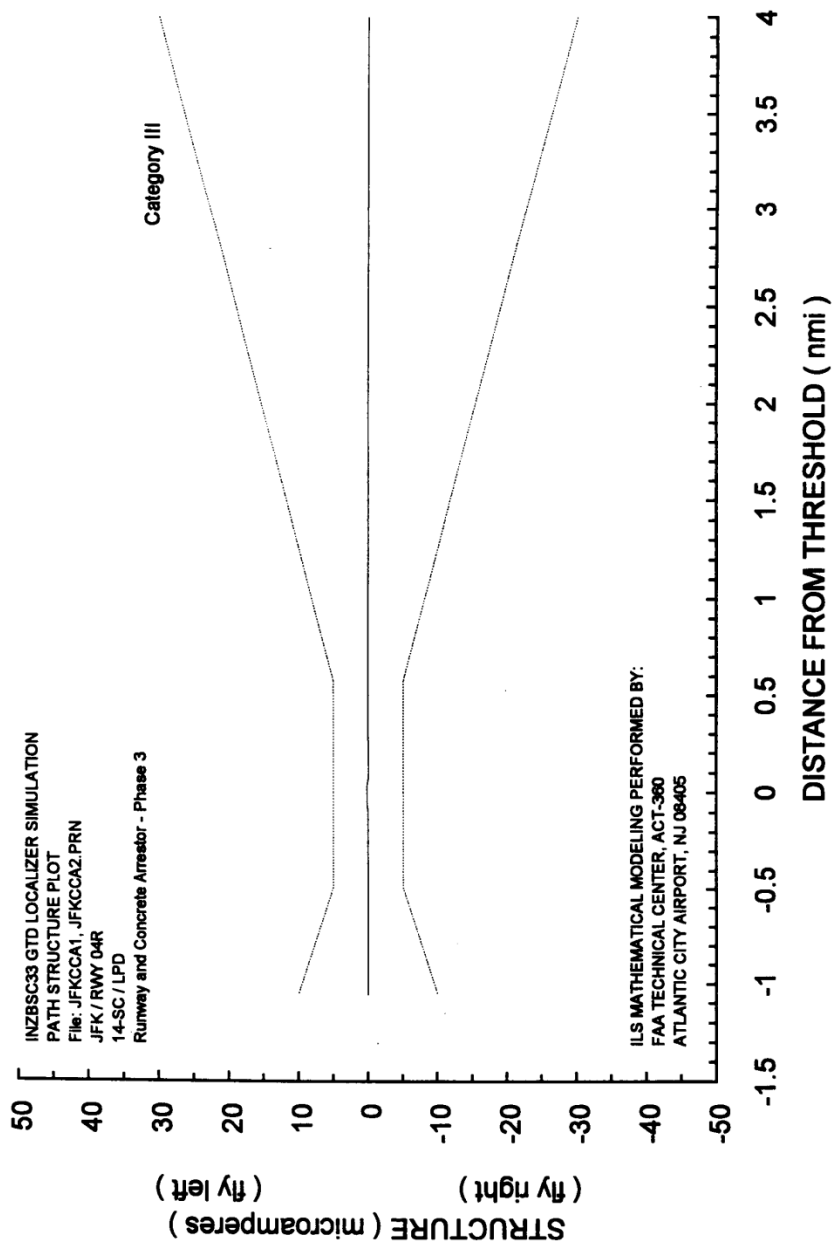
Figure 5. Modeled Path Structure from Concrete Arrestor – Phase 3.
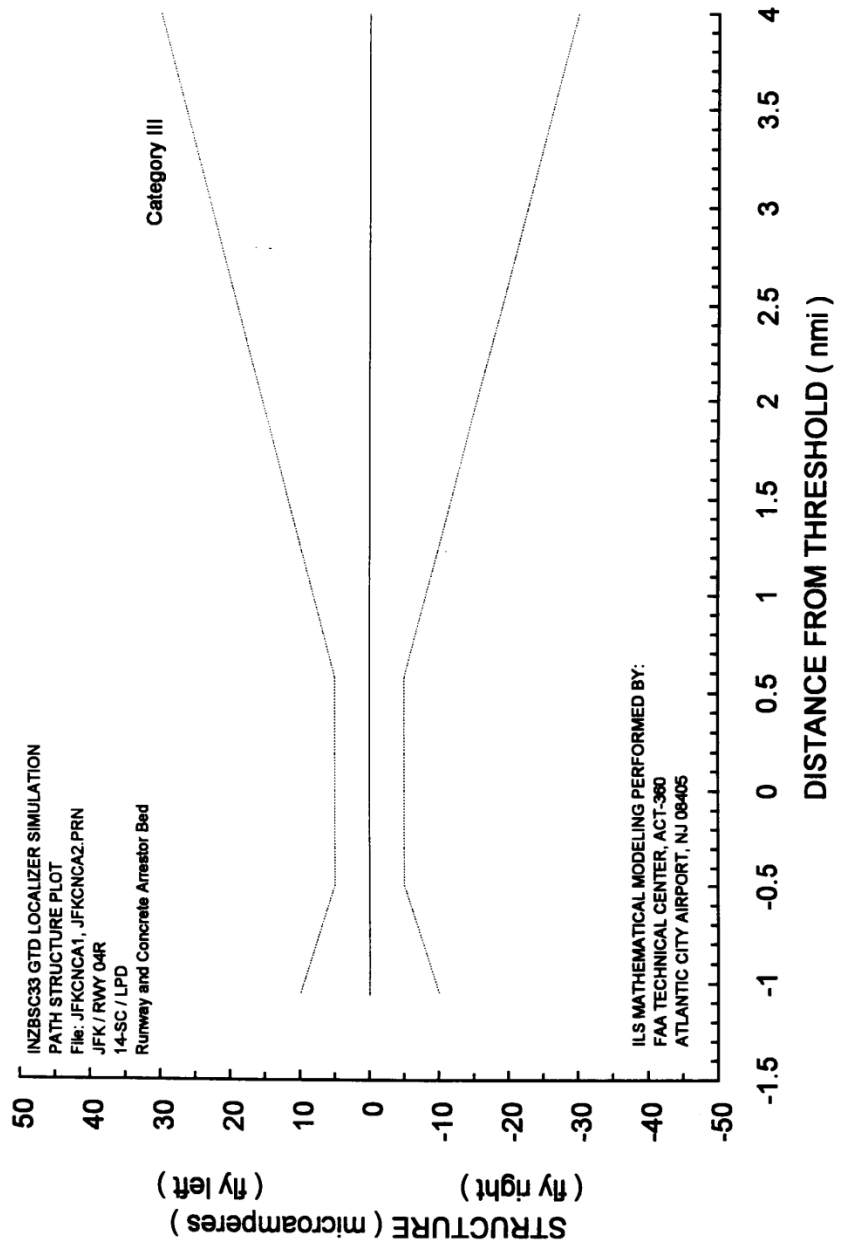
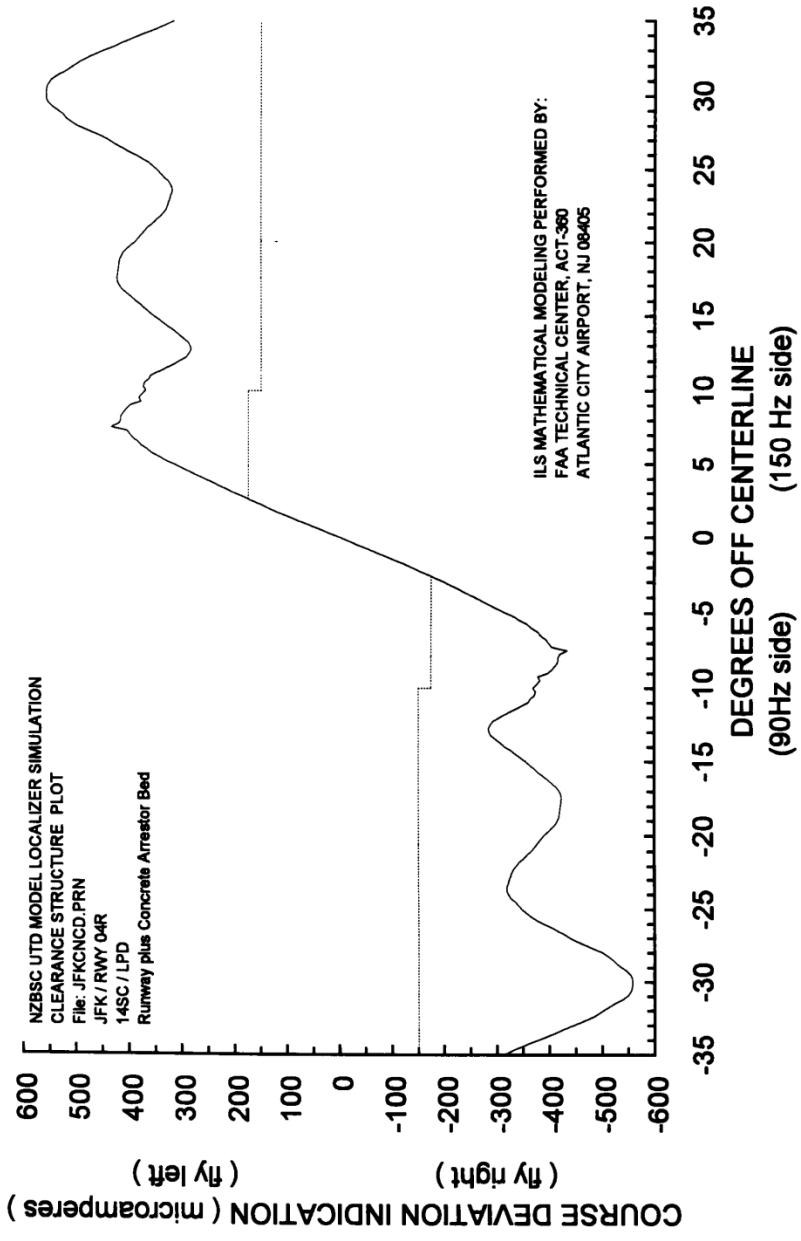Figure 6. Modeled Path Structure from Completed Concrete Arrestor Pad.

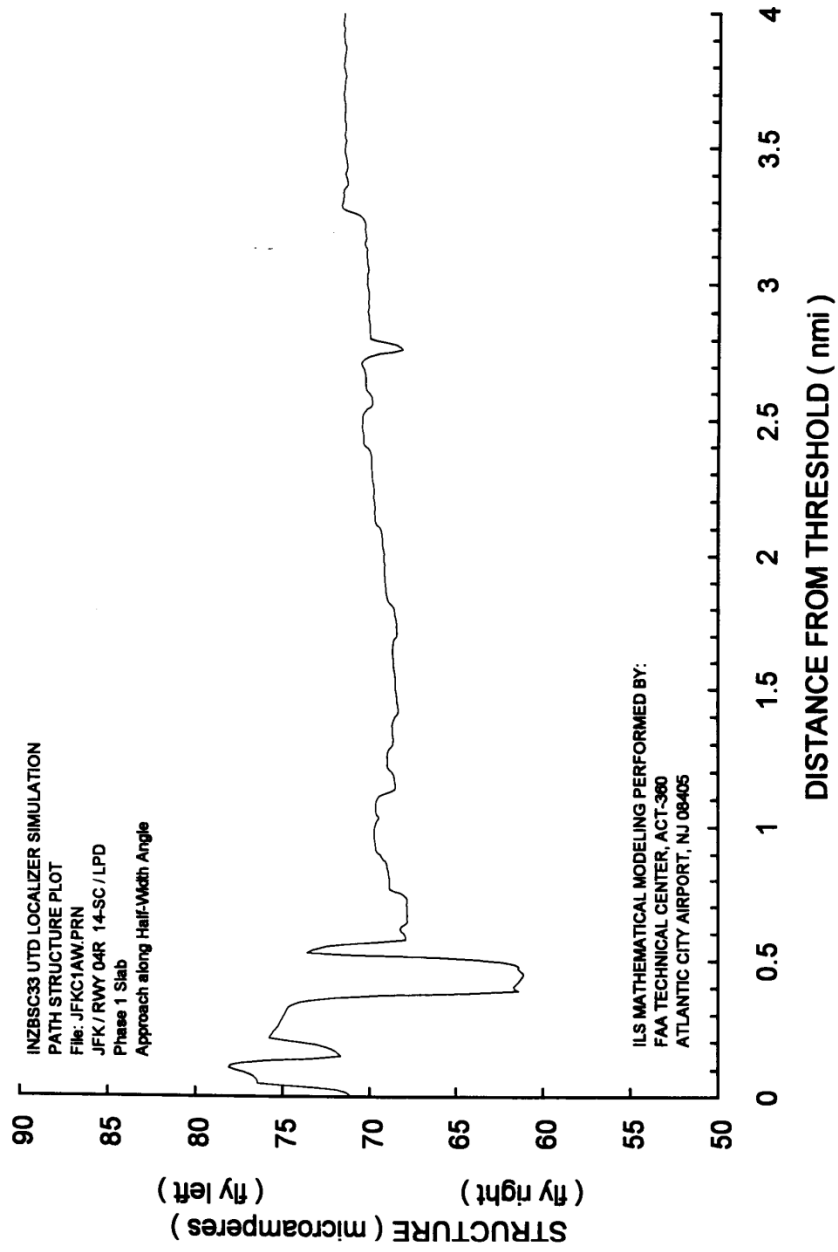Figure 7. Modeled Clearance Structure at JFK International.

Figure 8. CDI from Phase 1 Arrestor for Approach along Half-Width Angle.

`

Memorandum

**U.S. Department
of Transportation**

**Federal Aviation
Administration**

Subject: **INFORMATION:** ILS Math Modeling for La Guardia
Concrete Arrestor Bed Installations

Date: July 30, 1998

From: Technical Program Manager, ACT-360

Reply to
Attn. of:

To: Jim White, Civil Engineer, AAR-410

BACKGROUND: Mr. Jim White of AAR-410 requested math modeling of the effects of concrete
arrestor beds to be placed at the ends of Runways 13 and 22 at La Guardia Airport.

The concrete arrestor is 152 wide (symmetrically placed about the extended runway centerline) and
272 (runway 22) to 324 ft (runway 13) long. The arrestor pad begins at 35 ft from the runway end (in
the overrun area); at 9 inches above the surrounding ground and rises (towards the localizer) to 24
inches higher than the surrounding ground over a distance of 160 ft at which point it levels off for the
remaining length. The concern is that a discontinuous step in the reflecting ground plane so close to the
array may affect navigational performance.

The Runway 22 localizer is 14-10 dual-frequency Mark 20 log-periodic dipole (LPD) array, providing
a Category II approach. It is set back 7365 feet from threshold on centerline. Runway 22 is also served
by an 8-element self-clearing LPD localizer directional aid (LDA). This array is aligned -10° off
centerline, and provides a noise abatement procedure to the airport.

The Runway 13 localizer is to be a 14-10 dual-frequency Mark 20 log-periodic dipole (LPD) array,
providing an assumed Category I approach. It is set back 7382 feet from threshold on centerline, and
has not been commissioned at the time of this writing.

MATH MODELING PERFORMED: The Ohio State University Near-Zone Basic Scattering Code
(NZBSC33) was used to model the effects of the concrete arrestor and terrain. The NZBSC33
program uses the Uniform Theory of Diffraction (UTD) to calculate fields in the presence of scattering
surfaces in 3 dimensions. Scattering surfaces are defined by a connected sequence of flat multi-sided
plates.

Standard array geometry and excitation were assumed for all localizers. Each LPD antenna was modeled as 7 dipoles having geometry consistent with a typical FA-9913 LPD localizer antenna. The currents on each dipole have been previously determined using a Method of Moments program called NEC-2. The dipole excitations were multiplied by the array distributions and the geometry offset by the array dimensions in order to synthesize the localizer. A partial orbit was modeled under nominal conditions to determine the scaling factor for each course width. The modeled localizer sites and arrestors are shown in Figure 1.

The Category I centerline approaches were modeled as straight inbound flights descending along extended runway centerline at the glide path angle from 4 nmi into threshold, where the simulation ended at a height equal to the TCH. Category II approaches continued down to 12 feet above ground, where it leveled off until termination at ILS Point D. A post-processor then computed course deviation indication (CDI) from the electric field output of NZBSC33. The approach data was corrected by applying a low-pass filter representative of CDI needle damping. The LDA approach was modeled as described in the US Terminal Procedures NE2-66.

RESULTS: Table 1 lists the modeling results for the approaches. The first column lists the runway and array, the second column describes the arrestor as dry or wet (as after rain when we would expect the surface to be perfectly conducting), the third column lists the peak error in terms of Category tolerances, and the last column lists the range from threshold at which the peak occurs.

Table 1. Modeled Localizer Approach Performance

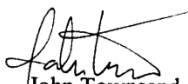| Runway / Array ILS Category	Configuration	Percent of Category Tolerances	Range (nmi)
22 / 14-10 Cat II	Dry	0.4	1.23
	Wet	0.6	2.31
22 / LDA Cat I	Dry	2.8	0.81
	Wet	2.0	0.81
13 / 14-10 Cat I	Dry	10.3	0.17
	Wet	3.1	2.28

Figures 2 through 4 illustrate the modeled clearance orbits in the presence of the arrestor bed. The clearances are worse for the wet (perfectly conducting) cases. Some clearance restrictions might appear due to the presence of the arrestor bed.

The effects of a uniform layer of snow up to 3 feet deep on the arrestor were also incrementally modeled to see if it would have any impact on the guidance. Little change was observed on the approaches; while the pattern on the clearances changed, the impact on restrictions remained about the same. Figures 5 and 6 illustrate the effect on the Runway 22 LDA performance of 1 and 3 feet of wet snow on the concrete arrestor.

CONCLUSIONS: Mathematical modeling indicates that the concrete arrestor beds will have negligible effect in the localizer approach region within ±10° of centerline. The arrestor may have some impact in the localizer clearance region, which may result in restrictions on the use of the localizer beyond ±10° from centerline. Based upon modeling results, a uniform layer of snow up to 3 feet deep should have little effect on localizer performance.

Flight checks are recommended to validate these conclusions.

If you have any questions about this modeling or for any other modeling requirements we can assist you with, please contact Jesse Jones by telephone at (609) 485-4573 or FAX at (609) 485-5451.

John Townsend
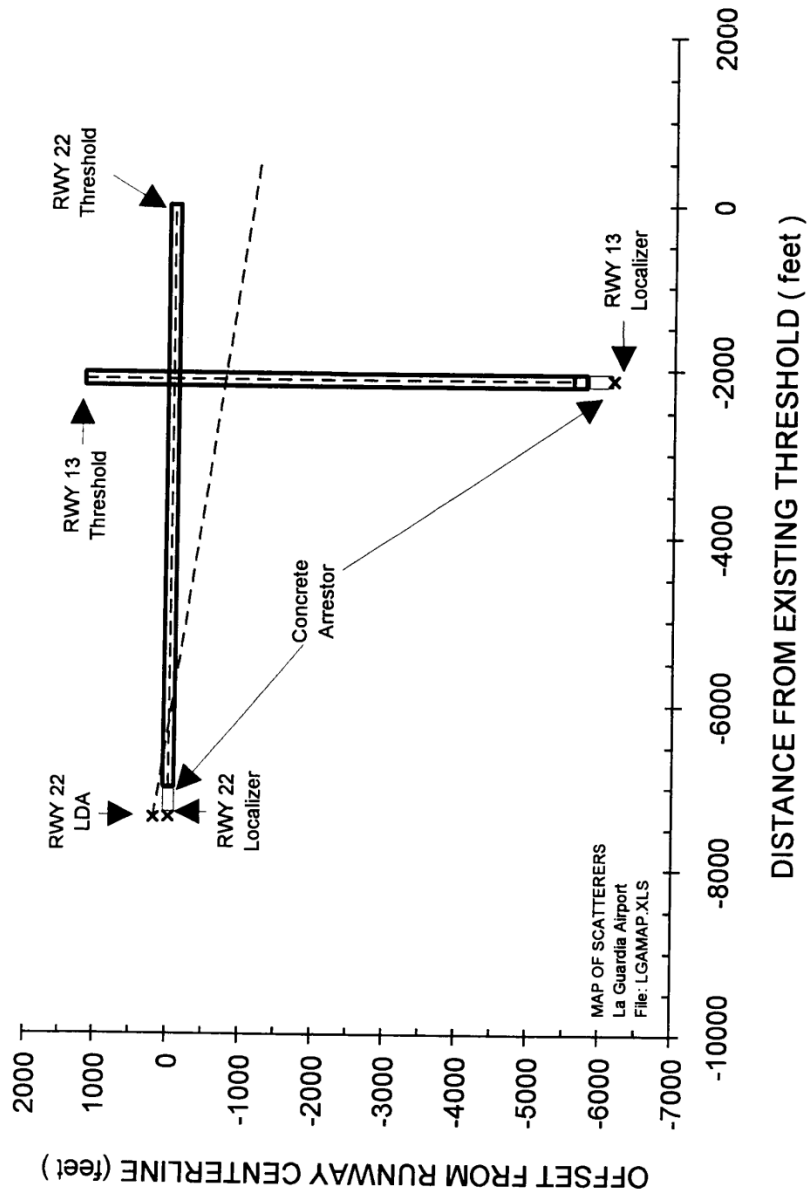
cc:
Gary Skillicorn, AND-740

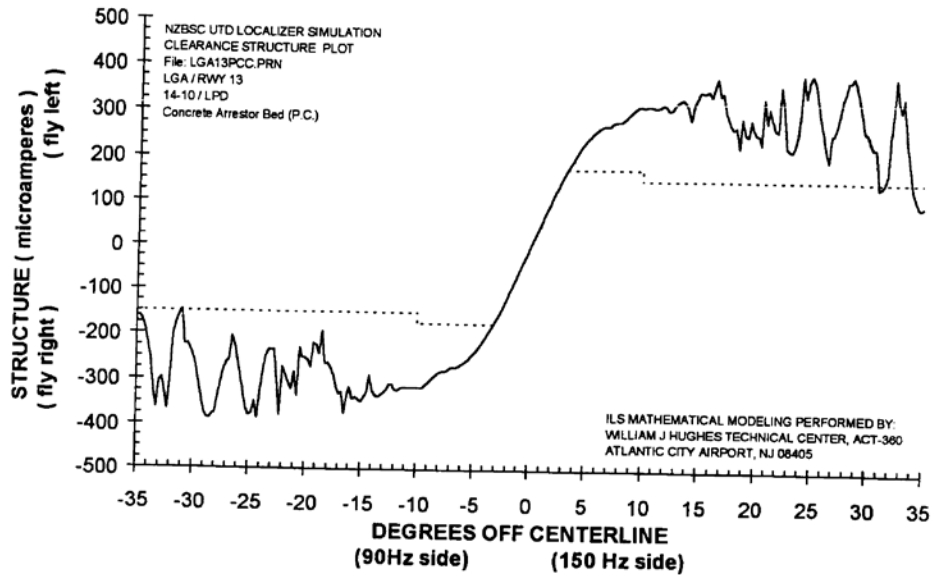Figure 1. Layout of Modeled Structures at La Guardia Airport.

Figure 2a. Clearance Orbit for LaGuardia Runway 13
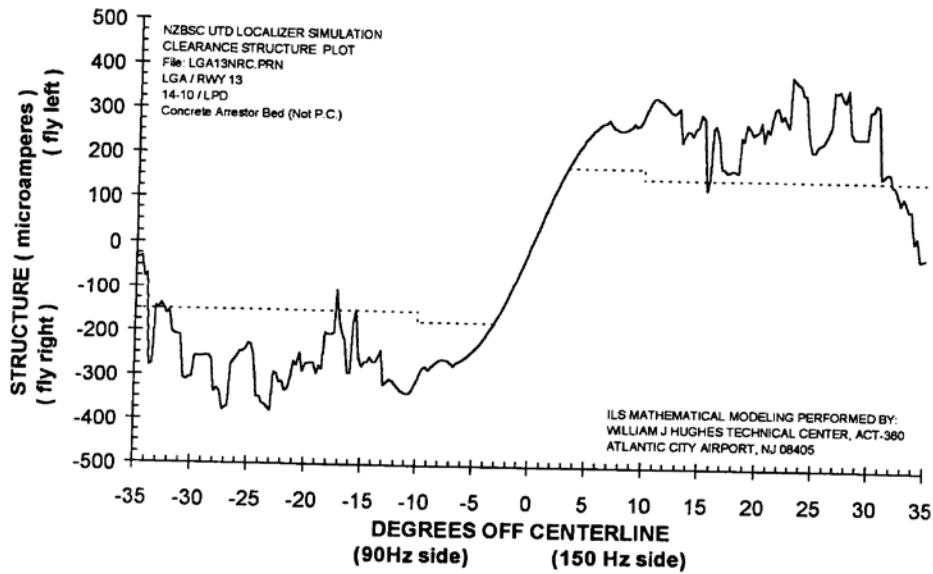Wet Concrete Arrestor.

Figure 2b. Clearance Orbit for LaGuardia Runway 13
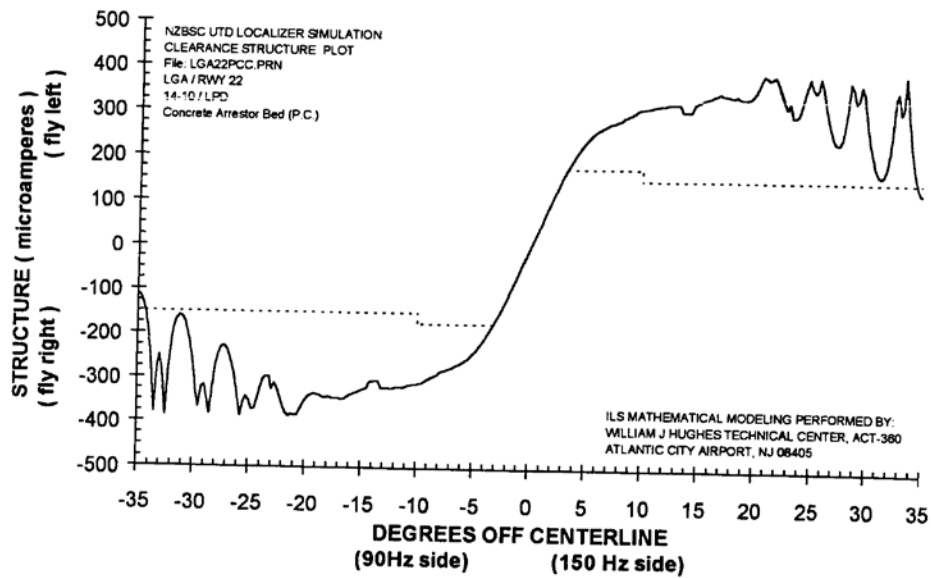Dry Concrete Arrestor.

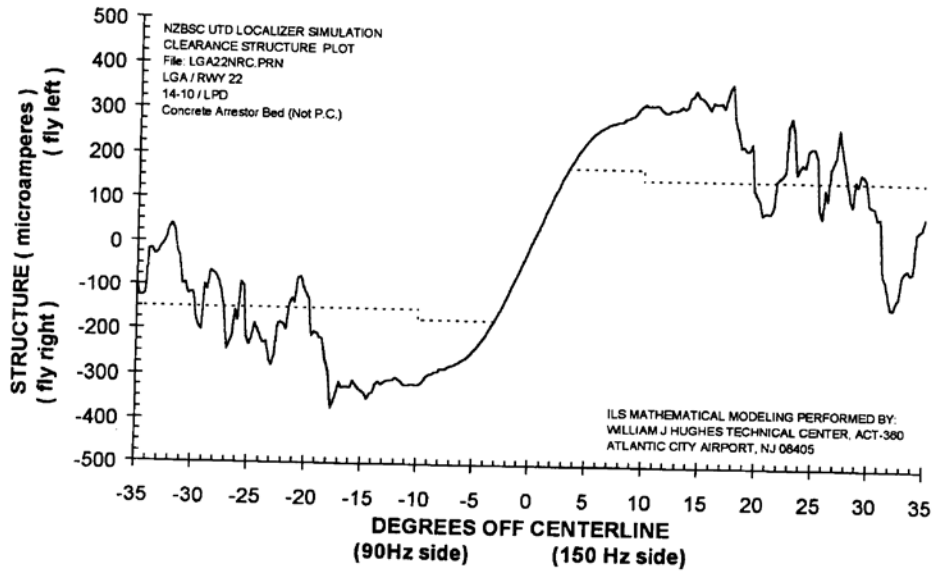Figure 3a. Clearance Orbit for LaGuardia Runway 22
Wet Concrete Arrestor.

Figure 3b. Clearance Orbit for LaGuardia Runway 22
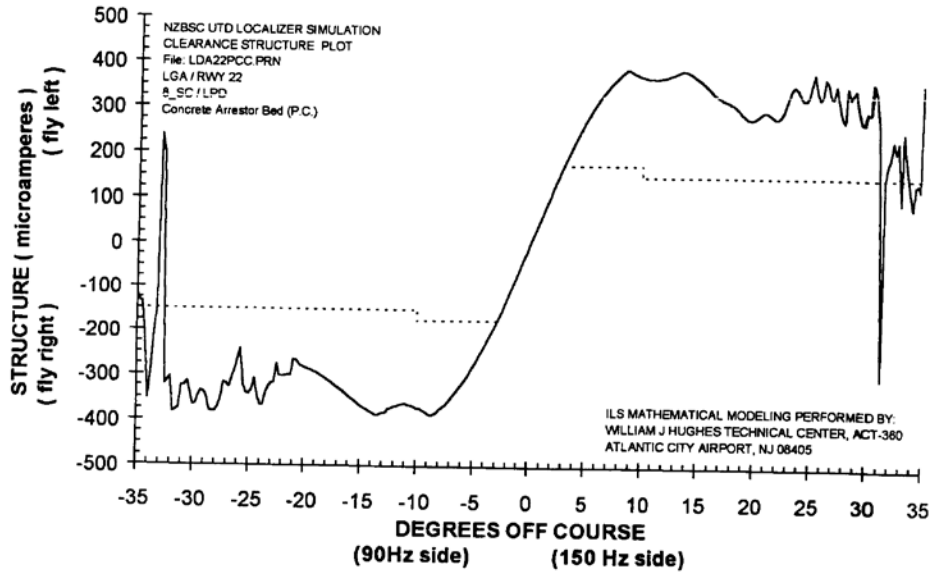Dry Concrete Arrestor.

Figure 4a. Clearance Orbit for LaGuardia Runway 22 LDA
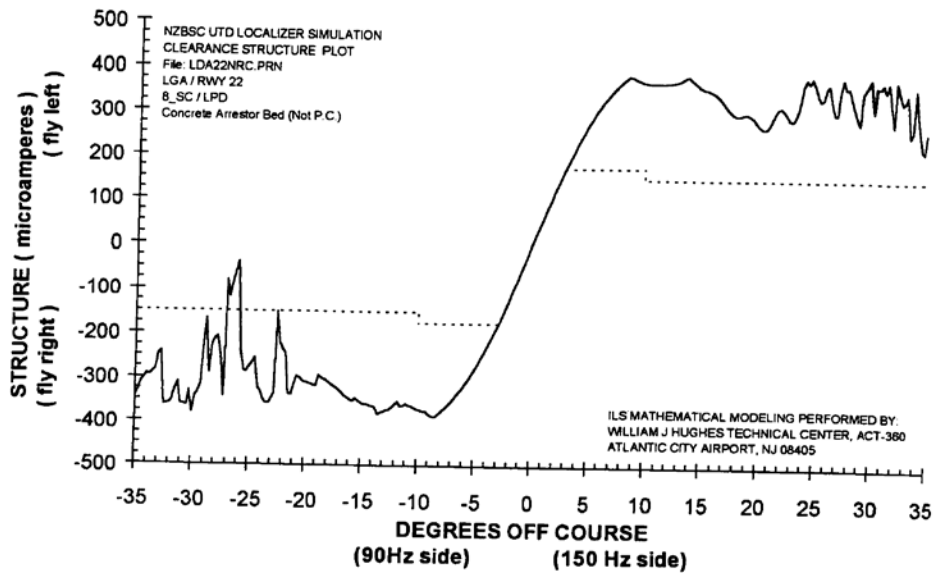Wet Concrete Arrestor.

Figure 4b. Clearance Orbit for LaGuardia Runway 22 LDA
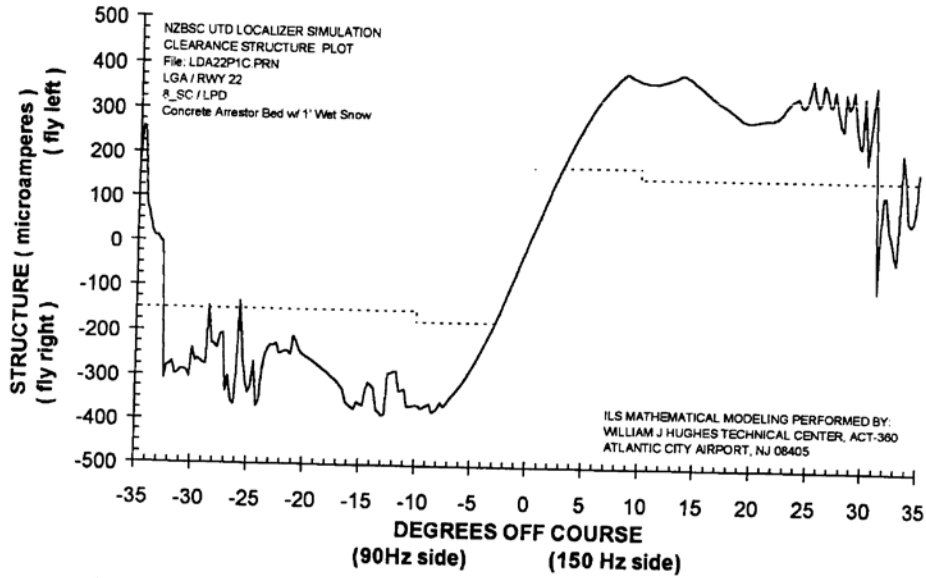Dry Concrete Arrestor.

Figure 5. Clearance Orbit for LaGuardia Runway 22 LDA
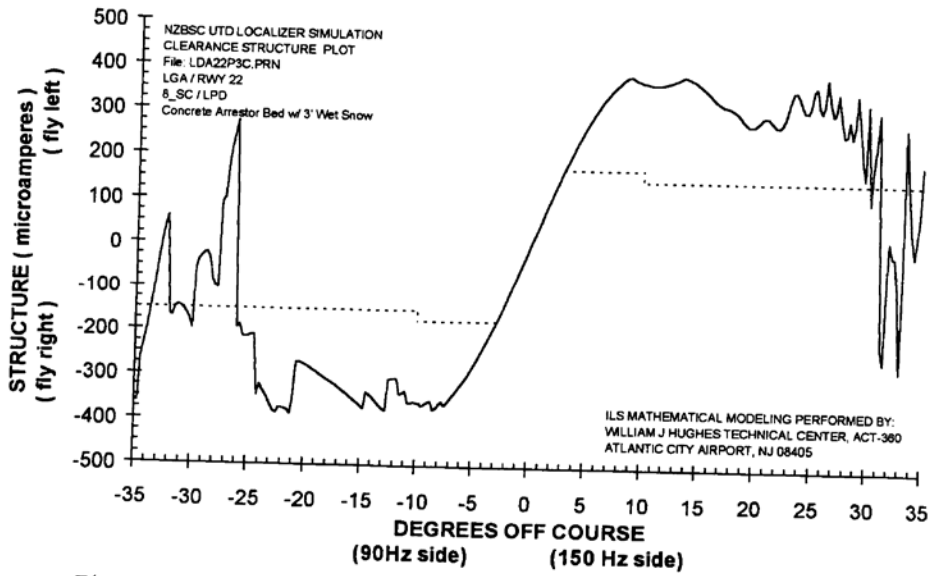Concrete Arrestor with 1 Foot of Wet Snow.

Figure 6. Clearance Orbit for LaGuardia Runway 22 LDA
Concrete Arrestor with 3 Feet of Wet Snow.

APPENDIX C—SUMMARY OF MEASURED DATA AND RECOMMENDATIONS FOR TESTING ON PLATFORM BEHIND FEDERAL AVIATION ADMINISTRATION WIND TUNNEL

Summary of Measured Data and
Recommendations for Testing on Platform Behind FAA Wind Tunnel

Geoffrey J. Frank
28 September 2000

On September 20, 2000 data was acquired behind the FAA's wind tunnel to determine if conditions behind the wind tunnel could be used to represent conditions measured on the Runway 22 Overrun Area at LaGuardia Airport (LGA)[1]. This data was acquired on top of the platform recently constructed behind the wind tunnel. The data are summarized in Section 1. The data were correlated with data measured at LGA and used to estimate equivalent exposure times that could be used to represent the conditions at LGA. The estimated exposure times are presented in Section 2.

1 Data Acquisition

Data was acquired behind the FAA's wind tunnel to determine if conditions behind the wind tunnel could be used to represent conditions measured on the Runway 22 Overrun Area at LaGuardia Airport (LGA)[1]. Data were acquired at three locations to map wind speed, temperature, ground vibration, sound pressure level (SPL), and lift pressure on the platform that has been fabricated behind the wind tunnel. The three locations at which data were acquired are:

Location 1 – on the flat portion of the platform just behind the ramp;
Location 2 – in the middle of the platform;
Location 3 – at the back of the platform.

The instruments used for the first set of measurements were mounted to a plywood base. The plywood base was directly attached to the cement top of the platform. This mounting system resulted in wind speed measurements 16 inches above the ground, temperature measurements 12 inches above the ground, and sound pressure measurements 4 inches above the ground. Vibration measurements were made at Location 1 only with an accelerometer mounted directly to the platform near Location 1. The instrumentation with the plywood base is shown in Figure 1. A second set of measurements was made to acquire uplift pressure data. This data was also acquired using instruments attached to a plywood base. The instrumentation used for measuring uplift pressure is shown in Figure 2.

---

[1] See G.J. Frank and M.P. Bouchard, "Vibration, Pressure, Wind Speed, and Temperature Measurements on Runway 22 Overrun Area at LaGuardia Airport," UDR-TR-2000-00083, University of Dayton Research Institute, August, 2000 for a summary of the conditions measured at LGA.

For the first set of measurements (wind speed, temperature, acoustic pressure and ground vibration) each of the instrumentation channels was sampled at 2,000 samples per second. Windows of 250 data points (corresponding to 1/8-second of data) were used to compute values in standard engineering units, which were stored in a data file. Voltages measured from the wind speed and temperature transducers were used to compute averages over each 1/8-second window. The average voltages were then converted to wind speed (in miles per hour) and temperature (in degrees Fahrenheit) and stored to the data file. Voltages from the accelerometer and microphone were passed through an electronic 3-Hz high-pass filter and then used to compute root-mean-square (RMS) averages. The acceleration level (in g's) and the sound pressure level (in dB) were computed from the RMS averages and stored in the data file. Typical measured data are shown in Figure 3. The data were recorded as the wind tunnel speed was increased from idle to full power. Data was recorded at 4 engine settings: idle, 70% rated speed, 85% rated speed, and 100% rated speed.

For the second set of measurements (uplift pressure), the data were sampled at 2,000 samples per second. Windows of 250 data points (corresponding to 1/8-second of data) were used to compute values in standard engineering units, which were stored in a data file. Voltages measured from the pressure transducer were used to compute averages over each 1/8-second window. The average voltages were then converted to uplift pressure (in psi) and stored to the data file. Typical measured data are shown in Figure 4.

Data such as that shown in Figures 3 and 4 are summarized in Table 1 for each of the three locations. Both maximum values and average values are listed.

2 Estimated Exposure Times Equivalent to Operational Usage at LGA

Based on the data summarized in Table 3 and the data measured at LGA[1], estimates were made of the amount of time required at various power settings to be equivalent to one month's exposure at LGA. The estimates use power settings of 85% rated speed, 90% rated speed, and 100% rated speed on the wind tunnel to give acoustic and wind speed conditions equivalent to specific ranges of conditions identified at LGA. Specifically, a correspondence was made between these power settings and data in the following ranges. The 90% rated speed range has been interpolated from the measured data at 85% and 100%. Corresponding ranges are:

% Rated Speed	Wind Speed Range	Acoustic Level Range
85	80-100 MPH	135-140 dB
90	100-120 MPH	140-145 dB
100	120 MPH and above	145 dB and above

Correlating data from Table 7 of Reference 1 with the ranges in the preceding table, it is possible to obtain estimates of the loading required for one month's equivalent exposure. Two estimates were made. One estimate was determined based on the maximum total time of wind speed or acoustic level in a given range. Table 3 summarizes the estimated time required at each power setting to provide an equivalent month's exposure using the maximum total time. The durations listed in Table 3 should be considered a conservative estimate of the loading. The other estimate was determined by averaging the loading durations from both wind speed and acoustic level in a given range. Table 4 summarizes the estimated time required at each power setting to provide an equivalent month's exposure using the average time assumption. The durations listed in Table 4 are less conservative than those listed in Table 3.

For testing at an equivalent 40 feet from the end of the LGA runway, the total times listed in Tables 3 and 4 have been divided up into cycles. These cycles are shown in Figures 5 (for the conservative loading) and 6 (for the less-conservative loading). The cycles shown in Figures 5 and 6 must be repeated 16 or 12 times, respectively, to achieve an equivalent month's exposure. The high number of repetitions has been chosen to produce short intervals at 100% rated speed, where the temperatures are on the order of 260 °F.
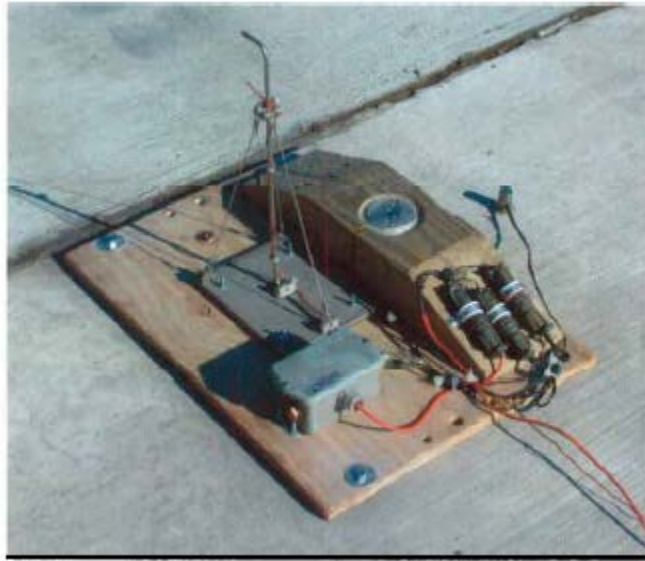
Figure 1. Instrumentation Used Behind Wind Tunnel to Measure Wind Speed, Temperature, Ground Vibrations and Sound Pressure Level

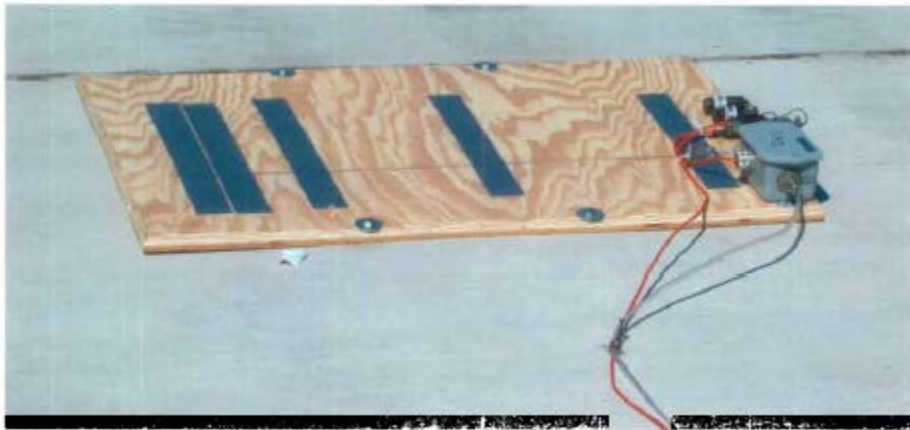Figure 2. Instrumentation Used Behind Wind Tunnel to Measure Uplift Pressure

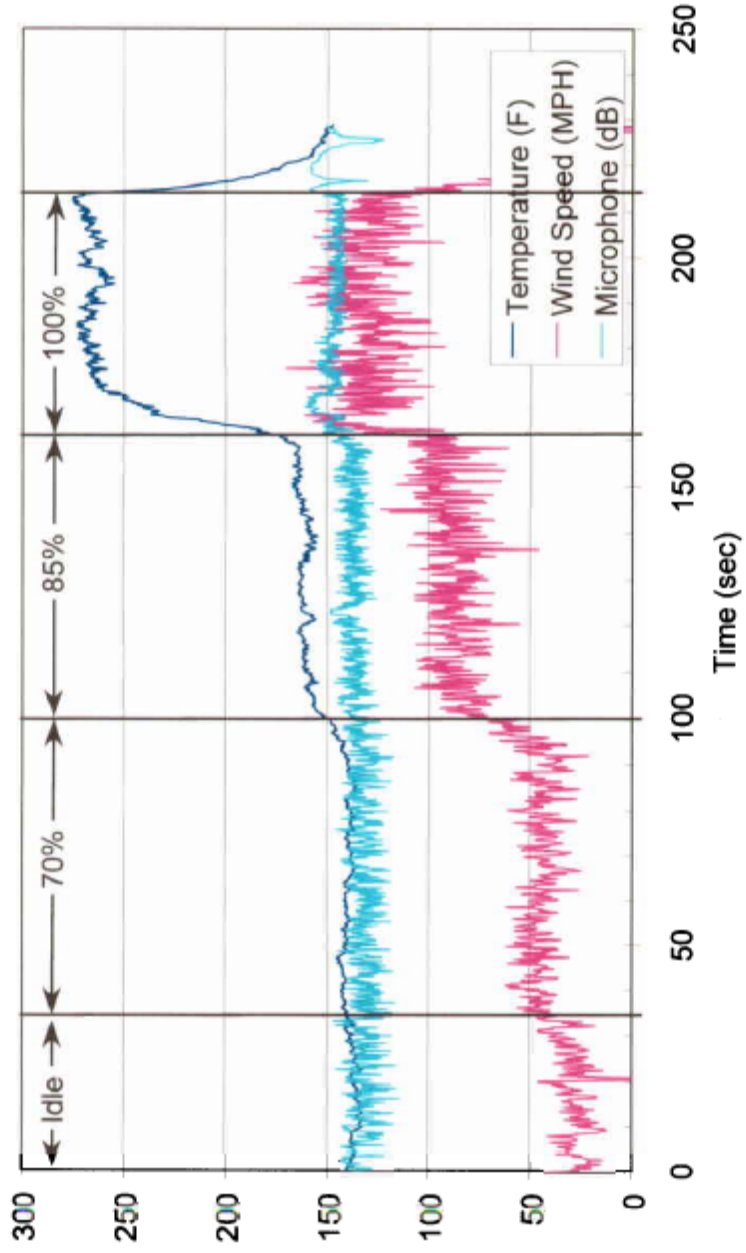Figure 3. Typical Data Showing Wind Speed, Temperature, Ground Vibrations and Sound Pressure Level at Location 1
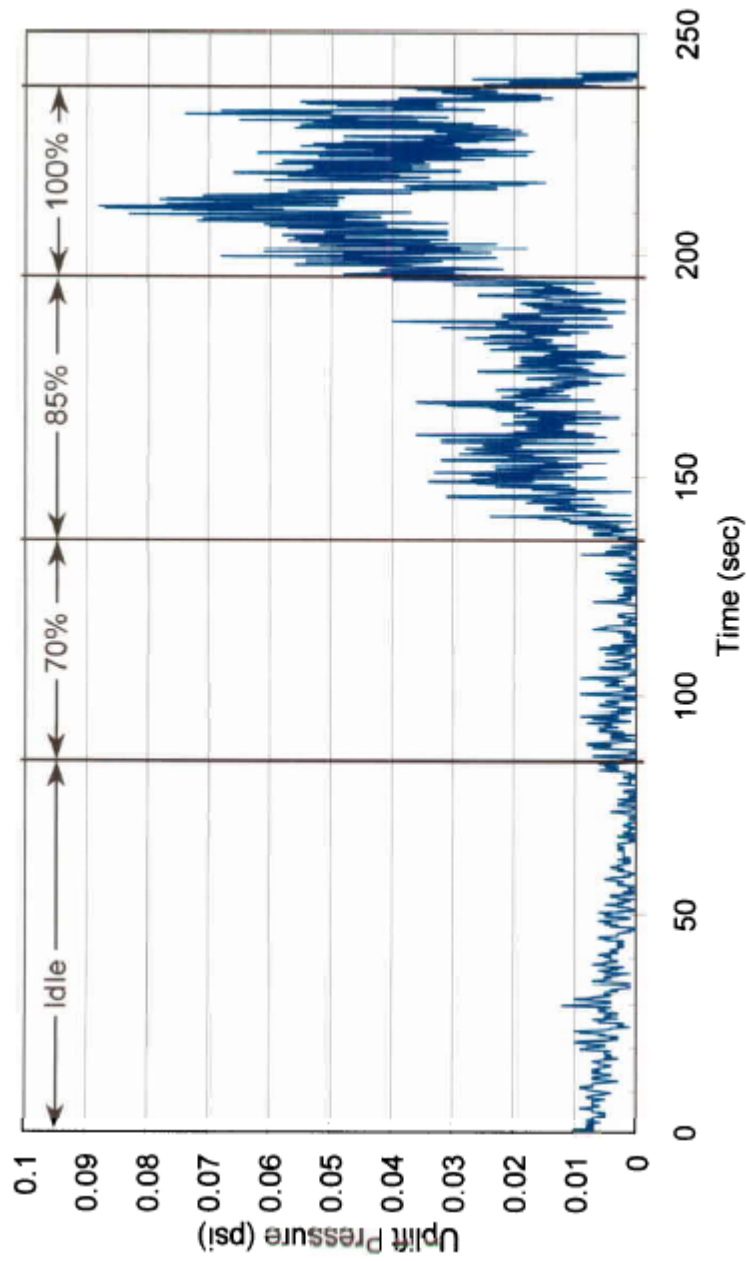
Figure 4. Typical Data Showing Uplift Pressure at Location 1

Recommended Profile for Simulating Exposure 40' from Runway at LGA
Using the FAA Wind Tunnel - Conservative Data Profile
(Repeat this Profile 16 Times for Each Months Equivalent Exposure)

Time (sec)	Power (% Rated Speed)
0	85
240	85
250	90
375	90
380	85
605	85
620	100
635	100
640	85

Figure 5. Recommended Wind Tunnel Setting for Simulating LGA Exposure 40' From End of Runway (Using Conservative Estimates of Loading) – Repeat Profile 16 Times for One Month's Equivalent Exposure
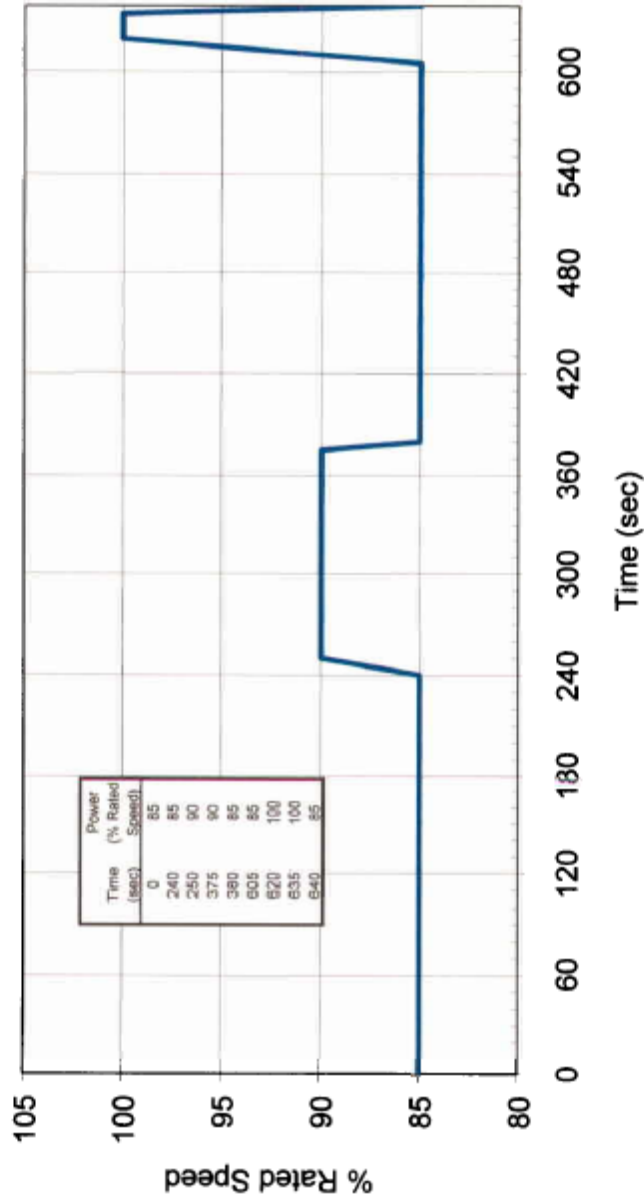
Recommended Profile for Simulating Exposure 40' from Runway at LGA
Using the FAA Wind Tunnel - Average Data Profile
(Repeat this Profile 12 Times for Each Months Equivalent Exposure)

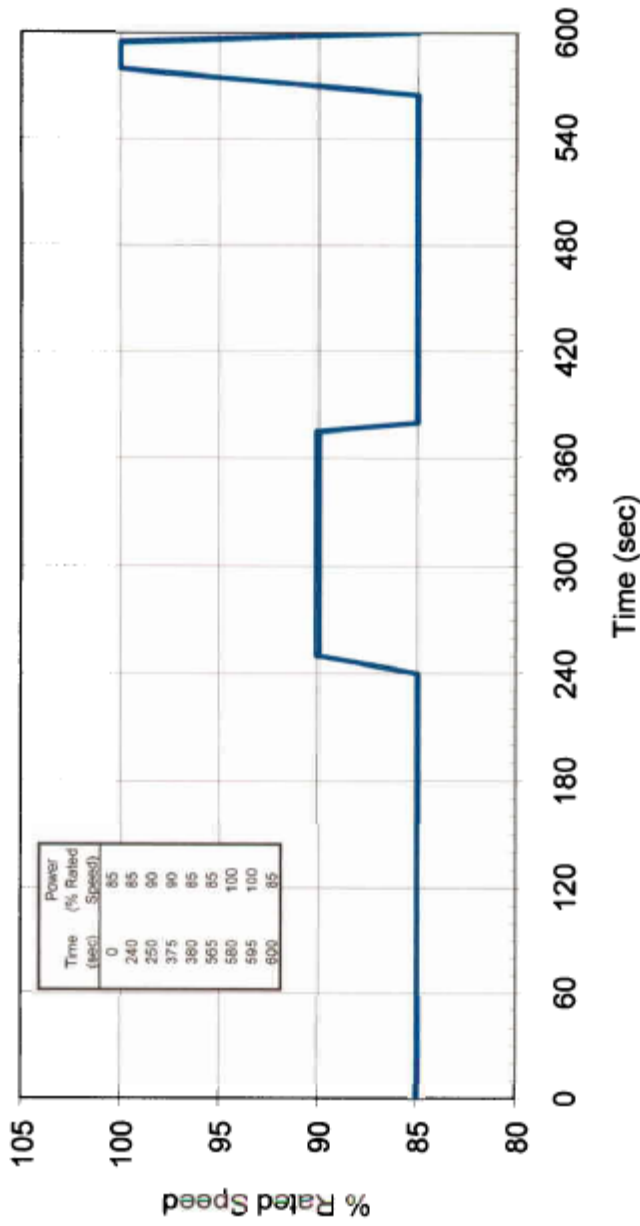| Time (sec)	Power (% Rated Speed)
0	85
240	85
250	90
375	90
380	85
565	85
580	100
595	100
600	85

Figure 6. Recommended Wind Tunnel Setting for Simulating LGA Exposure 40' From End of Runway
(Using Averaged Estimates of Loading) – Repeat Profile 12 Times for One Month's Equivalent Exposure

Table 1. Summary of Conditions on Platform

Location	Power Setting	Average Wind Speed (mph)	Maximum Wind Speed (mph)	Average Temperature (°F)	Maximum Temperature (°F)	Average SPL (dB ref 20E-6 Pa)	Maximum SPL (dB ref 20E-6 Pa)	Average Ground Vibration (Gms)	Maximum Ground Vibration (Gms)
1	idle	27.3	46.1	135.8	140.5	132.6	143.4	0.003	0.009
1	70%	44.8	61.9	139.5	142.9	132.0	143.2	0.006	0.017
1	85%	88.4	123.7	161.2	165.6	136.7	146.6	0.015	0.037
1	100%	131.5	170.2	265.8	273.7	146.8	156.3	0.091	0.160
2	idle	NA	NA	NA	NA	NA	NA	NA	NA
2	70%	31.4	55.8	139.5	142.2	129.4	141.5	NA	NA
2	85%	82.7	110.5	160.8	165.5	135.0	147.2	NA	NA
2	100%	124.8	155.1	265.1	271.7	144.6	154.3	NA	NA
3	idle	0.5	23.0	132.6	138.8	129.5	145.8	NA	NA
3	70%	25.6	52.9	136.9	142.1	130.4	142.7	NA	NA
3	85%	73.1	98.1	155.5	162.5	134.1	147.6	NA	NA
3	100%	111.9	144.1	256.2	267.5	143.6	154.2	NA	NA

NA = data not available for this sensor at this condition

Table 2. Summary of Uplift Pressure Data

Location	Power Setting	Average Uplift Pressure (psi)	Maximum Uplift Pressure (psi)
1	idle	0.004	0.012
1	70%	0.003	0.009
1	85%	0.016	0.040
1	100%	0.044	0.088
2	idle	0.008	0.013
2	70%	0.014	0.020
2	85%	0.028	0.043
2	100%	0.044	0.078
3	idle	0.002	0.007
3	70%	0.009	0.012
3	85%	0.018	0.027
3	100%	0.027	0.043

Table 3. Estimates of Exposure Times Behind Wind Tunnel Equal to 1 Month Operation at LGA - Conservative Estimate

Power Setting	Equivalent Exposure Time for EMAS Bed 40 Feet from End of Runway (second/month operation)	Equivalent Exposure Time for EMAS Bed 115 Feet from End of Runway (second/month operation)	Equivalent Exposure Time for EMAS Bed 190 Feet from End of Runway (second/month operation)
85% rated speed	7,900	3,200	1,400
92% rated speed	2,000	600	180
100% rated speed	350	45	0

Table 4. Estimates of Exposure Times Behind Wind Tunnel Equal to 1 Month Operation at LGA - Estimate Based on Average Values

| Power Setting	Equivalent Exposure Time for EMAS Bed 40 Feet from End of Runway (second/month operation)	Equivalent Exposure Time for EMAS Bed 115 Feet from End of Runway (second/month operation)	Equivalent Exposure Time for EMAS Bed 190 Feet from End of Runway (second/month operation)
85% rated speed	5,500	2,200	720
92% rated speed	1,500	340	60
100% rated speed	185	25	0

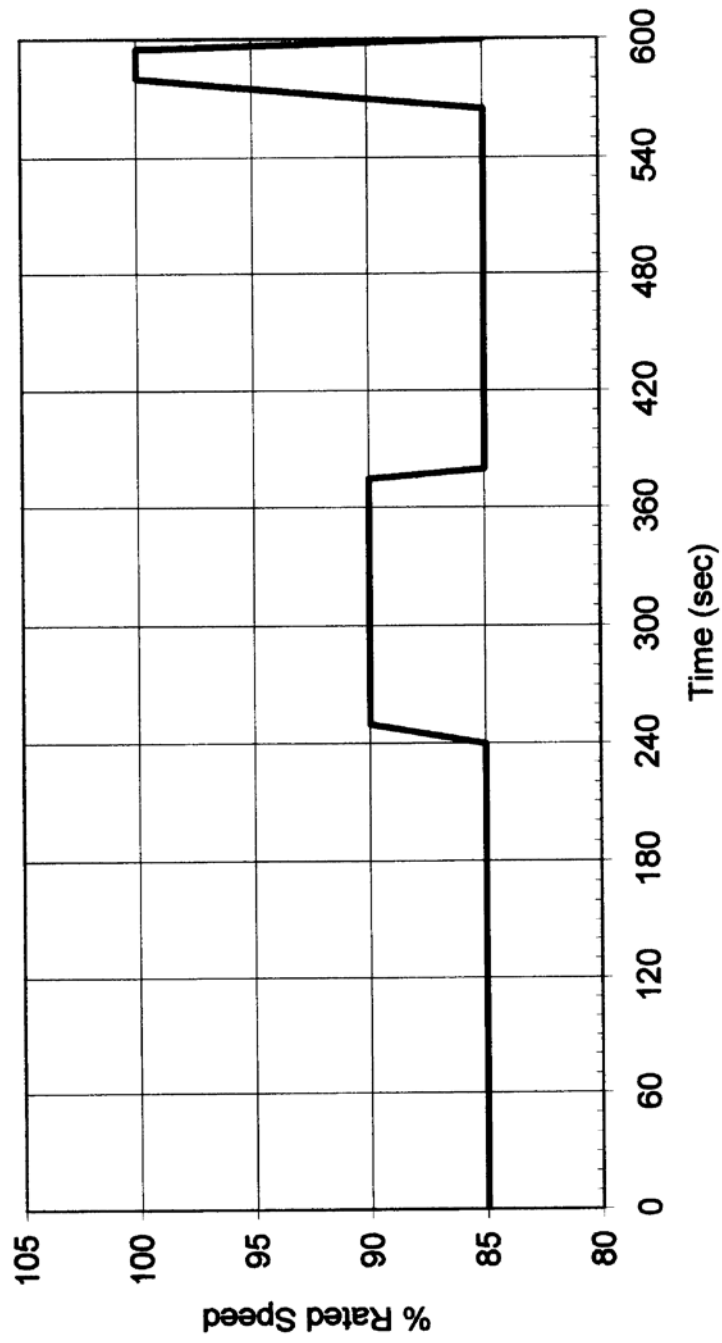Recommended profiles for simulating LGA conditions using FAA Wind tunnel

Conservative - 40' 16 repetition/month		Average - 40' 12 repetition/month		Conservative - 75' 14 repetition/month		Average - 75' 10 repetition/month		Conservative - 115' 8 repetition/month		Average - 115' 6 repetition/month	
Time (sec)	Power (% Rated Speed)	Time (sec)	Power (% Rated Speed)	Time (sec)	Power (% Rated Speed)	Time (sec)	Power (% Rated Speed)	Time (sec)	Power (% Rated Speed)	Time (sec)	Power (% Rated Speed)
0	85	0	85	0	85	0	85	0	85	0	85
240	85	240	85	180	85	180	85	180	85	180	85
250	90	250	90	190	90	190	90	190	90	190	90
375	90	375	90	280	90	280	90	265	90	240	90
380	85	380	85	290	85	290	85	275	85	250	85
605	85	565	85	485	85	470	85	445	85	395	85
620	100	580	100	500	100	485	100	460	100	410	100
635	100	595	100	515	100	495	100	465	100	415	100
640	85	600	85	520	85	510	85	480	85	430	85

Recommended Profile for Simulating Exposure 40' from Runway at LGA
Using the FAA Wind Tunnel - Conservative Data Profile
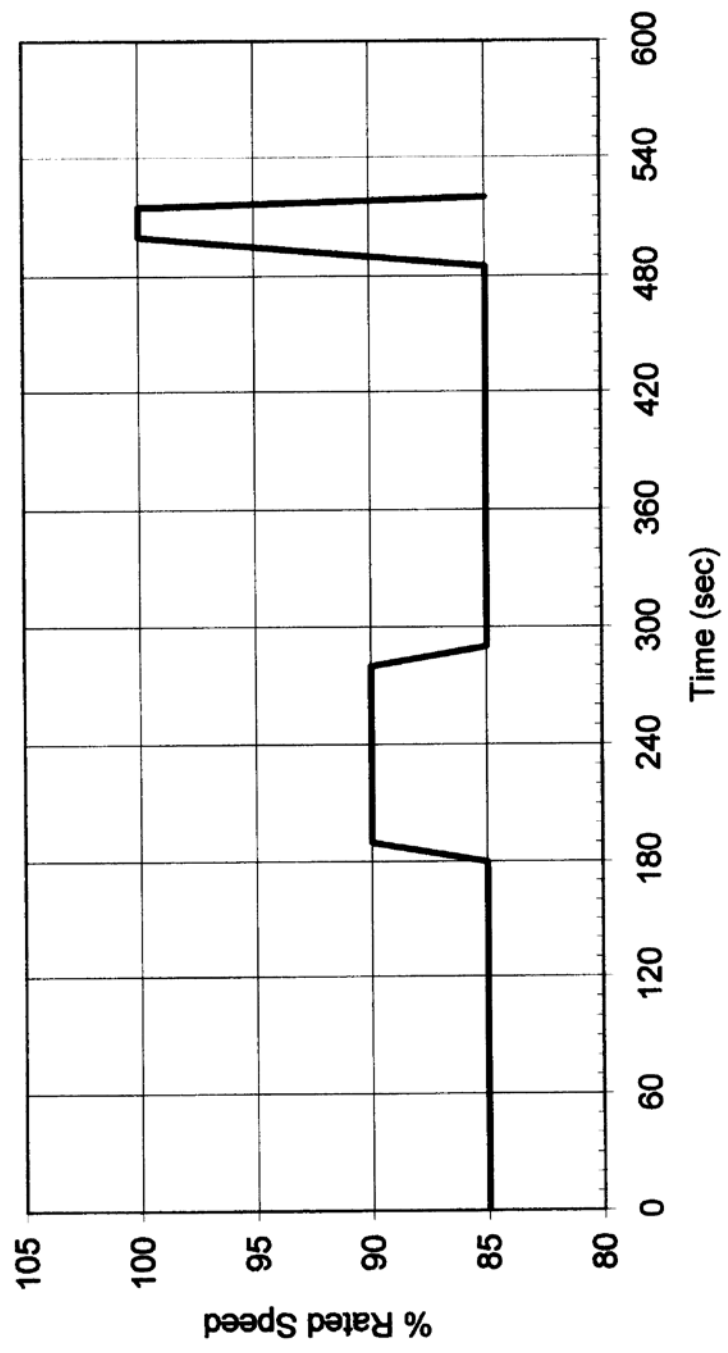(Repeat this Profile 16 Times for Each Month's Equivalent Exposure)
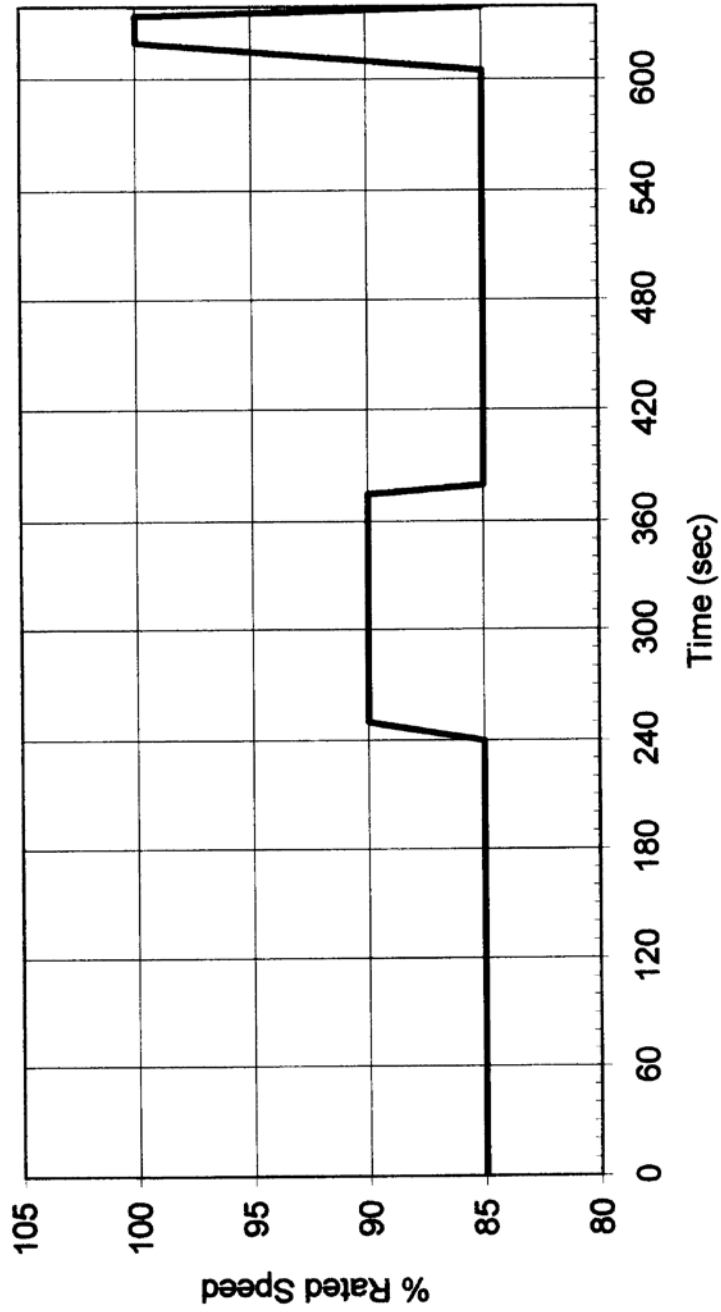
Recommended Profile for Simulating Exposure 40' from Runway at LGA
Using the FAA Wind Tunnel - Average Data Profile
(Repeat this Profile 12 Times for Each Month's Equivalent Exposure)

Recommended Profile for Simulating Exposure 75' from Runway at LGA
Using the FAA Wind Tunnel - Average Data Profile
(Repeat this Profile 14 Times for Each Month's Equivalent Exposure)
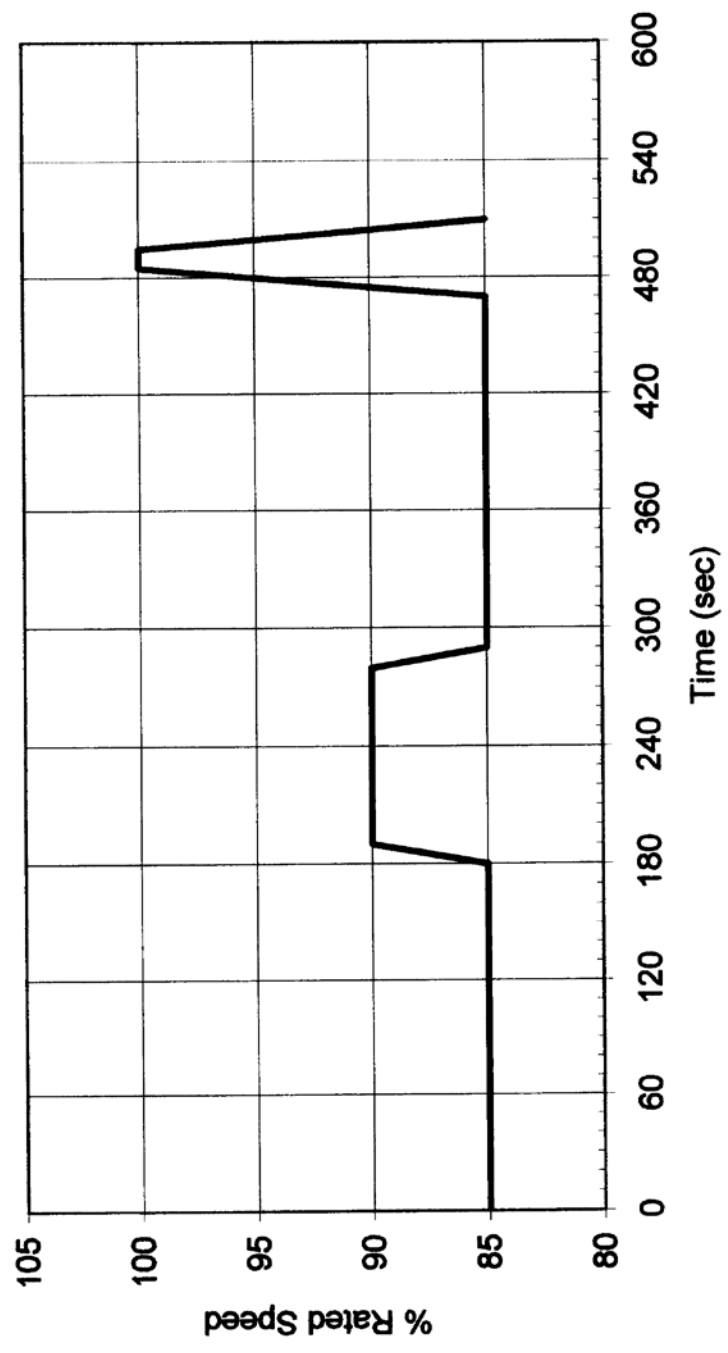
? CONSERVATIVE

Time (sec)

% Rated Speed

Recommended Profile for Simulating Exposure 75' from Runway at LGA
Using the FAA Wind Tunnel - Average Data Profile
(Repeat this Profile 10 Times for Each Month's Equivalent Exposure)

Recommended Profile for Simulating Exposure 115' from Runway at LGA
Using the FAA Wind Tunnel - Average Data Profile
(Repeat this Profile 8 Times for Each Month's Equivalent Exposure)
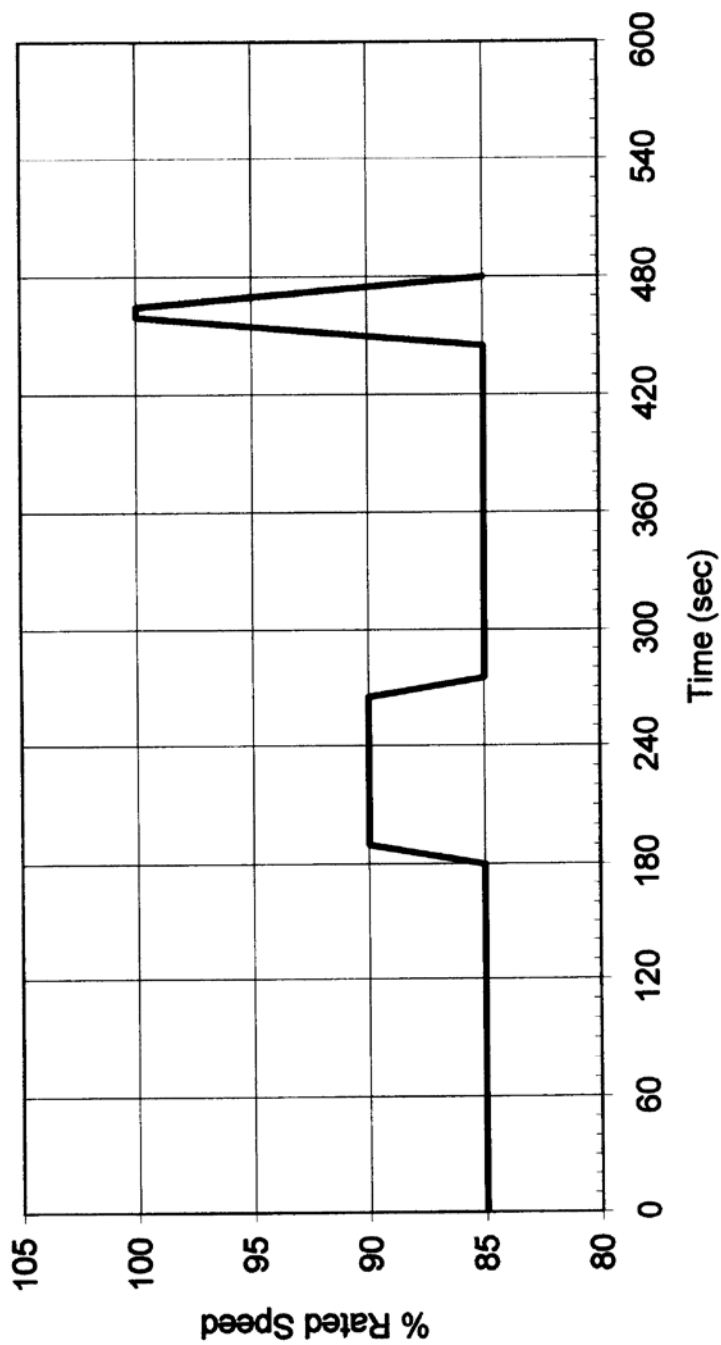
D-5

Estimates of Exposure Times Behind Wind Tunnel Equal to 1 Month Operation at LGA - Conservative Estimate

Power Setting	Equivalent Exposure Time for EMAS Bed 40 Feet from End of Runway (second/month operation)	Equivalent Exposure Time for EMAS Bed 115 Feet from End of Runway (second/month operation)	Equivalent Exposure Time for EMAS Bed 190 Feet from End of Runway (second/month operation)	Equivalent Exposure Time for EMAS Bed 75 Feet from End of Runway (second/month operation)
85% rated speed	7,900	3,200	1,400	5,700
92% rated speed	2,000	600	180	1,350
100% rated speed	350	45	0	210

Estimates of Exposure Times Behind Wind Tunnel Equal to 1 Month Operation at LGA - Estimate Based on Average Values

Power Setting	Equivalent Exposure Time for EMAS Bed 40 Feet from End of Runway (second/month operation)	Equivalent Exposure Time for EMAS Bed 115 Feet from End of Runway (second/month operation)	Equivalent Exposure Time for EMAS Bed 190 Feet from End of Runway (second/month operation)	Equivalent Exposure Time for EMAS Bed 75 Feet from End of Runway (second/month operation)
85% rated speed	5,500	2,200	720	4,000
92% rated speed	1,500	340	60	960
100% rated speed	185	25	0	110

Location	Power Setting	Average Wind Speed (mph)	Maximum Wind Speed (mph)	Average Temperature (°F)	Maximum Temperature (°F)	Average SPL (dB ref 20E-6 Pa)	Maximum SPL (dB ref 20E-6 Pa)	Average Ground Vibration (Grms)	Maximum Ground Vibration (Grms)
1	idle	27.3	46.1	135.8	140.5	132.6	143.4	0.003	0.009
1	70%	44.8	61.9	139.5	142.9	132.0	143.2	0.006	0.017
1	85%	88.4	123.7	161.2	165.6	136.7	146.6	0.015	0.037
1	100%	131.5	170.2	265.8	273.7	146.8	156.3	0.091	0.160
2	idle	NA	NA	NA	NA	NA	NA	NA	NA
2	70%	31.4	55.8	139.5	142.2	129.4	141.5	NA	NA
2	85%	82.7	110.5	160.8	165.5	135.0	147.2	NA	NA
2	100%	124.8	155.1	265.1	271.7	144.6	154.3	NA	NA
3	idle	0.5	23.0	132.6	138.8	129.5	145.8	NA	NA
3	70%	25.6	52.9	136.9	142.1	130.4	142.7	NA	NA
3	85%	73.1	98.1	155.5	162.5	134.1	147.6	NA	NA
3	100%	111.9	144.1	256.2	267.5	143.6	154.2	NA	NA

ENGINEERED MATERIAL ARRESTOR SYSTEMS JET
BLAST RESISTANT COATING EVALUATION

R. F. Cook

July 27, 2001

Galaxy Scientific Corporation
2500 English Creek Avenue, Bldg. C
Egg Harbor Twp., NJ 08234-5562

1

TABLE OF CONTENTS

LIST OF FIGURES

ENGINEERED MATERIAL ARRESTOR SYSTEMS JET BLAST RESISTANT COATINGS

INTRODUCTION

An entirely passive arrestor system for safely stopping commercial aircraft resulting from a runway overrun is being developed. The first such arrestor was installed at JFK International Airport in 1996. That arrestor demonstrated its design objective by safely stopping a SAAB 340 aircraft, traveling at high speed, after it passed the runway end.

As with any new technology, over time some problems become apparent. The Engineered Material Arrestor System (EMAS) was found to be susceptible to water intrusion due to failure of the finish waterproofing coating that is applied after the EMAS basic material is installed. It was also found that the severe aircraft jet blast in the area where the EMAS is installed could rapidly erode the EMAS material. The Engineered Arresting Systems Corporation (ESCO) that produces the EMAS is proposing a tested jet blast resistant (JBR) coating as a solution to these two problems. The purpose of this report is to comment on the JBR coating in terms of overall EMAS performance.

The basic EMAS material (a controlled strength cellular cement (CC)) is formed as blocks, generally four feet square and heights ranging from six inches to 30 inches. The proposed solution is to place a 5/16 inch thick fiber glass reinforced cement plate and a ¼ inch thick soft polyester foam layer under the plate on top of the basic block. A like cement plate is also placed on the bottom of the block. The entire block is then wrapped with a polyester scrim and sealed to prevent water intrusion. This is the jet blast resistant coating.

The current mathematical model used in performing aircraft braking performance while in the EMAS assumes the EMAS material is essentially homogeneous throughout and that the material strength is a given. The introduction of the above materials on the top surface to prevent moisture intrusion and erosion of the EMAS material tends to violate these assumptions and must be taken into account or it must be shown that the addition of these materials is insignificant in terms of EMAS braking performance.

An extensive environmental safety area study, a FAA wind-tunnel EMAS durability test, limited size EMAS installation at LaGuardia and small wheel loads test program to determine the structural integrity of this solution has been conducted. Some of the results are presented in this report.

SAFETY AREA ENVIRONMENT

For a solution to the above-mentioned problems it was necessary to determine the EMAS environment produced by aircraft jet exhaust using the runway for takeoff and landing. A study was conducted to determine jet exhaust speed and duration, temperature, acoustic and acceleration information in the area to be occupied by the EMAS. ESCO and the

2

FAA established a program to test the encapsulated EMAS blocks in the significant parts of this environment. This program is underway in the FAA wind-tunnel and thus far it has shown the proposed coating solution to be satisfactory.

An additional test being conducted at LaGuardia with an abbreviated EMAS has, thus far, also shown the proposed EMAS JBR coating to be acceptable in the true environment. The durability issue of the EMAS in the runway safety area appears to be satisfied.

SMALL WHEEL TEST

A small wheel test program was conducted to determine if the current computer simulation model used in predicting aircraft performance in the EMAS is still accurate or if modifications to the code are required. The program was based on the assumption that only small aircraft wheel loads would likely be affected by the addition of the EMAS JBR coating. The test consisted of pulling an instrumented wheel with a 19.5 x 6.75-8 King Air aircraft tire through several EMAS test beds at three different speeds; very slow, 15 knots and 30 knots. The test rig is shown below. Video coverage of the tests is available.
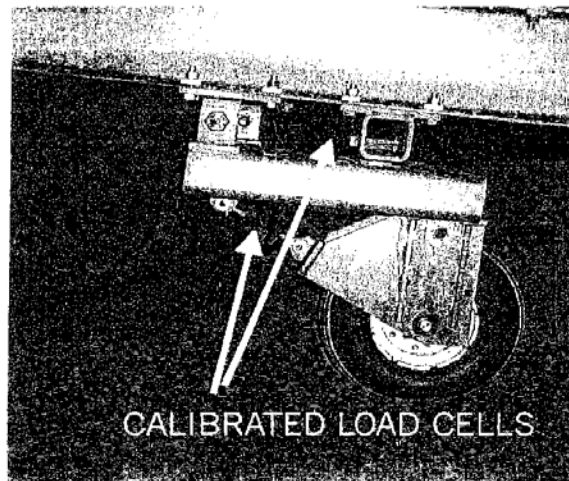

CALIBRATED LOAD CELLS

FIGURE 1 TEST RIG

Tests were conducted with JBR coated and uncoated blocks to determine any significant differences in vertical and drag loads. The mass above the wheel was adjusted to give about 3800 pounds vertical load in a static mode. This weight was selected by estimating the Beech 1900C aircraft wheel loads (since it is about the smallest commuter now operating) and it was found that the single main wheel load was about 3800 pounds at maximum take off weight. This weight is reduced as drag loads are applied due to the test rig design and may go as low as 3000 pounds.

3

Instrumentation was installed on the test rig to measure the vertical and drag wheel loads during each of the tests. Tire pressure was approximately 100 psi. Load cells were located as shown on the above photograph. Incremental loads were applied in the vertical and drag directions and measured with accurate scales to calibrate the load cells on the test rig. The load cell output was recorded and the proper calibration factors determined to convert recorded information to true vertical and drag loads.

TEST RESULTS

Three test bed configurations were tested. All used the basic "60 psi" strength cellular cement blocks. Figure 2 shows the beds used for the higher speed tests (15 and 30 knots). It should be noted that there are variations in the strengths of individual blocks in the test beds and there were also differences in the bed heights between the JBR coated and the uncoated beds. The uncoated beds were about 1 inch lower than the JBR coated beds because of the added layers for the JBR coating.

The slow speed tests were conducted on test beds using only three 8 inch high blocks (12 feet) located at the end of concrete slab that had a 5 inch depression giving a three inch high EMAS exposure to the wheel as it entered.

The computer simulation assumes the block strength is the same for each block but the real manufactured blocks vary in strength. That has been shown in earlier analysis to be insignificant so long as the strength is between the "specification" limits set by the FAA. The one inch (maximum) taller JBR coated bed would be expected to produce a different dynamic response than a one inch lower bed just because of its shape difference so the comparison between coated and uncoated test results is probably biased a little bit. The computer simulations of the test rig were made just for the uncoated test beds.

The first two tests conducted were the slow speed test on JBR coated and uncoated blocks. The primary reason for this test was just to show that the small wheel would penetrate the JBR coating and to get some indication of the gear loads relative to the uncoated bed.
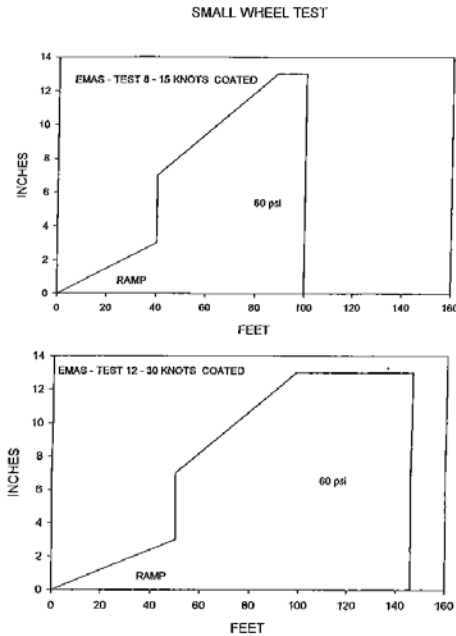
4

SMALL WHEEL TEST

FIGURE 2 TEST BED ELEVATIONS
(Note: the slope of the uncoated 30 knot test bed had a slope of 40 feet)

Figure 3 shows a comparison of the EMAS drag ratio, that is, the value of the drag force divided by the vertical force while in the EMAS. The drag ratio average of the simulation is considerably higher than the drag ratio averages of each of the two tests. (There was no data filtering in these analyses.) The simulation average drag ratio average is about 23 % higher than the average for the uncoated test and about 40 % higher than the JBR coated test. It was found after the coated test that the center block was an "80 psi" block instead of 60 psi. This reduced the penetration and average drag ratio that accounts for much of the difference in drag ratio. The higher simulation drag ratio and dynamic response results require further scrutiny.

Figure 4 presents the drag ratio comparison for the 15 knot tests and simulation. During the uncoated test the wheel sank below axle depth after about 14 seconds so that additional rig frontal area was engulfed in the EMAS and the wheel loads were influenced by this exposure. In order to minimize this effect only the initial responses (to 14.1 seconds) were considered as representative for this test. Comparison of the average drag ratio value for the JBR coated, uncoated and the uncoated simulation shows about a

5

E-7

2 to 6% difference, the JBR coating giving the smallest average drag ratio and highest percentage difference with simulation value although still quite close.

SMALL WHEEL TEST
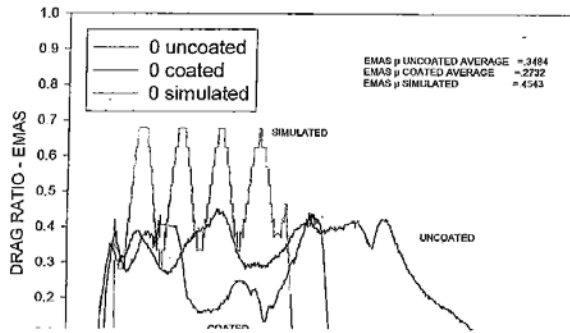0 KNOTS (SLOW) AT ESCO
EMAS 60 PSI

FIGURE 3 EMAS DRAG RATIO – SLOW SPEED

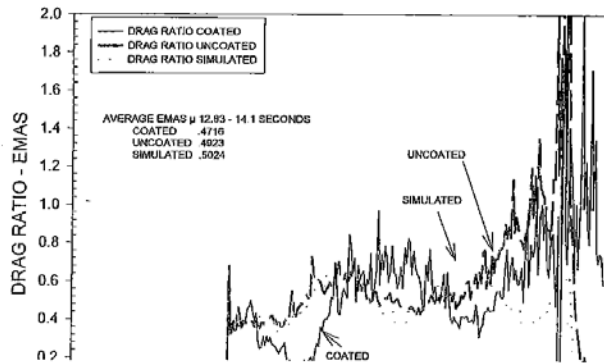SMALL WHEEL TEST
15 KNOTS AT ESCO
EMAS 60 PSI

FIGURE 4 EMAS DRAG RATIO – 15 KNOTS
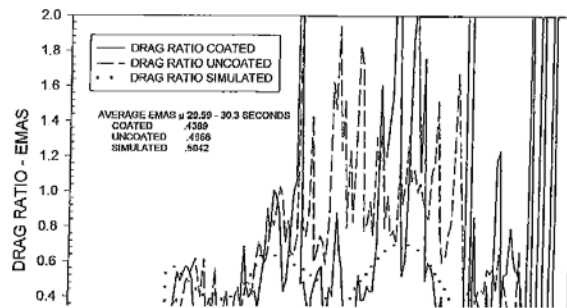
6

SMALL WHEEL TEST
30 KNOTS AT FAA
EMAS 60 PSI

FIGURE 5 EMAS DRAG RATIO – 30 KNOTS

Comparison of the 30 knot drag ratio test data showed similar results as obtained from the 15 knot test. Again the test rig wheel went below the axle depth shortly after the uncoated run began compromising the actual wheel loads; as a result, only the first second of data were averaged. As noted above, the average drag ratio was different for JBR coated, uncoated and simulated with the coated average being the lowest again. The difference between the JBR coated and simulated value was about 14 % and the difference between the uncoated and simulation about 1.5% indicating that the JBR coating does affect the drag ratio but it is still within a reasonable range of the simulation value.

From an EMAS performance standpoint these tests tend to indicate that the JBR coating is significant for small wheel loads and computer simulations should take this into account. It must also be noted, however, that the differences in JBR coated and uncoated are still close from a EMAS performance and gear loads standpoint.

The vertical and drag test data were filtered after the above analysis to remove most of the frequency content above 8 HZ. This was done in order to reduce the local test rig vibration input to load cells. As before, by limiting the time period of 12.8 to 14.1 seconds for the 15 knot test runs and 29.59 to 30.3 seconds for the 30 knot test runs a comparison of wheel loads can be made that are not influenced by other test rig components above the axle.

Figures 6, 7, 8, and 9 show a comparison of vertical and drag test rig loads for JBR coated, uncoated and uncoated simulation of the 15 knot and 30 knot tests. Vertical loads

7

for the 15 knot case were quite close but not as good for the 30 knot case. In a test of this type where the test rig is pulled over a surface with less than smooth elevation profile it is not expected that the "dynamics" will be the same as for a mathematic smooth surface and load values will vary. There were some differences in drag loads, however, that should be noted.
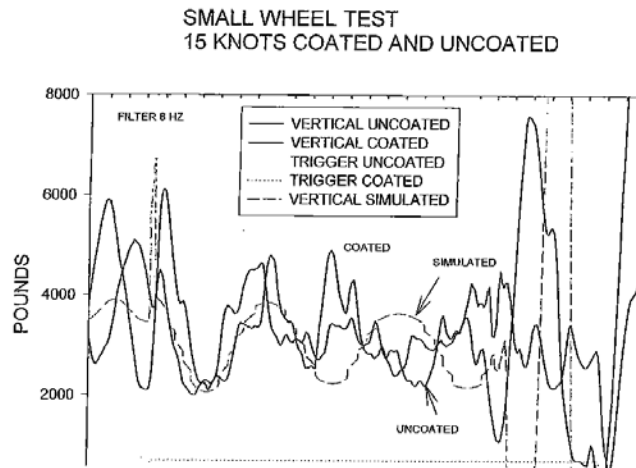
SMALL WHEEL TEST
15 KNOTS COATED AND UNCOATED

FIGURE 6 EMAS WHEEL VERTICAL LOADS – 15 KNOT

It appeared that the drag loads for both the 15 and 30 knot cases exhibited a divergent dynamic characteristic after the selected time periods which was not expected. The front of each test bed is sloped over 48 feet so that more depth of CC material is available to increase the drag load as the wheel progresses up this slope but the drag peaks continued to increase after reaching the maximum CC depth. This is most likely attributable to the test rig configuration and might have damped had a longer bed been available. This should be investigated further. It must also be noted that except for one small area near the end of the bed the wheel did not exceed the axle depth for the JBR coated test beds so most of this data from the test beds is considered good data.

In the drag ratio figures above there were some large spikes. These spikes are attributed to block boundary crossings and instrumentation noise rather than test bed performance. Block boundary crossing, particularly, the JBR coated blocks produce a non-homogeneous condition which will have to be accounted for in the prediction of EMAS performance of small aircraft.
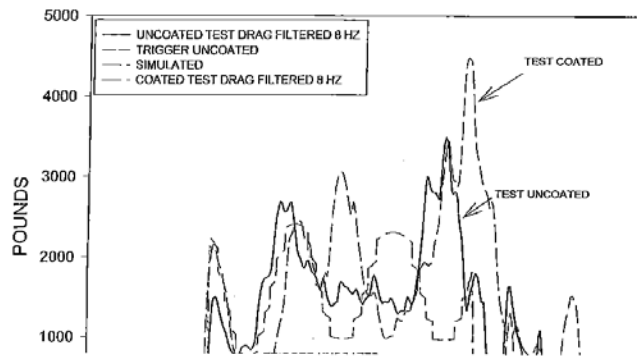
8

SMALL WHEEL TEST
15 KNOT COATED VS UNCOATED

FIGURE 7 EMAS WHEEL DRAG LOADS – 15 KNOT

SMALL WHEEL TEST
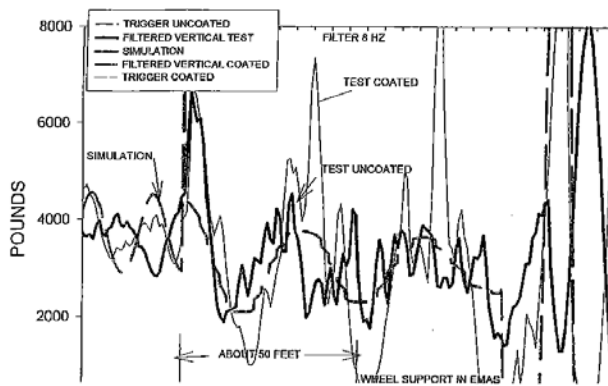COATED TEST 12 VS UNCOATED TEST 11
30 KNOTS

FIGURE 8 EMAS WHEEL VERTICAL LOADS - 30 KNOT

9

SMALL WHEEL TEST
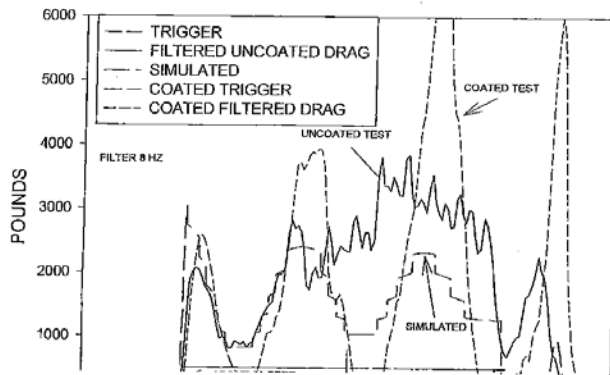COATED TEST 12 VS UNCOATED TEST 11
30 KNOTS

FIGURE 9 EMAS WHEEL DRAG LOADS – 30 KNOTS

SMALL WHEEL TEST
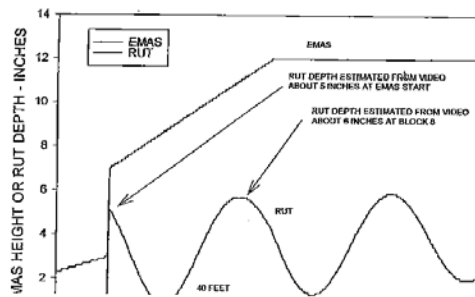30 KNOTS AT FAA
EMAS 60 PSI

FIGURE 10 EMAS WHEEL RUT DEPTH – 30 KNOTS (UNCOATED)

The simulation rut depth for the uncoated test bed was also checked for the 30 knot test, see Figure 10. This figure shows that the simulated rut depths agree well with that estimated from the video. However, as the test rig passed about 40

10

feet the wheel rut greatly increased but the simulation did not. This action also needs further scrutiny.

FOREIGN OBJECT DAMAGE

In general, the video of the JBR coated test beds showed that the coating tended to restrain the coating material flight so that the problem of Foreign Object Damage (FOD) should be no worse than coatings from the previously installed EMAS. The cement board on the EMAS upper surface probably has a somewhat greater strength than the previous coatings but it appears that any loose material is already well failed so that no big chunks would ejected. For aircraft with bigger wheels that cover more EMAS block area any not failed cement board material would be small and not likely to cause damage.

AIRCRAFT SIZE IMPLICATIONS

As mentioned earlier, the size of the wheel and test weight was selected as representative of one of the smallest commuter aircraft now in service. As the size of the aircraft get bigger, say the SAAB 340 the single main wheel load is about 6200 pounds at maximum take off weight and about 5000 pounds at landing weight, that is greater than the test wheel weight. The tire pressure for the SAAB main gear is about 100 psi, the same as tested. That is above the CC "60 psi" material strength so EMAS penetration would be expected. The nose gear, on the other hand, has a low tire pressure and may initially ride on the upper surface of JBR coated EMAS but may penetrate when braking causes higher nose gear loading. Generally for aircraft in the 25,000 to 50,000 pound range EMAS performance estimates may slightly less accurate but reasonable.

For an EMAS with base CC material strength of "80 psi" the smaller aircraft could be expected to ride on the surface of the JBR coated EMAS but this would most likely be true for an uncoated EMAS as well.

As the aircraft get bigger it is expected that the JBR coating, being a fixed strength application, will be more and more insignificant in producing gear loads beyond that predicted or measured while operating in an uncoated EMAS. For aircraft with gross weights above 25,000 pounds the JBR coating effect on loads may be significant but not by a substantial amount. Above 50,000 pounds the JBR coating affect on performance and gear loads will, most likely, be insignificant.

AIRCRAFT SPEED IMPLICATIONS

Aircraft speed is known to have a pronounced affect on landing gear loads because of the "dynamic pressure" that materially increases the CC strength as seen by the aircraft wheels. The current tests only went to 30 knots. The design criteria require that the EMAS be compatible with air carrier operations to at least 70 knots. While it is not possible from the present test program results to predict the affect of the JBR coating on gear loads of small aircraft at these higher speeds, we can probably assume that the penetration would be less, but this may or may not affect the drag ratio. The only way to

11

E-13

determine this high-speed effect is to conduct tests at higher speeds and conducting such tests is recommended.

CONCLUSIONS

The JBR coating affect on the EMAS performance and loads as presently predicted is likely to be to insignificant for larger aircraft, i.e., 50,000 pounds or greater, however, for aircraft in the 25,000 pound range, (SAAB 340) this is also true but with less accuracy. For smaller aircraft (Beech 1900) loads may be a little higher up to 30 knots and performance reduced. For speeds above 40 the predictions of performance and loads on these smaller aircraft may not be quite as accurate. Testing of the JBR coating up to 70 knots is recommended to provide data for improving computer modeling capability.

The present indications are that the JBR does affect the computer prediction accuracy of small aircraft performance and loads while engaged in an EMAS. The measured uncoated drag ratios and simulated drag ratios were very close 2% at 15 knots and 1.5% at 30 knots while the JBR coated drag ratios were not quite as close, 6% at 15 knots and 14% at 30 knots, but within reasonable engineering accuracy. It is cautioned, however, that this conclusion is based on very limited test data and could change with the availability of more test data. For aircraft weighing more than 25,000 pounds the computer program is still considered to be an suitable means of predicting "60 psi" EMAS stopping distance and loads although not with quite same accuracy as for heavier aircraft, i.e. 50,000 pounds or larger.

Foreign Object Damage does not appear to be any worse than that for the usual EMAS coatings. The JBR coating appears to restrain broken coating parts to the basic block thus keeping ejected pieces to a minimum.

Based on information to date, the JBR coating appears to be a good solution to the durability problem. The blocks are completely encapsulated to prevent water intrusion and the upper surface has adequate strength for any necessary traffic on the EMAS as well a high resistance to the expected aircraft jet exhaust environment.

No additional recommendations are made regarding fabrication, installation, and maintenance methods. The present solution appears to be a good one at this stage of the technology and only time will tell if additional changes are necessary.

12